

UCLA

UCLA Electronic Theses and Dissertations

Title

Discs Large Homolog 1: Identifying Molecular Mechanisms that Guide Functional Specificity in Lymphocytes

Permalink

<https://escholarship.org/uc/item/1377h3c1>

Author

Crocetti, Jillian Ann

Publication Date

2014

Peer reviewed|Thesis/dissertation

UNIVERSITY OF CALIFORNIA

Los Angeles

Discs Large Homolog 1: Identifying Molecular Mechanisms that Guide
Functional Specificity in Lymphocytes

A dissertation submitted in partial satisfaction of
the requirements for the degree of Doctor of Philosophy
in Molecular Biology

by

Jillian Ann Crocetti

2014

© Copyright by
Jillian Ann Crocetti
2014

ABSTRACT OF THE DISSERTATION

Discs Large Homolog 1: Identifying Molecular Mechanisms that Guide Functional Specificity in Lymphocytes

By

Jillian Ann Crocetti

Doctor of Philosophy in Molecular Biology

University of California, Los Angeles, 2014

Professor M. Carrie Miceli, Chair

Lymphocytes, including T and B cells, are the cornerstone of the adaptive immune response. Recognition of foreign antigen by the T cell receptor or B cell receptor (collectively known as immunoreceptors) triggers transcriptional and cytoskeletal changes leading to proliferation, differentiation and execution of cell specific effector functions. Immunoreceptors have the unique ability to discriminate subtleties in antigen quality and translate these differences into specific biological responses. In T cells, scaffold protein Discs Large Homolog 1 (Dlg1) associates with signaling and cytoskeletal mediators including: Lck, Zap70, p38, ezrin and WASp. Through these interactions Dlg1 couples T cell receptor (TCR) stimulation to activation of MAPK p38 and transcription factor NFAT, and facilitates cytoskeletal events including receptor clustering, actin polymerization and cell-mediated cytotoxicity. This thesis identifies a role for Dlg1 in receptor clustering, synapse formation and p38 activation in B cells and examines the molecular mechanisms that individually and collectively regulate Dlg1-mediated pathways that guide functional specificity in lymphocytes. We show that T cells express two Dlg1 variants that form unique signaling complexes and drive distinct CTL effector responses. We also identify Dlg1 tyrosine phosphorylation as a key point of control required for

Dlg1-mediated transcriptional, but not cytoskeletal events. Finally, we use a novel inducible Dlg1 knockout model to characterize the role of Dlg1 *in vivo*. Together this work identifies changes in Dlg1 splice variant expression, recruitment, utilization and/or modification as a method to guide lymphocyte fate and function, and characterizes a knockout model that can be used to extend these findings in future studies.

The dissertation of Jillian Ann Crocetti is approved.

Jonathan Braun

Linda Baum

John Colicelli

Benhur Lee

M. Carrie Miceli, Committee Chair

University of California, Los Angeles

2014

I dedicate this work to my parents who have taught me both the value of hard work and the importance of balance. Your unwavering support has made all things possible. Thank you.

TABLE OF CONTENTS

ABSTRACT OF THE DISSERTATION.....	ii
LIST OF FIGURES.....	vii
LIST OF TABLES.....	x
ACKNOWLEDGEMENTS.....	xi
VITA.....	xiii
CHAPTER 1: Introduction.....	1
References.....	14
CHAPTER 2: Dlg1 splice variants direct CD8+ T cell function by coupling the TCR to p38- dependent pro-inflammatory cytokine production and/or WASp-dependent degranulation.....	18
References.....	49
CHAPTER 3: Phosphorylation of Discs large homolog 1 (Dlg1) by Lck is critical for p38 activation and pro-inflammatory cytokine gene expression in T cells.....	53
References.....	78
CHAPTER 4: The scaffolding protein synapse-associated protein 97 (SAP97/Dlg1) is required for enhanced signaling through isotype-switched IgG memory B cell receptors.....	82
References.....	116
CHAPTER 5: Discs large homolog 1 (Dlg1) facilitates BCR-induced alternative p38 activation in IgM+ B cells.....	120
References.....	136
CHAPTER 6: Conclusions.....	137
References.....	148

LIST OF FIGURES

Chapter 1

Figure 1-1	Dlg1 domain structure and sites of alternative splicing.....	11
Figure 1-2	Dlg1 mediates the alternative p38 pathway.....	12
Figure 1-3	Immunoreceptor signaling in T and B lymphocytes.....	13

Chapter 2

Figure 2-1	T lymphocytes express two Dlg1 splice variants due to alternative splicing: Dlg1AB and Dlg1B.....	35
Figure 2-2	Dlg1 alternative splice variants expressed by hematopoietic and non- hematopoietic cells.....	36
Figure 2-3	Dlg1AB selectively binds Lck and supports p38 phosphorylation while Dlg1B does not.....	37
Figure 2-4	Selective expression of Dlg1AB, but not Dlg1B promotes p38-dependent transcription of IFN γ	38
Figure 2-5	Dlg1AB over expression selectively enhances NFAT-dependent transcription of IFN γ and TNF α but not IL-2 or granzyme B, while Dlg1B does not.....	39
Figure 2-6	Dlg1AB knockdown selectively diminishes transcription of IFN γ and TNF α , but not IL-2 or granzyme B; while total Dlg1 knockdown impairs cytokine and granzyme B secretion.....	40
Figure 2-7	Dlg1 knockdown prevents optimal intracellular IFN γ production over a range of antigen concentrations.....	41
Figure 2-8	Dlg1 regulates optimal TCR-triggered, actin-dependent degranulation.....	42
Figure 2-9	Dlg1 truncations and WASp knockdown OT-1 hybridoma T cell lines.....	44
Figure 2-10	Dlg1-SH3 controls WASp activation to mediate degranulation.....	45
Figure 2-11	Dlg1 knockout decreases p38 activation, pro inflammatory cytokine production and CTL killing in CD8+ T cells from LCMV-infected mice.....	46

Chapter 3

Figure 3-1	A Dlg1-associated kinase phosphorylates Dlg1AB in response to TCR stimulation.....	71
Figure 3-2	Dlg1-associated Lck phosphorylated Dlg1 at tyrosine 222.....	72
Figure 3-3	Dlg1 Y222 phosphorylation is required for TCR-induced alternative p38 activation.....	73
Figure 3-4	Dlg1 Y222 is required for selective induction of TCR-triggered NFAT-, but not NFκB-dependent genes including pro-inflammatory cytokine IFNγ and TNFα....	74
Figure 3-5	Dlg1 Y222 phosphorylation is not required for antigen-dependent CTL degranulation.....	75
Figure 3-6	Acute Dlg1 KO impairs p38 activation, NFAT-dependent pro-inflammatory cytokine gene expression and target cell lysis in response to TCR stimulation...	76
Figure 3-7	Model of Dlg1-dependent signaling downstream of the TCR.....	77

Chapter 4

Figure 4-1	The cytoplasmic tail of mIgGs are highly conserved.....	103
Figure 4-2	The cytoplasmic tail of mIgG binds SAP97.....	104
Figure 4-3	SAP97 is the most abundant SAP family protein in B cells.....	105
Figure 4-4	The binding of SAP97 to the cytoplasmic tail of mIgG.....	106
Figure 4-5	IgG BCRs enhance the accumulation of SAP97 in the immunological synapse.....	107
Figure 4-6	IgG BCRs and SAP97 show increased colocalization and close molecular proximity after antigen binding.....	108
Figure 4-7	The accumulation of SAP97 at the immunological synapse and its colocalization with IgG and IgM BCRs in human B cells.....	109
Figure 4-8	The enhanced accumulation of IgG-BCRs in the immunological synapse and the increased recruitment of pSyk is SAP97-dependent.....	110

Figure 4-9	Knockdown of SAP97 has mild effects on the antigen-induced accumulation of IgM BCRs in the immunological synapse.....	111
Figure 4-10	The enhances accumulation of IgG-BCRs in the immunological synapse is SAP97-dependent.....	112
Figure 4-11	The SSVV motif in the mIgG cytoplasmic tails is required for the enhances accumulation of IgG BCRs into the immunological synapse.....	113
Figure 4-12	The extent of co-localization of IgG-SSVV/AAA mutant BCRs with SAP97 upon antigen engagement is substantially reduced to that of IgG-WT BCRs.....	114
Figure 4-13	Knockdown of SAP97 substantially impairs actuation of p38 MAPK.....	115

Chapter 5

Figure 5-1	Dlg1 expression profiles in T and B lymphocytes.....	131
Figure 5-2	Dlg1 forms a BCR-inducible complex with Lyn, Syk and p38 that facilitates p38 phosphorylation <i>in vitro</i>	132
Figure 5-3	BCR-inducible alternative p38 activation occurs in IgM+ B cells.....	133
Figure 5-4	BCR-induced NFAT-, but not NFB-dependent transcription is p38 dependent..	134
Figure 5-5	Dlg1 knockout impairs BCR-induced p38 phosphorylation and cytokine production in IgM+ B cells.....	135

Chapter 6

Figure 6-1	Current Model of MAGUK-Mediated Signaling.....	145
Figure 6-2	Dlg1 knockout impairs response to H1N1 influenza.....	146
Figure 6-3	Early memory formation is diminished in Dlg1 knockout mice after acute LCMV infection.....	147

LIST OF TABLES

Chapter 2

Table 2-1	Knockdown sequences clone into MGP or MRP.....	48
Table 2-2	RT-PCR Primers.....	48
Table 2-3	qPCR Primers.....	48

ACKNOWLEDGEMENTS

I would first like to thank my mentor, Carrie Miceli, for her guidance and support throughout my time in her lab. She has encouraged me to find my own path; and to be a well-rounded scientist and person, for which I am very grateful. I would also like to thank my committee members, Jonathan Braun, John Colicelli, Linda Baum and Benhur Lee for their time and thoughtful discussion. I would like to thank everyone in the Miceli Lab, past and present. To Derek, Genevieve and Richard for making the endless hours in lab go by more quickly. I would like to extend a special thank you to Lisa for being a great scientific resource and friend. I could not have made it through the early years of troubleshooting without your guidance, and the later years without our coffee dates. I would like to thank Oscar, for his patience with my many questions over the years, and for being a great scientific partner in crime. I would also like to thank Steve, Neil and Howard at the UCLA Office of Intellectual Property for their efforts in organizing the Technology Fellows program, which has taught me so much about bringing important discoveries out of the lab and into the world. To Ed for joining me at the end of my graduate school journey. For keeping me company while I change cell media on Saturday mornings, pretending that my science rants are interesting and understanding that frozen yogurt is a legitimate answer to a bad day. I could not have done this without you. Finally, to my parents for their unconditional love and support throughout the years. You have always encouraged me to fight through rough times, enjoy the good times and when all else fails—go to Hawaii! For all these things, and so many more—thank you.

I would like to acknowledge my funding sources throughout the years. The Microbial Pathogenesis Training Grant (NIH NIAID T32-AI067253) and the UCLA Molecular Biology Institute.

Chapters 2, 3 and 5 are versions of what will be first author and co-first author publications. Chapter 4 is a published co-author manuscript. The author directing each project is indicated in bold.

CHAPTER 2: Dlg1 splice variants direct CD8+ T cell function by coupling the TCR to p38-dependent pro-inflammatory cytokine production and/or WASp-dependent degranulation

AUTHORS: Silva, O.* , Crocetti, J.* , Humphries, L.A., Elsaesser, H., Brooks, D. & **Miceli, M.C.**

*authors contributed equally to this work

CHAPTER 3: Phosphorylation of Discs large homolog 1 (Dlg1) by Lck is critical for p38 activation and pro-inflammatory cytokine gene expression in T cells

AUTHORS: Crocetti, J., Silva O., Humphries, L.A., Tibbs, M. & **Miceli, M.C.**

CHAPTER 4: The scaffolding protein synapse-associated protein 97 (SAP97/Dlg1) is required for signaling through isotype-switched IgG memory B cell receptors

AUTHORS: Liu, W., Chen, E.* , Zhao, X.W.* , Wan, Z.P.* , Gao, Y.R.* , Davey, A.* , Huang, E., Zhang, L., Crocetti, J., Sandoval, G., Joyce, M.G., Miceli, M.C., Lukszo, J., Aravind, L., Swat, W., Brzostowski, J. & **Pierce, S.K.**

*authors contributed equally to this work

Chapter 4 was reprinted from: *Sci. Signal.* **5**, ra54 (2012).

CHAPTER 5: Discs large homolog 1 (Dlg1) facilitates BCR-induced alternative p38 activation in IgM+ B cells

AUTHORS: Crocetti, J., Humphries, L.A. & **Miceli, M.C.**

VITA

- 2006 Edmondson Summer Research Fellowship
University of Southern California
Los Angeles, California
- 2006-2007 Teaching Assistant, Protein Biochemistry & Immunology
University of California, Santa Barbara
Santa Barbara, California
- 2007 Bachelor of Science, Microbiology, Cum Laude
University of California, Santa Barbara
Santa Barbara, California
- 2008 Admitted to UCLA ACCESS Program
University of California, Los Angeles
Los Angeles, California
- 2009-2011 UCLA/NIH Microbial Pathogenesis Training Grant
University of California, Los Angeles
Los Angeles, California
- 2010-2011 Teaching Assistant, Microbial Pathogenesis & Immunology
Dept. of Microbiology, Immunology and Molecular Genetics
University of California, Los Angeles
Los Angeles, California
- 2011 Private Tutor, Graduate Level Immunology
ACCESS Department
University of California, Los Angeles
Los Angeles, California
- 2012 Graduate Student Scholar
Science Outside the Lab
Washington D.C.
- 2012-2014 Technology Transfer Fellow
Office of Intellectual Property & Industry Sponsored Research
University of California, Los Angeles
Los Angeles, California
- 2012-2014 Co-Chair, Molecular Biology Institute Retreat Planning Committee
Molecular Biology Institute
University of California, Los Angeles
Los Angeles, California

PUBLICATIONS

Silva, O.* , **Crocetti, J.***, Humphries, L.A., Elsaesser, H., Brooks, D. & Miceli, M.C. Dlg1 splice variants regulate p38-dependent and -independent CTL effector functions. (In preparation).

***indicates equal contribution**

Crocetti, J., Silva O., Humphries, L.A., Tibbs, M. & Miceli, M.C. Dlg1 phosphorylation is required for coordination of the TCR-induced p38 pathway in CD8+ T cells. (In preparation).

Crocetti, J., Humphries, L.A. & Miceli, M.C. Discs Large Homolog 1 (Dlg1) facilitates BCR-induced alternative p38 activation in IgM+ B cells. (In preparation).

Liu, W., Chen, E., Zhao, X., Wan, Z., Gao, Y., Davey, A., Huang, E., Zhang, L., **Crocetti, J.**, Sandoval, G., Joyce, M.G., Miceli, C., Lukszo, J., Aravind, L., Swat, W., Brzostowski, J. & Pierce, S.K. The scaffolding protein synapse-associated protein 97 is required for enhanced signaling through Isotype-switched IgG memory B cell receptors. *Sci. Signal.* **5**, ra54 (2012).

PRESENTATIONS

Crocetti, J.*, Humphries, L.A., Miceli, M.C. *Discs Large Homolog 1 (Dlg1) phosphorylation mediates p38-dependent functions downstream of the T cell receptor.* Immunology LA, Los Angeles, CA (2013).

Silva, O.* , **Crocetti, J.**, Humphries, L.A. , Miceli, M.C. *Discs Large Homolog 1 Splice Variants Couple T Cell Receptor Engagement to Distinct T Cell Effector Functions.* American Association of Immunologists Annual Meeting, Honolulu, HI (2013).

Crocetti, J.*, Humphries, L.A., Miceli, M.C. *Discs Large Homolog 1 (Dlg1) phosphorylation mediates p38-dependent functions downstream of the T cell receptor.* UCLA Molecular Biology Institute Retreat, Lake Arrowhead, CA (2012).

Silva, O.* , **Crocetti, J.**, Humphries, L.A. , Miceli, M.C. *Discs Large Homolog 1 Splice Variants Couple T Cell Receptor Engagement to Distinct T Cell Effector Functions.* Immunology LA, Malibu, CA (2011).

Silva, O.* , **Crocetti, J.**, Humphries, L.A. , Miceli, M.C. *Discs Large Homolog 1 Splice Variants Couple T Cell Receptor Engagement to Distinct T Cell Effector Functions.* American Association of Immunologists Annual Meeting, San Francisco, CA (2011).

Silva, O.* , **Crocetti, J.**, Humphries, L.A. , Miceli, M.C. *Discs Large Homolog 1 Alternative Splice Variants: Molecular Scaffolds Directing Specific T Cell Effector Functions.* UCLA MIMG Symposium, Los Angeles, CA (2011).

Crocetti, J.*, Humphries, L.A., Miceli, M.C. *Dlg1 Orchestrates Immunoreceptor-Dependent Alternative p38 Activation in B Lymphocytes.* UCLA Molecular Biology Institute Retreat, Lake Arrowhead, CA (2010).

CHAPTER ONE

Introduction

The immune system is a diverse collection of organs, tissues and cells distributed throughout the body responsible for protecting an organism from foreign pathogens and the onset of disease. A defining feature of the immune response is its ability to discriminate between self and non-self and mount a proper cellular response. The immune system can be separated into two distinct, but interconnected systems—the innate immune system and the adaptive immune system. The innate immune system is a first line of defense that provides rapid, but broad protection from pathogens. The cells of the innate immune system, which include macrophages, dendritic cells, eosinophils, basophils, neutrophils and natural killer cells, are triggered by recognition of repeating patterns of molecules that are common to most pathogens (1). The second line of protection is provided by the adaptive immune response, which relies on cues from the innate immune response to tailor its response to a particular invading pathogen. Specificity of the adaptive response relies on recognition of pathogens by a diverse set of immunoreceptors on the surface of B and T lymphocytes estimated to recognize as many as 25×10^6 distinct antigens (2). Each lymphocyte expresses an immunoreceptor, known as the B cell receptor (BCR) or the T cell receptor (TCR), of a single specificity through random gene rearrangement. Antigen recognition by these receptors triggers a dynamic set of cytoskeletal rearrangements and intracellular signaling pathways that control development, proliferation, energy, differentiation and cell-specific effector functions that dictate the adaptive immune response.

The TCR is a disulfide-linked membrane-anchored heterodimer normally consisting of the highly variable alpha (α) and beta (β) chains expressed as part of a complex with the invariant CD3 chain molecules (3). The TCR heterodimer is responsible for specific recognition of antigens, while the CD3 accessory molecules aid in intracellular signal transduction. T cell activation occurs when the TCR engages major histocompatibility complex (MHC)/peptide complexes (pMHC) on an antigen presenting cell (APC). The amount and affinity of the peptide antigen determines the strength of the TCR signal, and therefore guides the quality and intensity of the cellular response (4).

The mechanisms responsible for TCR signal initiation and resulting signal transduction cascades have been well studied. The TCR has no intrinsic enzymatic activity and instead depends on the kinase activity of Src-family tyrosine kinase Lck to initiate signaling. Following interaction of the TCR with pMHC, Lck phosphorylates the immunoreceptor tyrosine-based activation motifs (ITAMs) in the intracellular portion of CD3 ζ and CD3 ϵ . Phosphorylated ITAMs serve as a docking site for Syk-family tyrosine kinase Zap70, positioning it for activation by Lck-dependent phosphorylation (5). These early TCR-dependent signaling events are required for the activation of nearly all cytoskeletal and signaling pathways downstream of the TCR. However, the precision of TCR-triggered cellular responses dictates that these proximal signals not be diversified at random, but instead specified toward particular pathways (4). This dissertation explores the mechanisms by which scaffold protein Discs Large Homolog 1 (Dlg1) specifies lymphocyte function by channeling TCR, or BCR-proximal signaling molecules toward p38-specific transcriptional programs and WASp-dependent cytoskeletal events.

TCR Activation: Not All Signals Are Created Equal

Primary activation of naïve T cells requires interaction between an antigen-specific TCR and peptide-loaded APC. This initial TCR-APC interaction in naïve CD8⁺ T cells leads to the generation of cytotoxic T lymphocytes (CTLs) that produce pro-inflammatory cytokines and kill infected cells through release of lytic granules (6, 7). Conversely, activation of naïve CD4⁺ T cells has the potential to induce differentiation into multiple effectors with functional capabilities including: T helper 1 (Th1), T helper 2 (Th2), T follicular helper (Tfh) and regulatory T cells (Treg). Through the coordinated response of CD8⁺ and CD4⁺ T cells, the adaptive immune system eradicates pathogens, and provides immunological memory, which protects against re-infection with the same microbe through the retention of antigen-specific memory T cells (8-10).

One of the first consequences of T cell activation is dynamic actin-mediated re-organization of the cytoskeleton; where T cell receptors, intracellular signaling molecules and cytoskeletal components are recruited to interface between the T cell and APC. The resulting

molecular platform, often referred to as the immunological synapse, provides a framework for assembly and maintenance of signaling complexes that couple proximal signals initiated by Lck and Zap70 to the activation of MAPKs p38, JNK and ERK and transcription factors NFAT, NFκB and AP-1 (11, 12). Additionally, the immune synapse facilitates re-organization of the microtubule organizing complex (MTOC) and polarized trafficking of cytokines and lytic granules, which promotes directional secretion of cytokines and lytic factors (13, 14). The immune synapse can also dampen T cell activation by mediating TCR internalization, transducer ubiquitination and inhibitory receptor recruitment (15).

TCR-induced signaling cascades are not simple on-off pathways, but instead are complex cellular processes in which the T cell senses its environment and responds through activation of specific gene programs and delivery of effector molecules (4). The TCR/pMHC interaction is both sensitive and specific, requiring proper recognition of both the peptide and the MHC; however, it is relatively weak compared with many receptor-ligand pairs (3). Recently, it has been appreciated that both quantitative and qualitative differences in TCR-pMHC interactions (together referred to as TCR signal strength) influence events far downstream of TCR recognition (3). Indeed, weak TCR/pMHC interactions lead to delayed or impaired early signaling events, which result in decreased proliferation and impaired cell-specific effector functions or even lead to inactivation of the T cell referred to as clonal anergy (3). Inability of T cells to properly sense antigen quality has been linked to changes in the T cell repertoire that precede numerous autoimmune diseases (16). Therefore the understanding the mechanisms that translate TCR signal strength into appropriate biological responses including proliferation, differentiation and function may have important clinical implications.

Scaffold Proteins: Key Players in Signal Transduction

Scaffold proteins (also known as adaptors) have emerged as key regulators of intracellular signaling pathways capable of tuning molecular responses by channeling proximal signals toward specific downstream pathways (17). While scaffold proteins have no intrinsic

enzymatic activity, they contain multiple protein-binding domains, proline-rich motifs and/or phosphotyrosines, which coordinate the assembly of signaling complexes that coordinate particular pathways (4, 18). Two of the most extensively studied scaffold proteins in T cells are LAT and SLP-76. Upon TCR stimulation, LAT is phosphorylated by Zap70 and recruits SLP-76 to the plasma membrane where the two scaffolds nucleate a multi-molecular complex containing signaling proteins, calcium modulators and cytoskeletal regulators that activate MAPKs ERK and JNK and transcription factors NFAT, NF κ B and AP-1, mediate calcium flux and cytoskeletal re-arrangements (4, 19). While specific phosphorylation events are known to guide SLP76 activity toward certain pathway, the severe impairment of T cell development and function suggests that SLP-76/LAT complex does not necessarily specify signals downstream of the TCR, but rather is required for simultaneous activation of numerous pathways (4). Thus, the question of how TCR signals are tethered to *specific* downstream pathways remains unanswered.

Work from our lab and others have demonstrated that two membrane associated guanylate kinase (MAGUK) scaffold proteins, Dlg1 and CARMA1, play a major role in *specifying* signal transduction downstream of the TCR (20-23). MAGUKS are a ubiquitous class of multi-domain scaffold proteins found at the interface of cell:cell contacts, where they play an vital role in synapse formation, cell polarity, asymmetric division, receptor trafficking and signal transduction (24-26). Structurally, MAGUKs are characterized by the presence of one to three PDZ domains, an SH3 domain and a catalytically inactive guanylate kinase domain (26). While Dlg1 and CARMA1 share portions of this common region in their C-terminus, they have distinct N-terminal features that contribute to unique protein-protein interactions and endowing each scaffold with specific functions (Figure 1-1). In response to TCR stimulation, CARMA1 forms a complex with Bcl10, MALT1, TAK1 and TRAF6 in order to activate MAPK JNK1/2 and transcription factor NF κ B (27-30, Figure 6-1). Conversely, Dlg1 forms a complex with proximal tyrosine kinases Lck and Zap70 and MAPK p38 leading to the activation of p38 and transcription factor NFAT (23, Figure 6-1, Figure 1-2). Therefore, MAGUK family scaffold

proteins act as molecular conduits, funneling TCR-proximal signals toward specific downstream pathways and functions (Figure 6-1). Understanding the molecular mechanisms by which MAGUK scaffold proteins regulate downstream pathways will be vital in determining how TCR signals are specified and provide novel targets for pharmaceutical intervention.

Discs large homolog 1 (Dlg1) Guides TCR-dependent Signaling and Cytoskeletal Events

In response to TCR stimulation, Dlg1 mediates the alternative p38 activation pathway by forming a molecular complex with Lck, Zap70 and p38 (21, 23, 31) (Figure 1-2). Through juxtaposition these kinases, Dlg1 facilitates Lck-mediated activation of Zap70, and subsequent Zap70-dependent phosphorylation of p38 at tyrosine 323 (Y323) (23, 31, 32). Phosphorylation at Y323 triggers p38 auto-phosphorylation at threonine 180 (T180), up regulating p38 kinase activity (33). Indeed, Dlg1-mediated alternative p38 activation leads to downstream activation of NFAT-, but not NFkB-dependent transcription and production of pro-inflammatory cytokine IFN γ (23, 34, 35). Consequently, Dlg1 specifies early signal transduction toward p38 and NFAT leading to the induction of a discrete set of genes and therefore cellular functions.

In addition to selectively activating p38 and NFAT-dependent transcription, Dlg1 facilitates antigen-induced cytoskeletal re-arrangements (14, 36, 37). The association of Dlg1 with cytoskeletal regulators WASp and ezrin is hypothesized to facilitate T cell polarity by coupling TCR engagement to actin polymerization, the clustering of synaptic TCRs, and MTOC polarization. Knockdown of Dlg1 attenuates TCR triggered F-actin polymerization and the polarized recruitment of lipid rafts, TCR and the MTOC to the immune synapse, processes known to utilize WASp and ezrin (14, 38, 39). Given the involvement of Dlg1 in guiding both transcriptional activation and cytoskeletal re-organization, we hypothesized that Dlg1 plays a vital role in specifying T cell development, fate determination and effector function.

Indeed, utilizing knockdown systems, we and others have demonstrated a role for Dlg1 in CD4+ Th1 differentiation, CD4+FoxP3+ Treg suppressive activity and CD8+ CTL effector functions including cytokine production and contact-dependent cytotoxicity (23, 34, 35, 40).

Despite the tremendous progress toward understand the role of Dlg1 in guiding T cell development and effector function, the relative contributions of individual Dlg1 ligands Lck, Zap70, p38 and WASp has not been determined. It is also uncertain whether Dlg1-mediated transcriptional and cytoskeletal events are discrete or dependent pathways, and how these pathways are regulated. This dissertation explores these unanswered questions, with emphasis on Dlg1 alternative splicing (Chapter 2) and Dlg1 phosphorylation (Chapter 3) as key regulatory events that guide Dlg1-mediated events downstream of the TCR.

Post-Transcriptional and Post-Translational Dlg1 Modifications

Dlg1 is dynamically regulated by alternative splicing, phosphorylation, ubiquitination, and intramolecular interactions that dictate Dlg1 localization, conformation, stability and interaction partners (15, 37, 41-50). Such changes are thought to be critical for Dlg1-mediated T cell effector functions, and thus may be excellent targets for modulating Dlg1 activity.

Dlg1 contains four known areas of alternative splicing capable of generating unique Dlg1 scaffolds thought to have specific functional capacities (37, 51) (Figure 1-1). The first is in the 5'UTR, which regulates *dlg1* translation (52). The second region is in the N-terminus where a CXC α palmitoylation domain or L27 β oligomerization domain is expressed (53). The third is in the proline-rich region upstream of the first PDZ domain, where i1A and/or i1B regions can be expressed. Finally, splicing can occur between the SH3 and GUK domains in region known as the HOOK domain, where i2, i3, i4 and/or i5 can be expressed. Dlg1 splice variants play a role in the localization, stability and function in neurons and epithelial cells; however, a role for Dlg1 splicing has not been established in T cells. In chapter 2 of this dissertation we explore the expression of Dlg1 splice variants in T cells, and demonstrate their ability to regulate discrete pathways downstream of the TCR.

Phosphorylation dynamically regulates the structure and function of MAGUK protein complexes. In T cells, CARMA1 exists in an auto-inhibited form through intramolecular interactions. In response to TCR stimulation, CARMA1 localizes to the immune synapse where

it is phosphorylated by PKC θ , causing a conformational change that allows CARMA1 to associate with Bcl10 and MALT1, leading to activation of MAPK JNK and transcription factor NF κ B (54-56). Numerous studies in epithelial and neuronal cells have demonstrated that Dlg1 phosphorylation influences Dlg1 localization, stability and function (44-46). While tyrosine kinase activity has been attributed to Dlg1 complexes in T cells, a role for Dlg1 phosphorylation in regulating TCR signal transduction and resulting T cell function has not been explored (51). In chapter 3 of this dissertation, we determine that TCR-dependent Dlg1 tyrosine phosphorylation plays a key role in regulating Dlg1-mediated p38-dependent events including IFN γ production.

Dlg1 Knockout

Our group and others have demonstrated a role for Dlg1 in regulating TCR-dependent cytoskeletal and transcriptional events. However, the majority of these studies have been performed using siRNA knockdown, which are limited to *ex vivo* biochemical studies in dividing cells (14, 23, 34, 35, 38). The development of a *dlg1* knockout model would allow questions about T cell development and response to infection to be asked *in vivo*. Because mice harboring germline *dlg1*-null mutations show several developmental abnormalities and die perinatally, our group and others have developed *dlg1* knockouts specific to the lymphoid compartment (57). However, studies using this system that examined T cell development, differentiation and effector function have yielded mild and varying phenotypes (40, 58). Results from *dlg1* knockout models in neuronal systems suggest that functional abnormalities in non-acute *dlg1* knockouts are masked through compensation up regulation of other Dlg1 family members (40, 53). This dissertation utilizes an acute *dlg1* knockout system to demonstrate a functional requirement for Dlg1 in CD8 $^+$ T cell function *in vitro* (Chapter 3) and *in vivo* in the context of lymphocytic choriomeningitis virus (LCMV) infection (Chapter 2). These results confirm the role of Dlg1 *in vitro* and *in vivo*, we hope to use this system in future studies to determine the individual role of Dlg1 variants and point mutants *in vivo*.

The Evolving Role of Dlg1 in B cells

Despite their vast functional differences, early signaling events in B and T cells are fairly analogous (Figure 1-3). B cells express a B cell receptor complex (BCR) consisting of a membrane-bound B cell receptor (mIg) that associates at a 1:1 molar ratio with signaling complex Ig/Ig. In response to antigen recognition, the Ig/Ig ITAMs are phosphorylated by Src-family member Lyn creating a binding site for Syk family member Syk. Activated Syk then goes on to phosphorylate downstream adaptor and effector proteins including MAPKs that activate transcription factors resulting in up regulation of specific gene programs. Despite these similarities in early signal transduction, initial investigations suggest that the alternative p38 pathway is not employed in B cells (31).

Unlike the TCR, the mIg portion of the BCR is altered after initial antigen encounter with naïve B cells expressing either mIgM or mIgD and memory B cells expressing mIgG. The mIgG contains a 28 amino acid cytoplasmic tail that is thought to enhance intracellular signal transduction in memory B cells (Chapter 4). However, a specific role for the cytoplasmic tail of the mIgG has yet to be determined. In collaboration with Dr. Sue Pierce's lab, chapter 4 of this dissertation examines the role of Dlg1 (SAP97) in mediating BCR early signaling and cytoskeletal events in IgG⁺ memory B cells. In chapter 5, we investigate the mechanism of Dlg1-mediated p38 activation in IgM⁺ B cells. Together this work aims to define novel mechanisms of signal transduction in B cells, future studies will determine the role that Dlg1-mediated signaling plays in B cell development and effector function.

Aims of Dissertation

Diversification and specification of signal transduction downstream of lymphocyte immunoreceptors is known to fine tune cellular function in response to the quality and quantity of antigen. Scaffold proteins act as molecular bridges that connect extracellular signals to intracellular signaling pathways. Dlg1 is a scaffold protein known to specify TCR-proximal signals toward p38-dependent transcription and actin-dependent cytoskeletal events. This

dissertation explores the molecular mechanisms of Dlg1 regulation in T and B lymphocytes. Chapters 2 and 3 explore Dlg1 modifications that specify immunoreceptor signal transduction and functional output in CD8⁺ T cells including alternative splicing (chapter 2) and phosphorylation (chapter 3). Chapters 4 and 5 explore the possibility of Dlg1-mediated signaling events in IgM⁺ (chapter 5) and IgG⁺ (chapter 4) B cells.

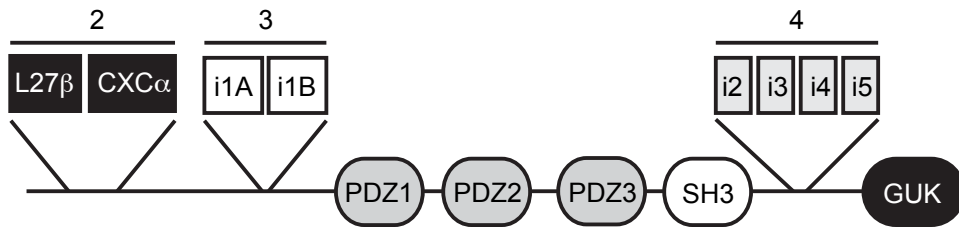


Figure 1-1: Dlg1 domain structure and sites of alternative splicing. Dlg1 is a multi-domain scaffold protein consisting of three PSD95/Dlg/ZO-1 (PDZ) domains, one Src-homolog 3 (SH3) domain and a catalytically inactive guanylate kinase domain (GUK). It also contains four regions of alternative splicing. Region 1 is in the 5' untranslated region (not pictured). Region 2 is in the N-terminus where either oligomerization domain L27β or palmitoylation domain CXCα is expressed. Region 3 is the proline-rich region where i1A, i1B or i1Ai1B is expressed. Region 4 is the HOOK domain where any combination of i2, i3, i4 and/or i5 can be expressed.

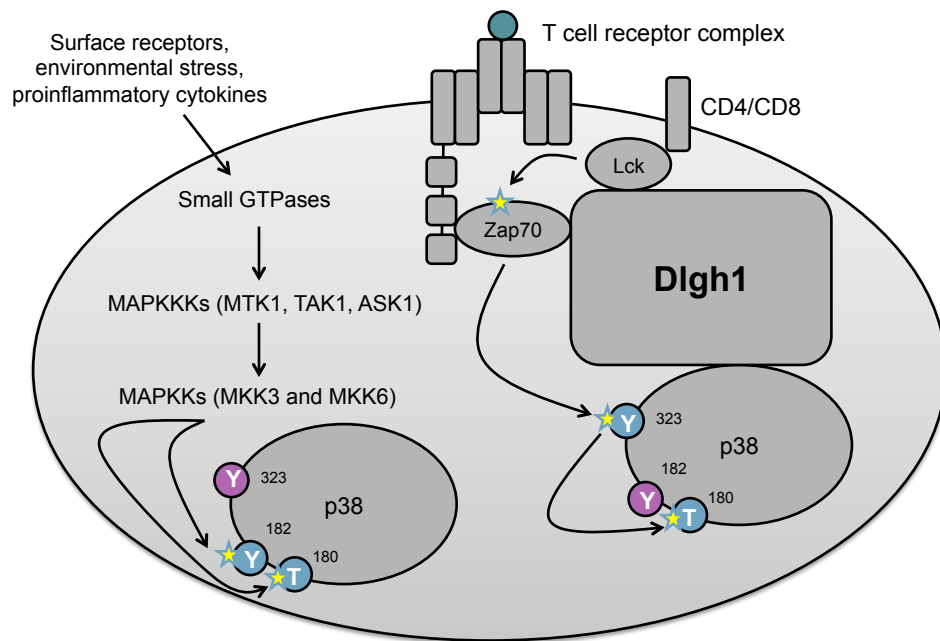


Figure 1-2: Dlg1 mediates the alternative p38 pathway. The canonical p38 pathway (left) occurs in response to environmental stress. Signaling is initiated by small GTPases and propagated by a three tiered MAK kinase cascade, which culminates in direct phosphorylation of p38 at T180 and Y182 by MKK3 or MKK6. The alternative p38 pathway (right) is initiated by TCR stimulation and is coordinated by scaffold protein Dlg1, which associates with Lck, Zap70 and p38. This complex facilitates p38 phosphorylation at Y323 by Zap70, leading to p38 auto-phosphorylation at T180.

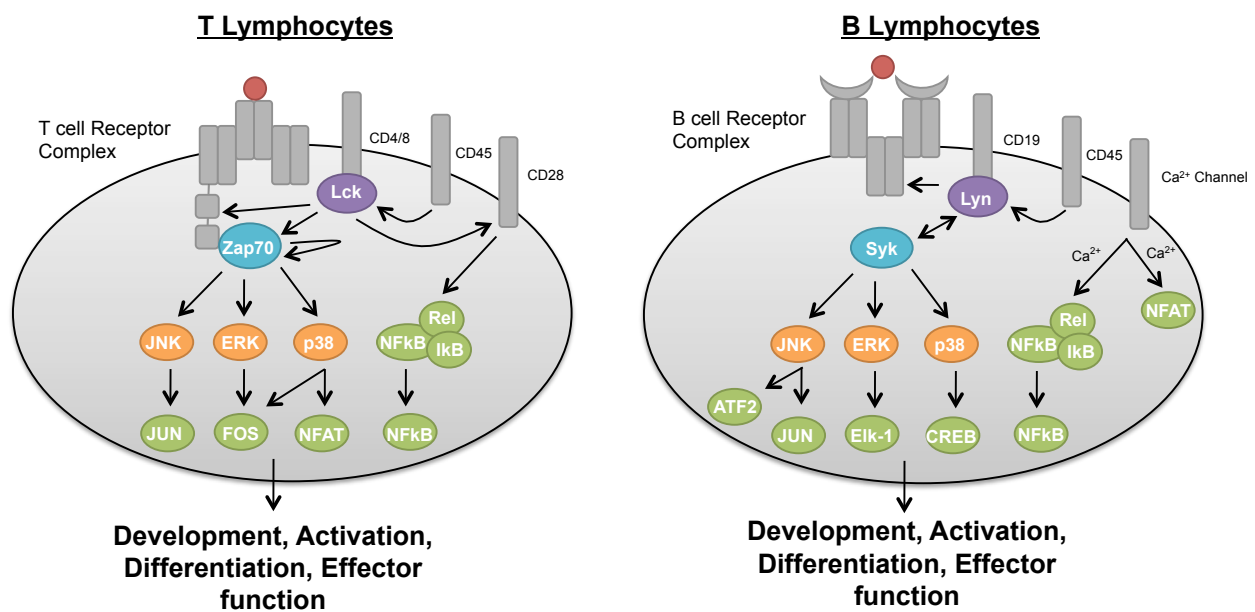


Figure 1-3: Immunoreceptor signaling in T and B lymphocytes. Signal transduction downstream of the immunoreceptors in B cell and T cells is quite analogous. The first level of activation is the Src family kinases (purple). These kinases phosphorylate ITAM motifs that form binding sites for Syk family kinases (blue). Once activated Syk family kinases activate a variety of MAP kinases (orange), which activate transcription factors (green) that regulate gene expression programs that guide development, activation, differentiation and effector functions.

REFERENCES

1. Janeway CA, Jr., Medzhitov R. 2002. Innate immune recognition. *Annu Rev Immunol* 20: 197-216
2. Arstila TP, Casrouge A, Baron V, Even J, Kanellopoulos J, Kourilsky P. 1999. A Direct Estimate of the Human $\alpha\beta$ T Cell Receptor Diversity. *Science* 286: 958-61
3. Corse E, Gottschalk RA, Allison JP. 2011. Strength of TCR-peptide/MHC interactions and in vivo T cell responses. *J Immunol* 186: 5039-45
4. Brownlie RJ, Zamoyska R. 2013. T cell receptor signalling networks: branched, diversified and bounded. *Nat Rev Immunol* 13: 257-69
5. Smith-Garvin JE, Koretzky GA, Jordan MS. 2009. T cell activation. *Annu Rev Immunol* 27: 591-619
6. Kaech SM, Wherry EJ. 2007. Heterogeneity and cell-fate decisions in effector and memory CD8+ T cell differentiation during viral infection. *Immunity* 27: 393-405
7. Kaech SM, Cui W. 2012. Transcriptional control of effector and memory CD8+ T cell differentiation. *Nat Rev Immunol* 12: 749-61
8. Kaech SM, Ahmed R. 2001. Memory CD8+ T cell differentiation: initial antigen encounter triggers a developmental program in naive cells. *Nature Immunology* 2: 415-22
9. Kaech SM, Hemby S, Kersh E, Ahmed R. 2002. Molecular and functional profiling of memory CD8 T cell differentiation. *Cell* 111: 837-51
10. Marshall HD, Kaech SM. 2013. Generating CD8 T cell heterogeneity: attack of the clones. *Immunity* 39: 203-5
11. Billadeau DD, Nolz JC, Gomez TS. 2007. Regulation of T-cell activation by the cytoskeleton. *Nat Rev Immunol* 7: 131-43
12. Fooksman DR, Vardhana S, Vasiliver-Shamis G, Liese J, Blair DA, Waite J, Sacristan C, Victora GD, Zanin-Zhorov A, Dustin ML. 2010. Functional anatomy of T cell activation and synapse formation. *Annu Rev Immunol* 28: 79-105
13. Huse M, Quann EJ, Davis MM. 2008. Shouts, whispers and the kiss of death: directional secretion in T cells. *Nature Immunology* 9: 1105-11
14. Lasserre R, Charrin S, Cuhe C, Danckaert A, Thoulouze MI, de Chaumont F, Duong T, Perrault N, Varin-Blank N, Olivo-Marin JC, Etienne-Manneville S, Arpin M, Di Bartolo V, Alcover A. 2010. Ezrin tunes T-cell activation by controlling Dlg1 and microtubule positioning at the immunological synapse. *EMBO J* 29: 2301-14
15. Lee K-H, Dinner AR, Tu C, Campi G, Raychaudhuri S, Varma R, Sims TN, Burack WR, Wu H, Wang J, Kanagawa O, Markiewicz M, Allen PM, Dustin ML, Chakraborty AK, Shaw AS. 2003. The Immunological Synapse Balances T Cell Receptor Signaling and Degradation. *Science* 302: 1218-22
16. Ohashi PS. 2002. T-cell signalling and autoimmunity: molecular mechanisms of disease. *Nat Rev Immunol* 2: 427-38

17. Shaw AS, Filbert EL. 2009. Scaffold proteins and immune-cell signalling. *Nat Rev Immunol* 9: 47-56
18. Dal Porto JM, Gauld SB, Merrell KT, Mills D, Pugh-Bernard AE, Cambier J. 2004. B cell antigen receptor signaling 101. *Mol Immunol* 41: 599-613
19. Koretzky GA, Abtahian F, Silverman MA. 2006. SLP76 and SLP65: complex regulation of signalling in lymphocytes and beyond. *Nat Rev Immunol* 6: 67-78
20. Gaide O, Favier B, Legler DF, Bonnet D, Brissoni B, Valitutti S, Bron C, Tschopp J, Thome M. 2002. CARMA1 is a critical lipid raft-associated regulator of TCR-induced NF-kappa B activation. *Nat Immunol* 3: 836-43
21. Rebeaud F, Hailfinger S, Thome M. 2007. Dlg1 and Carma1 MAGUK proteins contribute to signal specificity downstream of TCR activation. *Trends Immunol* 28: 196-200
22. Rincon M, Davis RJ. 2007. Choreography of MAGUKs during T cell activation. *Nature Immunology* 8: 126-7
23. Round JL, Humphries LA, Tomassian T, Mittelstadt P, Zhang M, Miceli MC. 2007. Scaffold protein Dlg1 coordinates alternative p38 kinase activation, directing T cell receptor signals toward NFAT but not NF-kappaB transcription factors. *Nat Immunol* 8: 154-61
24. Osborn O, Olefsky JM. 2012. The cellular and signaling networks linking the immune system and metabolism in disease. *Nat Med* 18: 363-74
25. Howard MA, Elias GM, Elias LA, Swat W, Nicoll RA. 2010. The role of SAP97 in synaptic glutamate receptor dynamics. *Proc Natl Acad Sci U S A* 107: 3805-10
26. Oliva C, Escobedo P, Astorga C, Molina C, Sierralta J. 2012. Role of the MAGUK protein family in synapse formation and function. *Dev Neurobiol* 72: 57-72
27. Wang D, You Y, Case SM, McAllister-Lucas LM, Wang L, DiStefano PS, Nunez G, Bertin J, Lin X. 2002. A requirement for CARMA1 in TCR-induced NF-kappa B activation. *Nat Immunol* 3: 830-5
28. Thome M. 2004. CARMA1, BCL-10 and MALT1 in lymphocyte development and activation. *Nat Rev Immunol* 4: 348-59
29. Rawlings DJ, Sommer K, Moreno-Garcia ME. 2006. The CARMA1 signalosome links the signalling machinery of adaptive and innate immunity in lymphocytes. *Nat Rev Immunol* 6: 799-812
30. Bionska M, Lin X. 2009. CARMA1-mediated NFkB and JNK activation in lymphocytes. *Immunological Reviews* 228: 199-211
31. Salvador JM, Mittelstadt PR, Guszczynski T, Copeland TD, Yamaguchi H, Appella E, Fornace AJ, Jr., Ashwell JD. 2005. Alternative p38 activation pathway mediated by T cell receptor-proximal tyrosine kinases. *Nat Immunol* 6: 390-5
32. Ashwell JD. 2006. The many paths to p38 mitogen-activated protein kinase activation in the immune system. *Nat Rev Immunol* 6: 532-40

33. Mittelstadt PR, Yamaguchi H, Appella E, Ashwell JD. 2009. T cell receptor-mediated activation of p38 α by mono-phosphorylation of the activation loop results in altered substrate specificity. *J Biol Chem* 284: 15469-74
34. Zanin-Zhorov A, Lin J, Scher J, Kumari S, Blair D, Hippen KL, Blazar BR, Abramson SB, Lafaille JJ, Dustin ML. 2012. Scaffold protein Disc large homolog 1 is required for T-cell receptor-induced activation of regulatory T-cell function. *Proc Natl Acad Sci U S A* 109: 1625-30
35. Adachi K, Davis MM. 2011. T-cell receptor ligation induces distinct signaling pathways in naive vs. antigen-experienced T cells. *Proc Natl Acad Sci U S A* 108: 1549-54
36. Brooks DG, Teyton L, Oldstone MB, McGavern DB. 2005. Intrinsic functional dysregulation of CD4 T cells occurs rapidly following persistent viral infection. *J Virol* 79: 10514-27
37. Lue RA, Brandin E, Chan EP, Branton D. 1996. Two independent domains of hDlg are sufficient for subcellular targeting: the PDZ1-2 conformational unit and an alternatively spliced domain. *J Cell Biol* 135: 1125-37
38. Round JL, Tomassian T, Zhang M, Patel V, Schoenberger SP, Miceli MC. 2005. Dlg1 coordinates actin polymerization, synaptic T cell receptor and lipid raft aggregation, and effector function in T cells. *J Exp Med* 201: 419-30
39. Burkhardt JK, Carrizosa E, Shaffer MH. 2008. The actin cytoskeleton in T cell activation. *Annu Rev Immunol* 26: 233-59
40. Humphries LA, Shaffer MH, Sacirbegovic F, Tomassian T, McMahon KA, Humbert PO, Silva O, Round JL, Takamiya K, Haganir RL, Burkhardt JK, Russell SM, Miceli MC. 2012. Characterization of in vivo Dlg1 deletion on T cell development and function. *PLoS One* 7: e45276
41. McLaughlin M, Hale R, Ellston D, Gaudet S, Lue RA, Viel A. 2002. The distribution and function of alternatively spliced insertions in hDlg. *J Biol Chem* 277: 6406-12
42. Godreau D, Vranckx R, Maguy A, Goyenville C, Hatem SN. 2003. Different isoforms of synapse-associated protein, SAP97, are expressed in the heart and have distinct effects on the voltage-gated K⁺ channel Kv1.5. *J Biol Chem* 278: 47046-52
43. Waites CL, Specht CG, Hartel K, Leal-Ortiz S, Genoux D, Li D, Drisdell RC, Jeyifous O, Cheyne JE, Green WN, Montgomery JM, Garner CC. 2009. Synaptic SAP97 isoforms regulate AMPA receptor dynamics and access to presynaptic glutamate. *J Neurosci* 29: 4332-45
44. Gardoni F, Mauceri D, Fiorentini C, Bellone C, Missale C, Cattabeni F, Di Luca M. 2003. CaMKII-dependent phosphorylation regulates SAP97/NR2A interaction. *J Biol Chem* 278: 44745-52
45. Mantovani F, Banks L. 2003. Regulation of the discs large tumor suppressor by a phosphorylation-dependent interaction with the beta-TrCP ubiquitin ligase receptor. *J Biol Chem* 278: 42477-86
46. Narayan N, Massimi P, Banks L. 2009. CDK phosphorylation of the discs large tumour suppressor controls its localisation and stability. *Journal of Cell Science* 122: 65-74

47. Wu H, Reissner C, Kuhlendahl S, Coblenz B, Reuver S, Kindler S, Gundelfinger ED, Garner CC. 2000. Intramolecular interactions regulate SAP97 binding to GKAP. *EMBO J* 19: 574-5751
48. Nakagawa T, Futai K, Lashuel HA, Lo I, Okamoto K, Walz T, Hayashi Y, Sheng M. 2004. Quaternary structure, protein dynamics, and synaptic function of SAP97 controlled by L27 domain interactions. *Neuron* 44: 453-67
49. Newman RA, Prehoda KE. 2009. Intramolecular interactions between the SRC homology 3 and guanylate kinase domains of discs large regulate its function in asymmetric cell division. *J Biol Chem* 284: 12924-32
50. Vandanapu RR, Singh AK, Mikhaylova M, Reddy PP, Kreutz MR, Sharma Y. 2009. Structural differences between the SH3-HOOK-GuK domains of SAP90/PSD-95 and SAP97. *Protein Expr Purif* 68: 201-7
51. Lue RA, Marfatia SM, Branton D, Chishti AH. 1994. Cloning and characterization of hdlg: The human homologue of the Drosophila discs large tumor suppressor binds protein 4.1. *Proc Natl Acad Sci U S A* 91: 9818-22
52. Cavatorta AL, Facciuto F, Valdano MB, Marziali F, Giri AA, Banks L, Gardiol D. 2011. Regulation of translational efficiency by different splice variants of the Disc large 1 oncosuppressor 5'-UTR. *Febs j* 278: 2596-608
53. Schluter OM, Xu W, Malenka RC. 2006. Alternative N-terminal domains of PSD-95 and SAP97 govern activity-dependent regulation of synaptic AMPA receptor function. *Neuron* 51: 99-111
54. Matsumoto R, Wang D, Blonska M, Li H, Kobayashi M, Pappu B, Chen Y, Wang D, Lin X. 2005. Phosphorylation of CARMA1 plays a critical role in T Cell receptor-mediated NF-kappaB activation. *Immunity* 23: 575-85
55. Sommer K, Guo B, Pomerantz JL, Bandaranayake AD, Moreno-Garcia ME, Ovechkina YL, Rawlings DJ. 2005. Phosphorylation of the CARMA1 linker controls NF-kappaB activation. *Immunity* 23: 561-74
56. Brenner D, Brechmann M, Rohling S, Tapernoux M, Mock T, Winter D, Lehmann WD, Kiefer F, Thome M, Krammer PH, Arnold R. 2009. Phosphorylation of CARMA1 by HPK1 is critical for NF-kappaB activation in T cells. *Proc Natl Acad Sci U S A* 106: 14508-13
57. Caruana G, Bernstein A. 2001. Craniofacial dysmorphogenesis including cleft palate in mice with an insertional mutation in the discs large gene. *Mol Cell Biol* 21: 1475-83
58. Gmyrek GB, Graham DB, Sandoval GJ, Blaufuss GS, Akilesh HM, Fujikawa K, Xavier RJ, Swat W. 2013. Polarity gene discs large homolog 1 regulates the generation of memory T cells. *Eur J Immunol* 43: 1185-94

CHAPTER TWO

Dlg1 splice variants direct CD8+ T cell function by coupling the TCR to p38-dependent pro-inflammatory cytokine production and/or WASp-dependent degranulation

ABSTRACT

Functionally diverse CD8⁺ T cells develop in response to antigenic stimulation with differing capacities to couple TCR engagement to downstream functions. However, mechanisms of diversifying TCR responsiveness are largely uncharacterized. Here we describe two alternative splice variants of scaffold protein Dlg1: Dlg1AB and Dlg1B. Dlg1AB, but not Dlg1B associates with Lck, coupling TCR stimulation to p38 activation and pro-inflammatory cytokine production. Conversely, both Dlg1AB and Dlg1B bind and activate WASp facilitating actin-mediated degranulation. Furthermore, we demonstrate that p38 activation, pro-inflammatory cytokine production and CTL killing are defective in Dlg1 knockout mice during acute viral infection. Our data support a model where Dlg1 selectively regulates TCR-triggered pro-inflammatory cytokine production and CTL killing through the expression of alternative splice variants.

INTRODUCTION

Antigen-specific CD8⁺ cytotoxic T lymphocytes (CTLs) are essential effectors against intracellular pathogens. Recognition of antigen by the T cell receptor (TCR) on a CTL induces several discrete effector functions; including the production of pro-inflammatory cytokines and lysis of infected cells through targeted release of cytotoxic granules (degranulation). Although the functionality of CTLs is often thought of as homogeneous, recent evidence suggests that a spectrum of functionally diverse CTLs are produced in response to infection (1). In fact, pro-inflammatory cytokine production and degranulation can be uncoupled in lung-resident CTLs during influenza infection depending on the concentration and presentation of the antigen. This selective functionality is hypothesized to clear virus without causing excessive tissue damage and inflammation (2). Thus, while degranulation and pro-inflammatory cytokine production are both induced through TCR recognition of antigen, it is evident that components downstream of the TCR can be selectively activated to guide these two possible functions. Identifying the mechanisms that individually regulate inflammation versus degranulation is vital to understanding how to selectively control the harmful effect of excess inflammation while maintaining the ability to kill virally infected or oncogenic cells.

Scaffold proteins have emerged as key molecular intermediates coupling extracellular receptors to intracellular signaling pathways, thus having the potential to influence functional outcomes of TCR engagement (3). Discs large homolog 1 (Dlg1), a membrane associated guanylate kinase (MAGUK) scaffold protein co-localizes with the TCR complex at the immunological synapse (IS) during T cell activation (4, 5). At the IS, Dlg1 juxtaposes tyrosine kinases Lck and ZAP70 with p38 mitogen-activated protein kinase (MAPK), facilitating a TCR-induced alternative p38 activation pathway (6). Dlg1-dependent p38 activation leads to selective activation of NFAT, but not NF κ B through S54 phosphorylation of NFATc2, and the downstream production of IFN γ (7). Additionally, Dlg1 controls antigen-induced actin polymerization, polarized TCR and lipid raft synaptic clustering, MTOC orientation and cytotoxicity in CTLs (4, 8,

9). Most recently, Dlg1 has been shown to regulate the formation and function of Treg, Thelper and memory cell subsets (10-12).

Despite the growing evidence in knockdown systems to support a role for Dlg1 in regulating T cell polarity, signaling and effector responses, recent attempts to extend these studies into Dlg1 knockout models has been largely unavailing (10). We and others have proposed that compensatory mechanisms may be responsible for the lack of functional defects seen in these models, since highly related proteins Dlg3 (SAP102) and (PSD95) Dlg4 are also expressed in T cells (10, 13). Therefore, an acute knockout of Dlg1 may overcome the issues of compensation allowing for more accurate assessment of the functional role of Dlg1 (10, 14).

Dlg1 facilitates specific signaling and cytoskeletal pathways by associating with and activating protein ligands; therefore, changes in Dlg1 structure that alter binding partners could have a significant effect on Dlg1-mediated pathways (4, 5, 7, 9, 12, 15). The core structure of Dlg1 contains: three PSD95/Dlg/ZO-1 (PDZ) domains, a Src homology 3 (SH3) domain and a guanylate kinase (GUK) domain. In addition, Dlg1 has four known areas of alternative splicing: (i) a site in the 5UTR that regulates *dlg1* translation (ii) a proline-rich region upstream of PDZ1 that can contain i1A and/or i1B proline-rich domains (iii) a region between SH3 and GUK, often referred to as the HOOK domain, that can contain exons i2, i3, i4 and/or i5 (iv) and, an N-terminal region that can contain either a CXC α palmitoylation domain or L27 β oligomerization domain (8, 16-19). Characterization of Dlg1 splice variants in epithelial, neuronal and cardiac cells demonstrates that a specific subset of the total possible variants are expressed in each cell type, and that each of these variants demonstrate differential functional capabilities (17, 19-21). However, which Dlg1 splice variants are expressed in T cells, and the role that these variants play in coordinating T cell functions has yet to be determined.

Here we demonstrate that CD8+ CTLs selectively couple TCR signals to pro-inflammatory cytokine production and/or degranulation through the expression two distinct Dlg1 splice variants. We show that two major Dlg1 protein variants are expressed in T cells: Dlg1 L27 β -i1A-i1B-i3i5 (Dlg1AB) and Dlg1-L27 β -i1B-i3i5 (Dlg1B). Moreover, we find that Dlg1AB and

Dlg1B form distinct complexes endowing them with different functional capabilities. Dlg1AB, but not Dlg1B associates with Lck and promotes the alternative p38 pathway and transcriptional activation of NFAT-dependent pro-inflammatory cytokines. In contrast, both Dlg1AB and Dlg1B facilitate lytic factor degranulation which depended on interaction of WASp with the Dlg1 SH3 domain. Dlg1 regulated WASp activation by facilitating the opening of WASp after antigen recognition. Additionally, we show that Dlg1 is required for optimal pro-inflammatory cytokine production and granule-mediated killing utilizing an acute Dlg1 knockout model in the context of acute viral infection. Taken together, our findings demonstrate that Dlg1 plays a critical role in antigen-specific pro-inflammatory cytokine production and target cell killing *in vivo*; and identifies a mechanism by which Dlg1 splice variants selectively regulate these functions through the formation of distinct signaling complexes.

RESULTS

T cells express two distinct Dlg1 protein variants due to alternative splicing

To investigate if alternative splicing of *dlg1* occurs in T cells we developed PCR primers that flanked the i1A/i1B or i2/i3/i4/i5 splicing regions (Figure 2-1). We performed RT-PCR on cDNA obtained from murine T cells including: freshly isolated CD8+ T cells, *in vitro* differentiated CTL, Th1 and Th2, and T cell hybridomas, followed by DNA sequencing of individual PCR products. Assessing the i1A/i1B region we observed two RT-PCR products in all T cells surveyed, which based on size and sequencing, were found to be the i1B and i1Ai1B exon combinations. All T cells surveyed also expressed the i3i5 and i2i5 splice combinations. Similar results were also seen in non-T cells (Figures 2-1 & 2-2). All T cells expressed L27 β (Figure 2-1), CXCA was not assessed in this study. Based on these findings, at least four possible *dlg1* transcripts are expressed in T cells, with differences in the inclusion of i1A and the inclusion of i3 or i2 (Figure 2-1).

To explore which *dlg1* variants were expressed on the protein level, each of the four splice variants sequences were over expressed in T cells. The migration distances of Dlg1 in resulting cells were compared to endogenous Dlg1 that runs as a protein doublet at 130kDa and 120kDa.

The 130kDa band best corresponded with Dlg1 L27 β -i1Ai1B-i3i5 or Dlg1 L27 β -i1Ai1B-i2i5, and the 120kDa band best corresponded with Dlg1 L27 β -i1B-i3i5 (Figure 2-1).

To determine which of the Dlg1 splice variants were endogenously expressed, we selectively targeted the L27 β , i1A, i1B or i3 exons for knockdown. We were unable to target the i2 exon as it was only 36bp. Targeting the L27 β , i1B or i3 exons ablated expression of both Dlg1 bands, indicating that the majority of Dlg1 protein variants expressed in T cells contained these exons. When i1A was targeted a selective loss of the 130kDa Dlg1 protein variant was observed, indicating that the 130kDa Dlg1 variant contained i1A, while the 120kDa Dlg1 variant did not (Figure 2-1). Similar results were observed in 3T3 fibroblasts (Figure 2-2). These data demonstrated that at least two protein variants of Dlg1, which migrate as distinct bands on SDS PAGE, are expressed in T cells due to alternative splicing: Dlg1-L27 β -i1Ai1B-i3i5 (Dlg1AB) and Dlg1-L27 β -i1B-i3i5 (Dlg1B) (Figure 2-1).

Dlg1AB associates with Lck and facilitates alternative p38 activation

Dlg1AB differs from Dlg1B by the presence of the proline-rich i1A domain. The i1A domain is predicted to form two polyproline helical domains, one within the i1A domain and one at the junction between i1A and i1B, that may facilitate interaction with SH3-containing proteins (18). Previous studies demonstrate that Lck interacts with the N-terminal region of Dlg1 via its SH3 domain (4, 22). Thus, to determine if the i1A-domain was required for Lck association we performed pulldown assays with GST-tagged Dlg1AB or Dlg1B. We found that only Dlg1AB could pulldown Lck, while both proteins could pulldown the PDZ binding protein p38 (Figure 2-3).

Lck is required for TCR-induced p38 activation leading to NFAT-dependent transcription (7, 23). Thus, we hypothesized that Dlg1 splice variants may differentially regulate the alternative p38 pathway. To assess the role of Dlg1 splice variants in p38 activation, we utilized a selective knockdown strategy to diminish Dlg1AB expression (using miR i1A) or total Dlg1 expression (using miR i1B) in CD8⁺ CTLs (Figure 2-3). When stimulated through the TCR there

was a significant decrease in total cellular p-p38 in both total and Dlg1AB-specific knockdown cells compared to control. Moreover, cells expressing only Dlg1B (miR i1A) were not significantly different from cells expressing no Dlg1 (miR i1B) (Figure 2-3). To further examine this finding, we generated stable *dlg1* knockdown T cells by targeting the 3UTR of *dlg1*, allowing subsequent re-expression of Dlg1AB or Dlg1B (Figure 2-4). When Dlg1 complexes were isolated from these cells, we found both variants were able to associate with p38; however, only Dlg1AB was able to facilitate TCR-induced p38 phosphorylation (Figure 2-3). Collectively, our results show that Dlg1AB orchestrates alternative p38 activation through association with Lck.

Dlg1 splice variants independently regulate TCR-induced pro-inflammatory cytokine production and cytokine/lytic factor release

We and others have demonstrated that alternative p38 activation leads to induction of NFAT-dependent transcription of IFN γ (7, 12). To assess the role of p38 and Dlg1 splice variants in coordinating NFAT activation we over expressed Dlg1AB or Dlg1B in CD8⁺ CTLs. We found that Dlg1AB, but not Dlg1B, enhanced TCR-induced expression of the NFAT-dependent gene NFATc1. The enhanced NFATc1 gene expression was p38-dependent, and selective as the NF κ B-dependent gene I κ B α was not affected (Figure 2-5).

The ability to selectively channel proximal TCR signals to p38 and NFAT has the potential to specify downstream function in CD8⁺ T cells. We therefore examined the impact of splice variant expression on TCR-induced IFN γ , TNF α , IL-2 and granzyme B gene expression. Expression of IFN γ and TNF α were significantly increased in cells over expressing Dlg1AB, but not Dlg1B; while neither Dlg1AB nor Dlg1B enhanced IL-2 or granzyme B gene expression (Figures 2-4 & 2-5). Furthermore, inhibition of p38 activity blocked the enhanced IFN γ gene expression seen with Dlg1AB over expression (Figure 2-4). To further explore splice variant contributions to TCR-triggered function, we performed splice variant specific knockdown in CD8⁺ CTLs. Loss of Dlg1AB (using miR i1A) reduced TCR-induced IFN γ and TNF α gene expression to levels equivalent to total Dlg1 knockdown, while not affecting IL-2 or granzyme B

gene expression (Figure 2-6). Accordingly, intracellular cytokine analysis demonstrated that total Dlg1 knockdown prevented optimal IFN γ production, but did not affect intracellular IL-2 protein production in response to anti-CD3/anti-CD28 or antigen at several antigen concentrations (Figure 2-7). Together, these results show that Dlg1AB channels TCR-dependent signals toward p38-dependent pro-inflammatory cytokine gene expression, while Dlg1B does not.

We previously reported that Dlg1 knockdown impairs the amount of IL-2 secretion and CTL killing activity (4). To determine the role of Dlg1 splice variants in controlling release of cytokines and lytic factors we examined the impact of select and total Dlg1 knockdown on TCR-triggered accumulation of cytokines and granzyme B in culture supernatants. Dlg1AB knockdown yielded a decrease in IFN γ and TNF α secretion, but not IL-2 or granzyme B. However, knockdown of both Dlg1AB and Dlg1B led to a further drop in IFN γ and TNF α compared to Dlg1AB knockdown alone, and a significant decrease in IL-2 and granzyme B secretion (Figure 2-6). Together our data support a model where Dlg1AB is required for expression of pro-inflammatory cytokines, while both Dlg1 variants regulate a common secretion pathway utilized by both cytokines and lytic factors.

Dlg1AB and Dlg1B support TCR-triggered p38-independent, actin-dependent degranulation

T cell receptor engagement on CD8⁺ CTLs induces actin-dependent polarized release of granzyme B containing granules to effect contact-dependent killing (24). To explore Dlg1 regulation of CTL degranulation, we examined the consequences of Dlg1 variant expression and pharmacologic inhibition in T cells in which endogenous Dlg1 had been knocked down and selectively replaced with Dlg1AB or Dlg1B (Figures 2-4 & 2-8). We found that re-expression of either Dlg1AB or Dlg1B rescued and enhanced antigen-induced degranulation, measured by exposure of CD107a on the T cell surface (Figure 2-8). Pretreatment with varying concentrations of p38 inhibitor SB203580 had no effect on degranulation (Figure 2-7). Similar results were observed in primary OT-1 CTLs, as p38 inhibition did not greatly affect degranulation or granzyme B secretion (Figure 2-8). In contrast, pretreatment with actin inhibitor

cytochalasin D prevented degranulation, indicating that polymerization of actin, but not p38, was required for degranulation (Figure 2-8).

We next examined the effects of total versus select Dlg1AB knockdown on TCR-induced actin polymerization in CD8+ CTLs. While total Dlg1 knockdown impaired TCR-triggered actin polymerization, selective Dlg1AB knockdown had no effect; suggesting that actin polymerization, like degranulation, is p38-independent and can be facilitated by either splice variant (Figure 2-8). Accordingly, pretreatment of CTLs with SB203580 had no effect on antigen-induced actin polymerization (Figure 2-8). Taken together these findings elucidate a p38-independent, actin-dependent pathway whereby both Dlg1 variants can promote actin reorganization events guiding CTL granule release.

Dlg1 controls WASp activation to promote degranulation

To investigate the molecular basis of Dlg1-mediated actin polymerization and degranulation we generated T cells that selectively expressed Dlg1B variants or truncations thereof to test their ability to promote degranulation, as several cytoskeletal effectors are known to associate with the C-terminal half of Dlg1 (7, 8, 25) (Figure 2-9). Total Dlg1 knockdown impaired degranulation; re-expression of full length Dlg1B variants containing either i2 or i3, or truncated Dlg1B proteins lacking the GUK or HOOK domains rescued and enhanced degranulation to higher levels than observed in cells expressing endogenous Dlg1. Conversely, expression of truncated Dlg1 proteins lacking the SH3 domain (SH3, PDZ3, PDZ2) were unable to rescue the effects of Dlg1 knockdown on degranulation despite being expressed to similar levels (Figures 2-9 & 2-10).

We previously showed that the Dlg1 SH3 domain could bind WASp, an actin regulator known to promote F-actin polymerization and granule release in murine T cells (7, 26). Knockdown of WASp with two different target sequences dramatically reduced antigen-induced degranulation in T cells (Figure 2-10). Furthermore, re-expression of Dlg1 variants in Dlg1/

WASp double knockdown cells was unable to rescue antigen-induced degranulation, suggesting that WASp was required for Dlg1-mediated degranulation (Figures 2-9 & 2-10).

WASp is held in an auto-inhibited “closed” state by intra- or intermolecular interactions between the VCA and GBD domains (27). Disruption of the VCA-GBD interaction results in “opening” and activation of WASp. We hypothesized that Dlg1 may open WASp by binding its proline-rich domain, like other SH3-containing proteins (27). To test this hypothesis we utilized a conformation-specific antibody which recognizes the open conformation of activated WASp (28). Total Dlg1 knockdown led to a decrease in the number of cells with “open” WASp after antigen recognition, while not affecting total WASp protein levels (Figures 2-10). Together these data identify Dlg1 association with and activation of WASp as a novel regulatory mechanism for TCR-triggered, Dlg1-mediated actin polymerization and degranulation.

Acute Dlg1 knockout diminishes p38 activation, cytokine production and target cell killing in response to acute viral infection

We and others have demonstrated that Dlg1 plays a vital role in T cell development, activation and effector responses utilizing knockdown methods *in vitro* (4, 7, 9, 10, 12, 29). However, attempts to extend these studies into Dlg1 knockout systems did not yield striking functional differences possibly due to compensation of other Dlg family members (10, 29). In order to demonstrate a role for Dlg1 during the context of an acute viral infection, we developed an acute Dlg1 knockout mouse model where Dlg1^{fl/fl} ER-Cre mice are injected with tamoxifen to knockout Dlg1 (30). Using this system we achieved complete genomic recombination and loss of Dlg1 protein (Figures 2-11). After Dlg1 knockout, mice were infected with LCMV Armstrong and CD8+ T cell function assessed. Dlg1 knockout (Dlg1^{KO}) mice had fewer CD8+p-p38+ cells and lower p-p38 mean fluorescence intensity (gMFI) in the CD8+ population compared to wild type (Dlg1^{WT}) (Figure 2-11). While there was no difference in granzyme B production, the Dlg1^{KO} mice had a significant a defect in CTL killing activity of CD8+ splenocytes measured by CD107a staining and direct lysis of GP33-pulsed target cells (Figures 2-11). We did not observe a

change in proliferative capacity of the CD8+ or the CD8+GP33+ populations in the spleen or liver of Dlg1^{KO} mice (Figure 2-11). However, there was a significant decrease in the absolute number of CD8+ and CD8+GP33+ cells in the liver in Dlg1^{KO} (Figures 2-11). Finally, there was a significant defect in the antigen-specific production of pro-inflammatory cytokines in CD8+ T cells from the liver (Figures 2-11). Together, these results are the first evidence that Dlg1 knockout results defects in CD8+ T cell function *in vivo*, and provides context for our Dlg1 splice variant findings.

DISCUSSION

Our results identify the expression of Dlg1 splice variants as a previously unrecognized mechanism by which CD8+ T cells selectively regulate functionality downstream of the TCR. Our work identifies two discrete TCR signaling pathways regulated by Dlg1 in CD8+ T cells: Dlg1- and p38-mediated up regulation of pro-inflammatory cytokine gene expression and Dlg1- and WASp-mediated degranulation and CTL killing. Further we show that these pathways are individually regulated by two Dlg1 splice variants: Dlg1AB and Dlg1B. Dlg1AB uniquely binds Lck and orchestrates alternative p38 activation and pro-inflammatory cytokine production; while both Dlg1AB and Dlg1B can bind and activate WASp to facilitate actin-mediated CTL granule release. In a Dlg1 knockout model CTL responses are impaired, with decreased p38 activation, IFN γ /TNF α production and CTL killing in response to acute viral infection; lending context to our splice variant discoveries. Future studies in mouse models expressing a single variant of Dlg1 will provide a more comprehensive understanding of the role of inflammation versus CTL killing in the context of viral infection, cancer and autoimmunity.

Polarity proteins and cytoskeletal regulators have been hypothesized to work cooperatively to control lytic factor degranulation and cytotoxicity in CD8+ T lymphocytes (31). Dlg1, a member of the Scribble polarity network, and cytoskeletal regulator WASp are both required for optimal contact-dependent cytotoxicity (4, 32). Furthermore, both control key processes required for lytic factor degranulation including lytic synapse formation/reformation,

actin polymerization, and MTOC dynamics (4, 9, 33-35). In this study we discovered a molecular link between Dlg1 and WASp that promotes p38-independent TCR-triggered degranulation requiring both WASp and Dlg1 SH3. We propose that Dlg1 SH3 associates with the proline-rich domain of WASp, to disrupt WASp VCA-GBD interactions; allowing WASp-dependent actin polymerization, CTL synapse formation/reformation, granule polarization and release of lytic factors. Dlg1 may additionally oligomerize, cluster and/or localize WASp; aggregating lipid rafts and TCRs at the immunological synapse (36, 37).

TCR-induced cytokine production is regulated by a complex network of transcription factors and feedback mechanisms (38). Here we demonstrate that Dlg1AB selectively induces transcription of IFN γ and TNF α , but not IL-2 or granzyme B through activation of p38 and NFAT. This is in keeping with reports that granzyme B gene expression is regulated by NF κ B activation (39). While NFATc2 is known to regulate IFN γ , TNF α , and IL-2 gene expression, only TCR-induced IFN γ and TNF α expression were selectively impacted by Dlg1 knockdown. One possible explanation is that NFATc1 compensates for NFATc2 in Dlg1-deficient cells to enable TCR triggered IL-2 production. Dlg1 regulates NFATc2 through p38-dependent phosphorylation of S54. Since NFATc1 lacks a phosphorylatable serine residue in its trans-activation domain, we predict it would not be affected by Dlg1AB knockdown. This suggestion is consistent with published findings demonstrating that NFATc1 and NFATc2 have redundant abilities to induce IL-2, but not TNF α (40-42).

CD8⁺ T lymphocytes that develop in response to antigen exposure show a broad range of functionality, with differing capacities to produce and secrete unique combinations of cytokines and cytotoxic effectors in response to TCR triggering (1). Specific pathogens evoke different constellations of functionally distinct subsets, a phenomenon proposed to customize optimal T cell responsiveness for eradicating a given pathogen while limiting damage to surrounding tissues (2). We propose that changes in Dlg1 splice variant expression in CD8⁺ T cells can fine-tune CTL functionality. Indeed, it has been reported that the Dlg1 i1A exon is within the top 1-2% of exons excluded from mRNA transcripts in human T cells following activation (43). Exclusion

of the i1A exon would lead to decreased Dlg1AB and increased Dlg1B. Our data support a model where these cells would maintain the ability to lyse target cells and release cytokines while specifically dampening the production of potentially harmful pro-inflammatory cytokines.

In addition to its role in CD8⁺ CTLs, Dlg1 also regulates the development and function of CD4⁺ T cells; selectively promoting Th1 and Treg function, while impairing Th2 function (7, 10, 12, 44). Here we demonstrate that *dlg1AB*, *B*, and *i2i5*, *i3i5* exon combinations are expressed in Th1 and Th2 cells. While both alternative p38 activation and WASp activation have similarly been implicated in Th1/Th2 skewing, which Dlg1 splice variants and Dlg1-guided processes are responsible for specifying TCR triggered functionality in CD4⁺ cells has yet to be elucidated (10, 12, 44, 45). We hypothesize that involvement of TCR signaling scaffolds, including Dlg1 splice variants, play a major role in diversifying and specifying T cell responsiveness. Future studies aimed at understanding Dlg1 activity in diverse CD8⁺ and other T cell subpopulations will test this hypothesis. Through understanding the detailed molecular mechanisms involved in specifying TCR signaling and functionality, we hope to elucidate pathways that can serve as discrete targets for therapeutic intervention and aid in our basic understanding of the regulation of functional output during T cell development and activation.

METHODS

Mice and Dlg1 Knockout

OT-1 TCR transgenic mice (46). The generation of Dlg1^{flox/flox} mice, which have loxP sites flanking the *dlg1* exon encoding a portion of PDZ1 and PDZ2 have been previously described (30). These mice were crossed with ER-Cre transgenic mice (Jackson Lab) and offspring (ER-Cre Dlg1^{flox/+}) were crossed with Dlg1^{flox/flox} mice to generate ER-Cre Dlg1^{flox/flox} mice. For knockout, 6-to-8 week old mice were injected IP with 2mg tamoxifen or mock solution (ethanol and sunflower seed oil) per day for 5 consecutive days. Mice were then used 14-21 days later. All mice were maintained and used in accordance with the University of California Los Angeles Chancellor's Animal Research Committee.

Cell Culture

Spleen and lymph node cells were obtained from 8- to 14-week old OT-1 mice. CD8⁺ cells were sorted using CD8a Ly-2 microbeads (Miltenyi 130-049-401) and stimulated in vitro with plate-bound anti-CD3/anti-CD28 or MEF.B7.OVA antigen presenting cells for 48-72 hrs in complete media composed of RPMI 1640 medium with 10% FCS, sodium pyruvate, 50nM β -meraptoethanol, penicillin, streptomycin and glutamine followed by expansion in rIL-2 (100 units/mL) for an additional 3-4 days to generate primary mouse CTLs. BI-141 murine T cell hybridoma cells were maintained in complete media. OT-1 hybridoma T cells were maintained as in (7). MEF.B7.OVA cells stably expressing H-2K^b, B7.1, and OVA₂₅₇₋₂₆₄ were maintained as in (4). H-2K^b EG.7 cells constitutively expressing OVA₂₅₇₋₂₆₄ and EL-4 cells were maintained in as in (47).

Retrovirus Production and Infections

293T cells were transfected with pCL-Eco and either knockdown or overexpression constructs using TransIT 293 (Mirus 2705) per manufacturer's instructions. After 48 hrs, viral supernatant was harvested, 0.45 μ m filtered and used to infect activated primary OT-1 cells or T cell-lines via spin infection in the presence of polybrene (8 μ g/mL) at 1250g for 90 mins at room temperature. For primary cell infections, T cells were infected after 48-72 hrs of stimulation with anti-CD3/anti-CD28. Two spin-infections were performed on cells 24 hrs apart. Infected primary T cells were used for functional assays 24-48 hrs after the last spin-infection.

RT-PCR and qPCR

T cells were stimulated with platebound anti-CD3 (2 μ g/mL) and anti-CD28 (2 μ g/mL) antibodies or left unstimulated. RNA was isolated and reverse-transcribed as in (7). For RT-PCR, 2.0 μ L of cDNA was used for PCR amplification with annealing temperatures of 62°C and 58°C for the i1A/i1B and i2/i3 primer sets respectfully. qPCR analysis was performed using Sybreen as in (7). Primers used for RT-PCR and qPCR analysis can be found in Table S2.

GST-pulldowns, Immunoprecipitations and Immunoblotting

Stimulated OT-1 hybridoma lysates for IPs and pulldowns were generated by incubating 4×10^7 cells with anti-CD3 and anti-CD28 followed by antibody crosslinking using donkey anti-hamster secondary for 15 mins at 37°C. Cells were lysed in the presence of protease and phosphatase inhibitors and cleared by centrifugation. For GST pulldown assays, lysates from stimulated or unstimulated OT-1 hybridoma cells were incubated for 2 hrs at 4°C with purified GST-alone or GST-Dlg1 fusion proteins. GST-precipitates were washed and then run on SDS-PAGE. IPs were performed as published (7). Proteins were separated by SDS-PAGE and transferred to nitrocellulose. Membranes, blocked with TBS plus 5% milk and 0.1% Tween-20, were incubated with primary antibodies (1:1000) overnight at 4°C, followed by incubation with HRP-conjugated secondary antibodies (1:5000) for either 4 hrs (Dlg1 blots) or 1 hr (all others) at room temperature. Signals were detected by chemiluminescence reagents (Western Lightening *Plus-ECL*; Pierce NEL104001EA).

ELISA

To detect protein expression of IFN γ , TNF α , IL-2, and Granzyme B in supernatants ELISAs were performed with Ready-Set-Go kits from eBioscience (88-7334, 88-7324, 88-7024, 88-8022) according to the manufacturer's instructions

Intracellular Cytokines

Primary mouse OT-1 CTLs were re-stimulated with either platebound anti-CD3 (2 μ g/mL) and anti-CD28 (2 μ g/mL) antibodies, EG.7 cells, or EL-4 cells pulsed with various concentrations of OVA₂₅₇₋₂₆₄ peptide for 4 hrs in the presence of GolgiPLUG (BD 555029). Cells were surface stained with CD8b-PE in FACS wash buffer (PBS + 3% FCS + 0.1% sodium azide) prior to overnight fixation and permeabilization with BD Cytofix/Cytoperm (BD 51-2090KZ) at 4°C. Cells were then washed in BD Permeabilization wash solution, stained for 30 mins with IFN γ -APC or IL-2-APC, washed and data collected using a BD FACS-Calibur.

Intracellular p-p38

For intracellular phospho-p38 analysis, T cells were stimulated with plate-bound anti-CD3 (5µg/mL) and anti-CD28 (20µg/mL) by quickly spin-contacting the cells to plates. After the stimulation, cells were immediately fixed in 4% PFA for 15 mins on ice. Cells were then harvested, washed with FACS buffer and permeabilized with ice cold methanol overnight at 4°C. Cells were then stained with Alexa Fluor647 Mouse anti-p38 MAPK (pT180/pY182) for 30 mins at room temperature, washed and immediately analyzed using a BD FACS-Calibur.

Degranulation

Primary mouse OT-1 CTLs or OT-1 hybridoma T cells and EL-4 cells pulsed with OVA₂₅₇₋₂₆₄ or EG.7 target cells were co-cultured (1:1) in 200µL media in 96-well U-bottom plates at 37°C for 3-4 hrs, in the presence of 1.0µL CD107a-APC, 1.0µL GolgiPLUG and 1.0µL GolgiSTOP. Cells were harvested, surface stained with CD8b-PE in FACS buffer, washed, fixed in 2% PFA and then analyzed using a BD FACS-Calibur

Actin Polymerization

Primary mouse OT-1 CTLs were spun onto adherent MEF.B7.OVA cells in 12-well plates and placed in an incubator for 15 mins. Cells were placed on ice and ice cold PBS was added. Cells were quickly harvested, spun down and resuspended in 200µL of BD Cytotfix/Cytoperm (BD Bioscience) for overnight fixation and permeabilization at 4°C. Cells were then washed in BD Permeabilization wash solution, stained for 1 hr with Alexa Fluor 647 phalloidin (0.3 units) and CD8b-PE (1:200) in 200µL BD Permeabilization wash solution, washed and fixed in 2% PFA. Data was collected using a BD FACS-Calibur.

Conformational Opening of WASp

OT-1 hybridoma T cells were stimulated with EG.7 cells (1:1) for 30 mins and then immediately fixed in 4% PFA on ice for 15 mins. Cells were then washed and surface stained with CD8b-PE. Cells were then permeabilized with the BD Cytofix/Cytoperm, washed and stained for 45 minutes at 4°C with anti-WASp 26E6 (1:200). Cells were washed, stained for 30 minutes at 4°C with Alexa Fluor647 AffiniPure F(ab)₂ Donkey Anti-Mouse IgG (1:1000). Cells were then washed, re-suspended in 2% PFA and analyzed with a BD FACS-Caliber.

LCMV Infection, Tissue Processing and Stimulation

Mice were infected with 2×10^4 plaque forming units of LCMV-Armstrong IP. Spleen and liver were processed as published (48). T cell stimulations were performed with LCMV-GP₃₃₋₄₁ peptide as published (49). LDH assay was performed with EL-4 cells pulsed with LCMV-GP₃₃₋₄₁ peptide at 5µg/ml for 2 hrs. Splenocytes from LCMV-infected mice were incubated with pulsed target cells at varying ratios for 4 hrs. Cytotoxicity was assessed using the CytoTox 96 assay (Promega G1780) according to manufacturer's instructions.

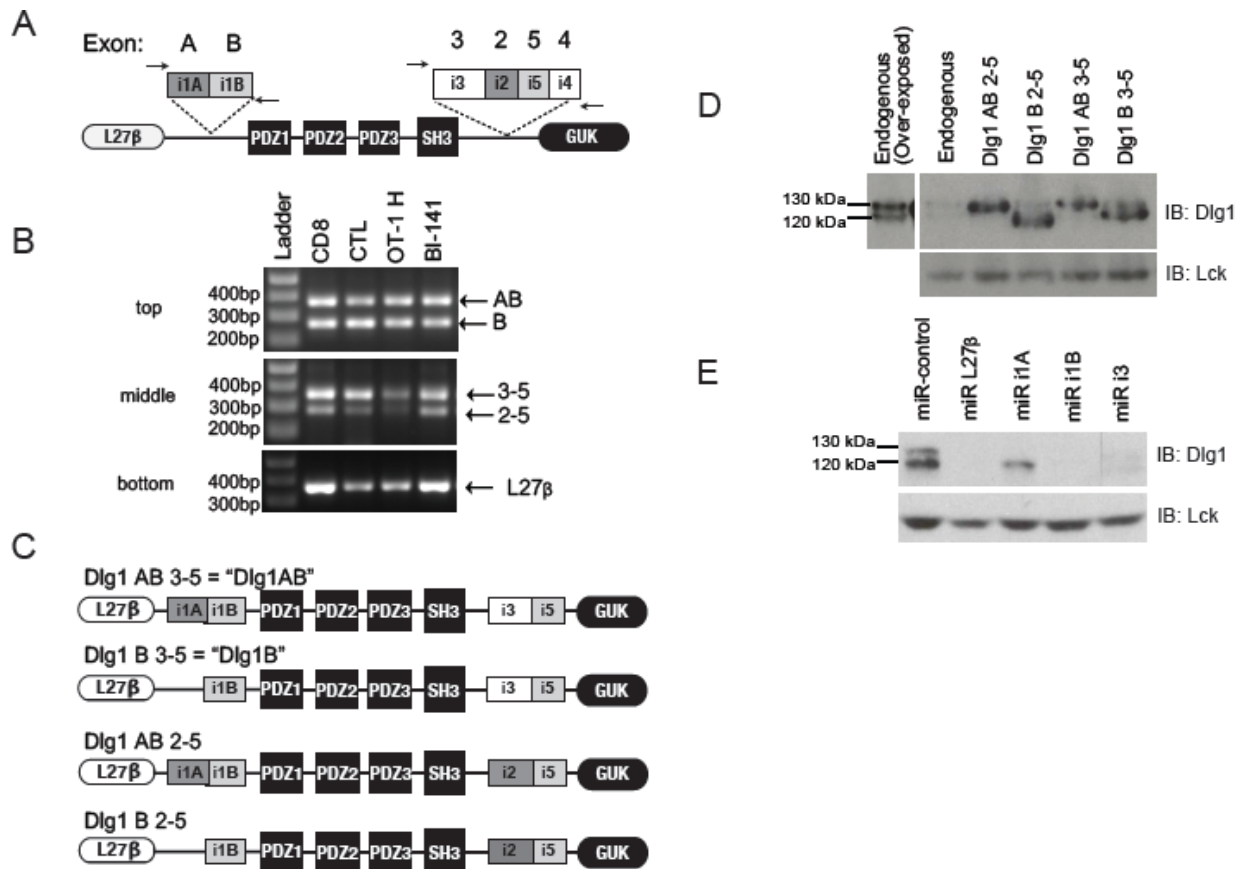


Figure 2-1: T lymphocytes express two Dlg1 protein variants due to alternative splicing: Dlg1AB and Dlg1B. (A) Schematic of the analyzed areas of splicing in *dlg1*. (B) RT-PCR of cDNA from different murine T cells (CD8 = purified unstimulated primary OT-1 CD8+ T cells; CTL = purified OT-1 CD8+ T cell stimulated *ex vivo* with CD3/CD28 and expanded in rIL-2; OT-1H = CD8+ OT-1 hybridoma T cell line; BI-141 T hybridoma cell) using primers that flank the i1A/i1B (top) or i2/i3/i4/i5 (middle) splice region. Primers that lie within L27β were also used (bottom). (C) Schematic of four possible *dlg1* transcripts expressed in T cells. (D) BI-141 T cells infected with viruses encoding different Dlg1 splice variants were analyzed via western blotting for Dlg1 expression; Lck was used as a loading control. (E) BI-141 T cells infected with knockdown viruses targeting L27β, i1A, i1B or i3 were analyzed via western blotting for Dlg1; Lck was used as a loading control.

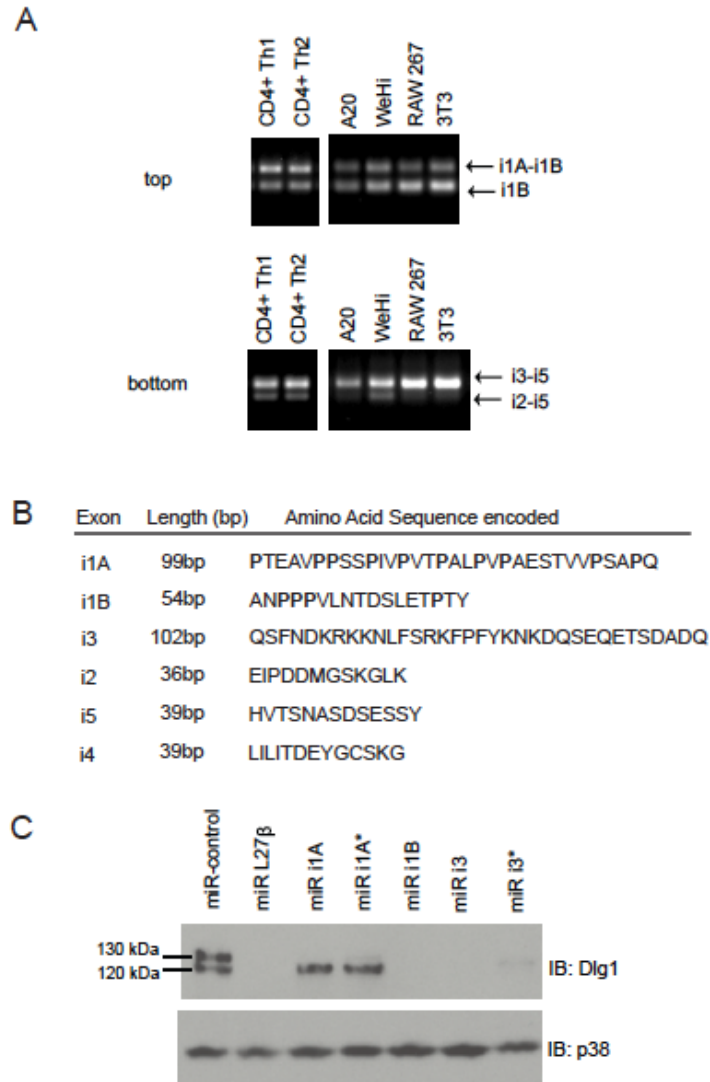


Figure 2-2: Dlg1 alternative splice variants expressed by hematopoietic and non-hematopoietic cells. (A) RT-PCR of cDNA from different murine hematopoietic and non-hematopoietic cells (CD4⁺ Th1 skewed cells, CD4⁺ Th2 skewed cells, A20 B cell line, WeHi B cell line; RAW267 macrophage cell line; 3T3 fibroblasts) using primers that flanks the i1A/i1B (top) and i2/i3/i4/i5 (bottom) splicing regions. (B) Nucleotide lengths of alternatively splice *dlg1* exons and encoded amino acid sequences. (C) 3T3 fibroblasts infected with miR-based knockdown viruses targeting specific regions of Dlg1 and analyzed for Dlg1 protein expression via immunoblotting; p38 was used as a loading control.

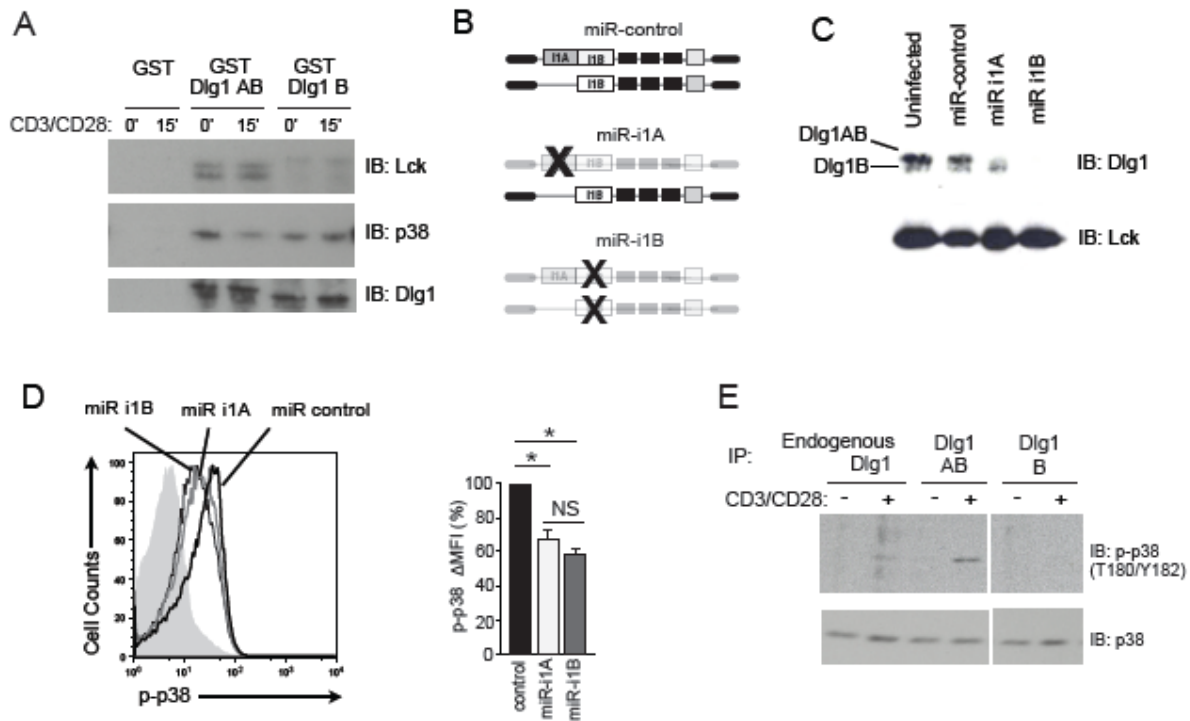


Figure 2-3: Dlg1AB selectively binds Lck and supports p38 phosphorylation while Dlg1B does not. (A) GST-tagged Dlg1AB and Dlg1B or GST-alone were incubated with protein lysate from unstimulated (0') or stimulated (15' mins) T cells. Associated Lck and p38 were identified by immunoblot. (B) Schematic representation of Dlg1 variants targeted for knockdown using miR-based knockdown viruses. (C-D) Purified primary OT-1 CD8⁺ T cells were stimulated with anti-CD3/anti-CD28 followed by infection with miR-based viruses. (C) SDS-PAGE of cell lysates assessing Dlg1 knockdown (D) Cells were re-stimulated with anti-CD3/anti-CD28 for 30 mins and stained for p-p38 (T180/Y182). CD8⁺GFP⁺ cells were gated and histograms of phosphorylated p38 are shown. The percentage of p38 phosphorylation relative to miR-control is quantified as Δ MFI (%), where Δ MFI = stimulated MFI - unstimulated MFI, and where miR-control is set to 100%. Error bars represent SD of means from three independent experiments. * $p < 0.05$. (E) OT-1 hybridoma T cells expressing endogenous Dlg1 or selectively re-expressing Dlg1AB or Dlg1B were left unstimulated (-) or stimulated with anti-CD3/anti-CD28 (+) for 15 mins, followed by immunoprecipitation with anti-Dlg1 and assessed for bound p38 T180/Y182 phosphorylation. Data is representative of three independent experiments.

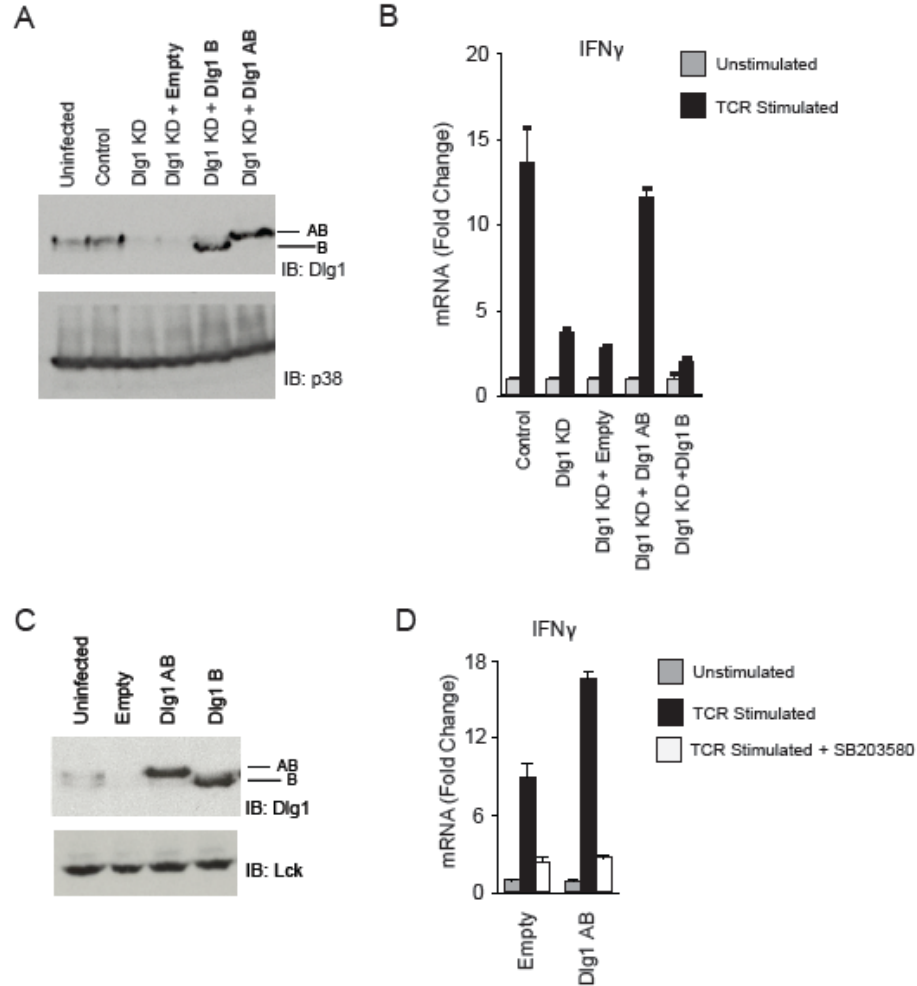


Figure 2-4: Selective expression of Dlg1AB, but not Dlg1B promotes p38-dependent transcription of IFN γ . (A-B) OT-1 hybridoma T cells were infected with the indicated Dlg1 re-expression (bold) and/or Dlg1 knockdown (KD) viruses. The Dlg1 knockdown (Dlg1 KD) construct targets the 3'UTR of *dlg1* allowing for re-expression of specific Dlg1 splice variants. (A) Cells were analyzed via protein immunoblotting for Dlg1; p38 was used as a loading control. (B) Cells were stimulated with anti-CD3/anti-CD28 or left unstimulated. RNA was isolated for qPCR analysis. mRNA was normalized to L32 and fold-increase in mRNA expression vs. unstimulated samples is shown. Error bars represent SD of samples analyzed in triplicate. Data are representative of at least three independent experiments. (C-D) BI-141 hybridoma T cells were infected with Dlg1-viruses to over express Dlg1 splice variants. (C) Cells were analyzed via protein immunoblotting for Dlg1; Lck was used as a loading control. (D) Cells were pretreated with 10 μ M SB203580 or carrier (DMSO) for 30 minutes. Cells were stimulated with anti-CD3/anti-CD28 for 2hrs or left unstimulated. RNA was isolated for qPCR analysis.

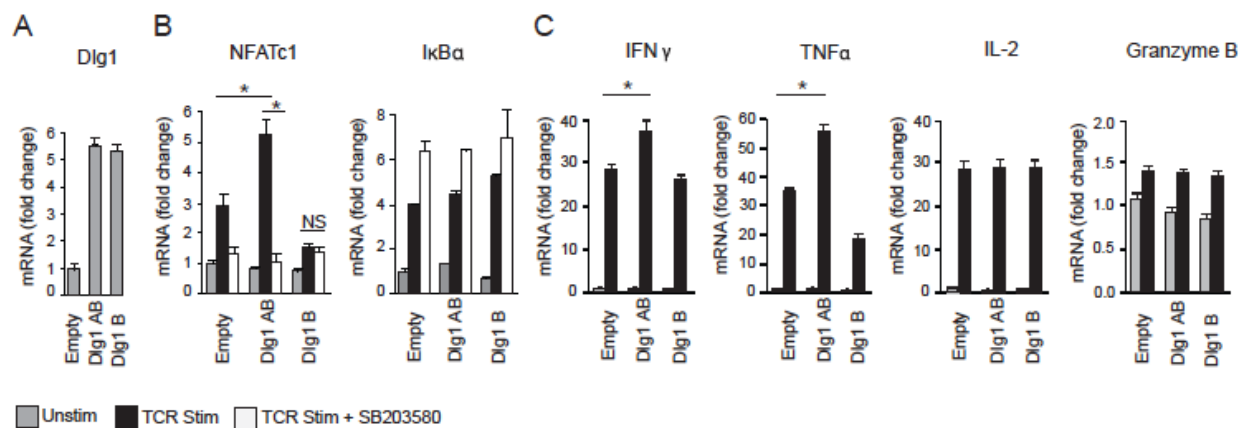


Figure 2-5: Dlg1AB over expression selectively enhances NFAT-dependent transcription of IFN γ and TNF α but not IL-2 or granzyme B, while Dlg1B does not. (A-C) Purified primary OT-1 CD8⁺ T cells were stimulated with anti-CD3/anti-CD28 followed by infection with control (Empty) or Dlg1-viruses. (A) Cells were isolated and assessed for Dlg1 over expression via qPCR. (B-C) Cells were re-stimulated with anti-CD3/anti-CD28 or left unstimulated in the presence or absence of 10 μ M p38 inhibitor (SB203580). RNA was isolated for qPCR analysis. mRNA was normalized to L32 and fold-increase in mRNA expression vs. unstimulated samples is shown. Error bars represent SD of samples analyzed in triplicate. * p < 0.05. Data are representative of three independent experiments.

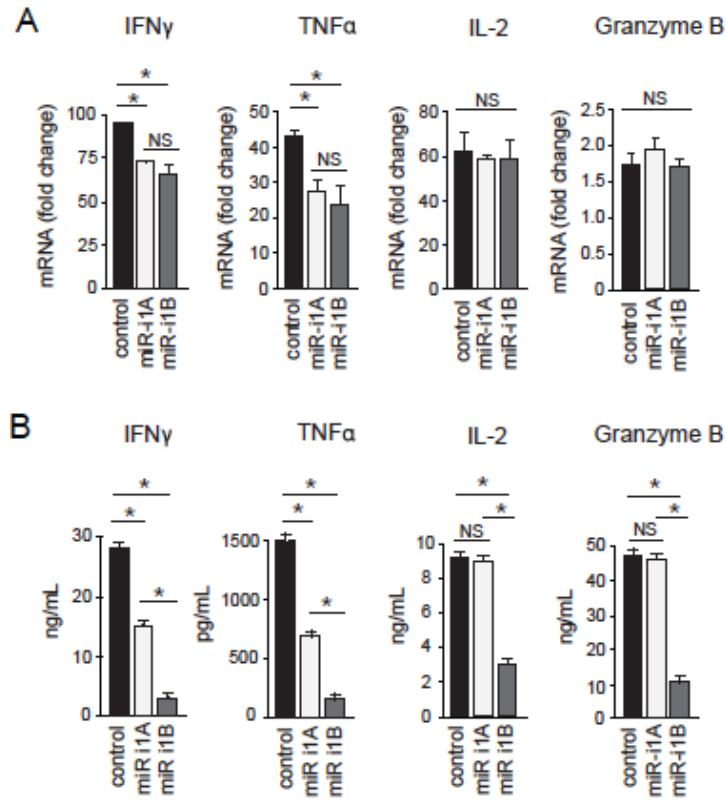


Figure 2-6: Dlg1AB knockdown diminishes transcription of IFN γ and TNF α , but not IL-2 or granzyme B; while total Dlg1 knockdown additionally impairs cytokine and granzyme B secretion. (A-B) Purified primary OT-1 CD8⁺ T cells were stimulated with anti-CD3/anti-CD28, followed by infection with miR-based viruses. (A) Cells were re-stimulated with anti-CD3/anti-CD28 for 4 hrs or left unstimulated. RNA was isolated for qPCR analysis. mRNA was normalized to L32 and the fold-increase in mRNA expression vs. unstimulated samples is shown. (B) Cells were re-stimulated with anti-CD3/anti-CD28 for 48 hrs and supernatants collected for ELISA analysis. Error bars represent SD of samples analyzed in triplicate. * $p < 0.05$. Data are representative of three independent experiments.

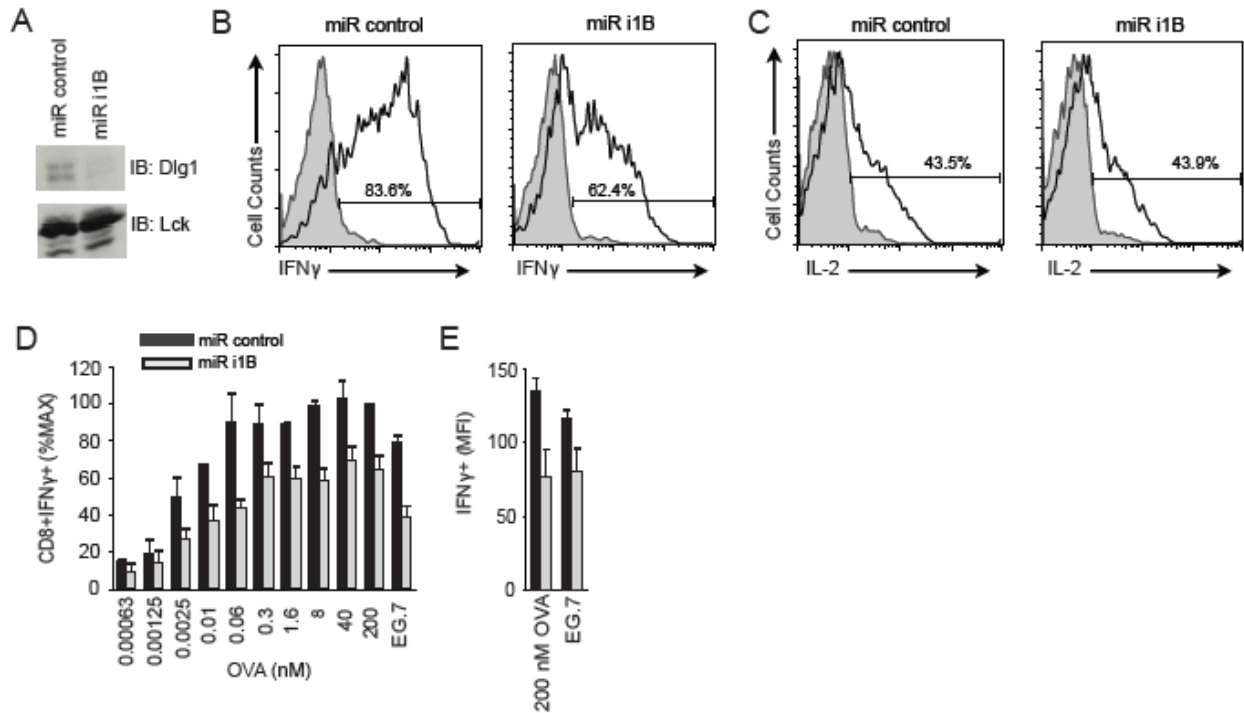


Figure 2-7: Dlg1 knockdown prevents optimal intracellular IFN γ production over a range of antigen-concentrations. (A-E) Purified primary OT-1 CD8 $^+$ T cells were stimulated with anti-CD3/anti-CD28 for 48 hrs, followed by infection with miR-based knockdown viruses. (A) Cells were analyzed via protein immunoblotting for Dlg1 knockdown; Lck was used as a loading control. (B-C) Cells were re-stimulated with anti-CD3/anti-CD28 for 4 hrs (black line) or left unstimulated (filled histogram) in the presence of GolgiPLUG and assessed for intracellular cytokines. (D-E) Cells were re-stimulated with EG.7 cells or EL-4 cells pulsed with various concentrations of OVA₂₅₇₋₂₆₄ peptide for 4 hrs in the presence of GolgiPLUG and assessed for intracellular cytokines. (D) CD8+IFN γ + (%MAX) was measured by setting the miR-control 200nM OVA condition to 100%. The mean and SD of three independent experiments is shown. (E) The mean and SD for the MFI of IFN γ + cells from three independent experiments is also shown.

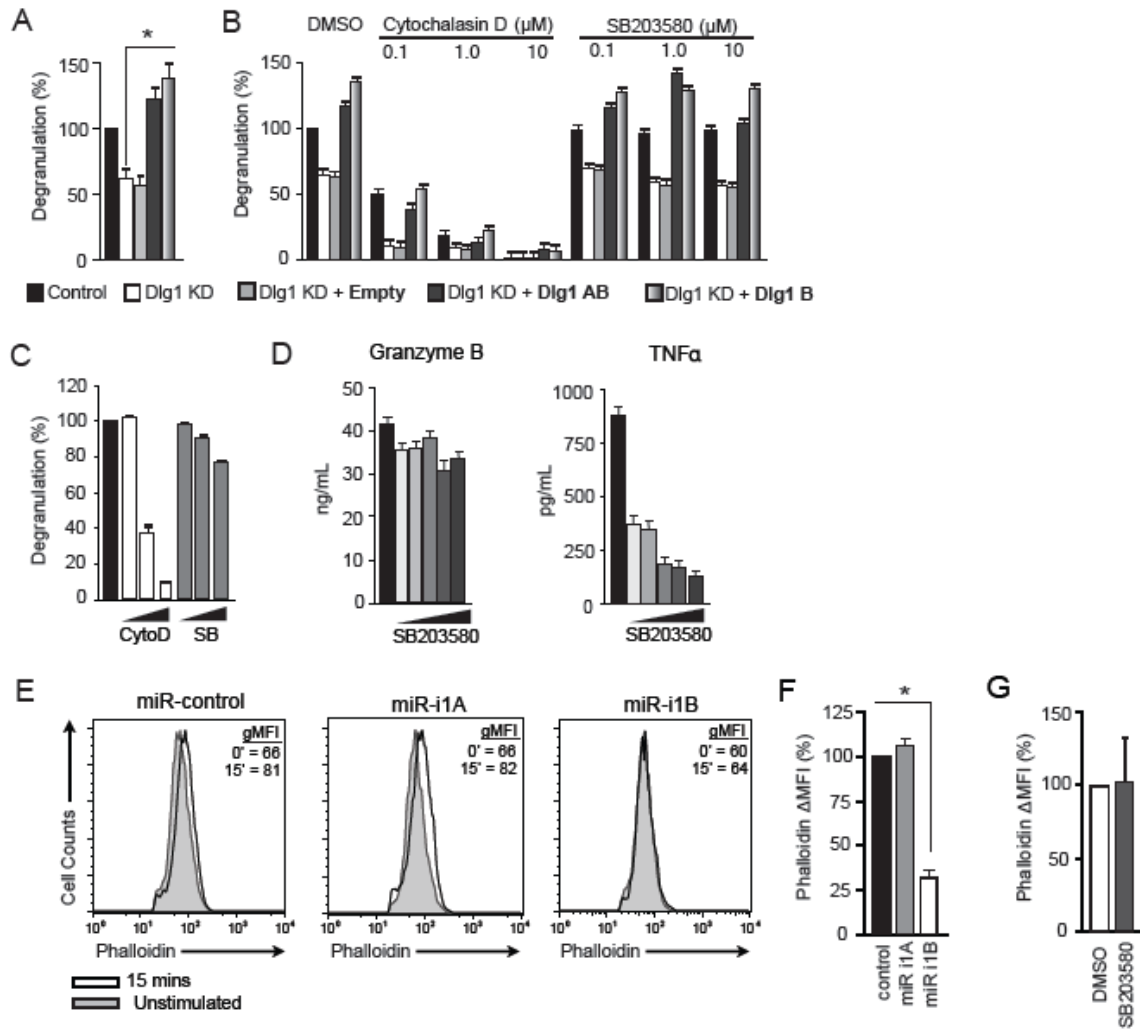


Figure 2-8: Dlg1 regulates optimal TCR-triggered, actin-dependent (p38-independent) degranulation. (A-B) OT-1 hybridoma CD8⁺ T cells were infected with re-expression (bold) and/or knockdown (KD) constructs. (A) Cells were stimulated with EG.7 cells in the presence of anti-CD107a. Relative degranulation was measured by setting the percentage of CD8⁺CD107a⁺ in the miR-control stimulated condition to 100%. Error bars represent SD of means from six independent experiments. **p* < 0.05. (B) Cells were pretreated with carrier (DMSO) or various concentrations of cytochalasin D or SB203580 prior to stimulation with EG.7 cells. Relative degranulation was measured as above. Error bars represent SD of samples analyzed in triplicate. Data is representative of at least two independent experiments. (C) Primary OT-1 CD8⁺ CTLs were pretreated with carrier (DMSO) or various concentrations of cytochalasin D (0.1, 1.0, 10 μM) or SB203580 (0.1, 1.0, 10 μM) prior to stimulation with EG.7 cells in the presence of anti-CD107a. Relative degranulation was measured by setting the percentage of CD8⁺CD107a⁺ in the stimulated DMSO condition (black bar) to 100%. Error bars represent SD of samples analyzed in triplicate. Data are representative of at least two independent experiments. (D) Primary OT-1 CD8⁺ CTLs were pretreated with carrier (DMSO) or various concentrations of SB203580 (0.625, 1.25, 2.5, 5, 10 μM) for 1 hr prior to stimulation with anti-CD3/anti-CD28 for 48 hrs. Supernatants were collected and analyzed via ELISA. Error bars represent SD of samples analyzed in triplicate. Data

are representative of at least two independent experiments. (E-F) Primary OT-1 CD8+ T cells were infected with miR-based knockdown viruses. (E) Cells were re-stimulated with MEF.B7.OVA cells for 15 mins and assessed for actin polymerization by intracellular phalloidin staining. Histograms of intracellular phalloidin for CD8+GFP+ cells is shown. Results are representative of four independent experiments. (F) The change in actin polymerization relative to miR-control was quantified as $\Delta\text{MFI} (\%)$, where $\Delta\text{MFI} = \text{stimulated MFI} - \text{unstimulated MFI}$, and where miR-control is set to 100%. Error bars represent SD of means from four independent experiments. $*p < 0.05$. (G) Primary OT-1 CD8+ CTLs were pretreated with 10 μM SB203580 or carrier (DMSO) for 30 mins. Cells were then stimulated with MEF.B7.OVA cells for 15 mins and assessed for intracellular phalloidin staining. The change in actin polymerization relative to DMSO was quantified as above. Error bars represent SD of means from three independent experiments.

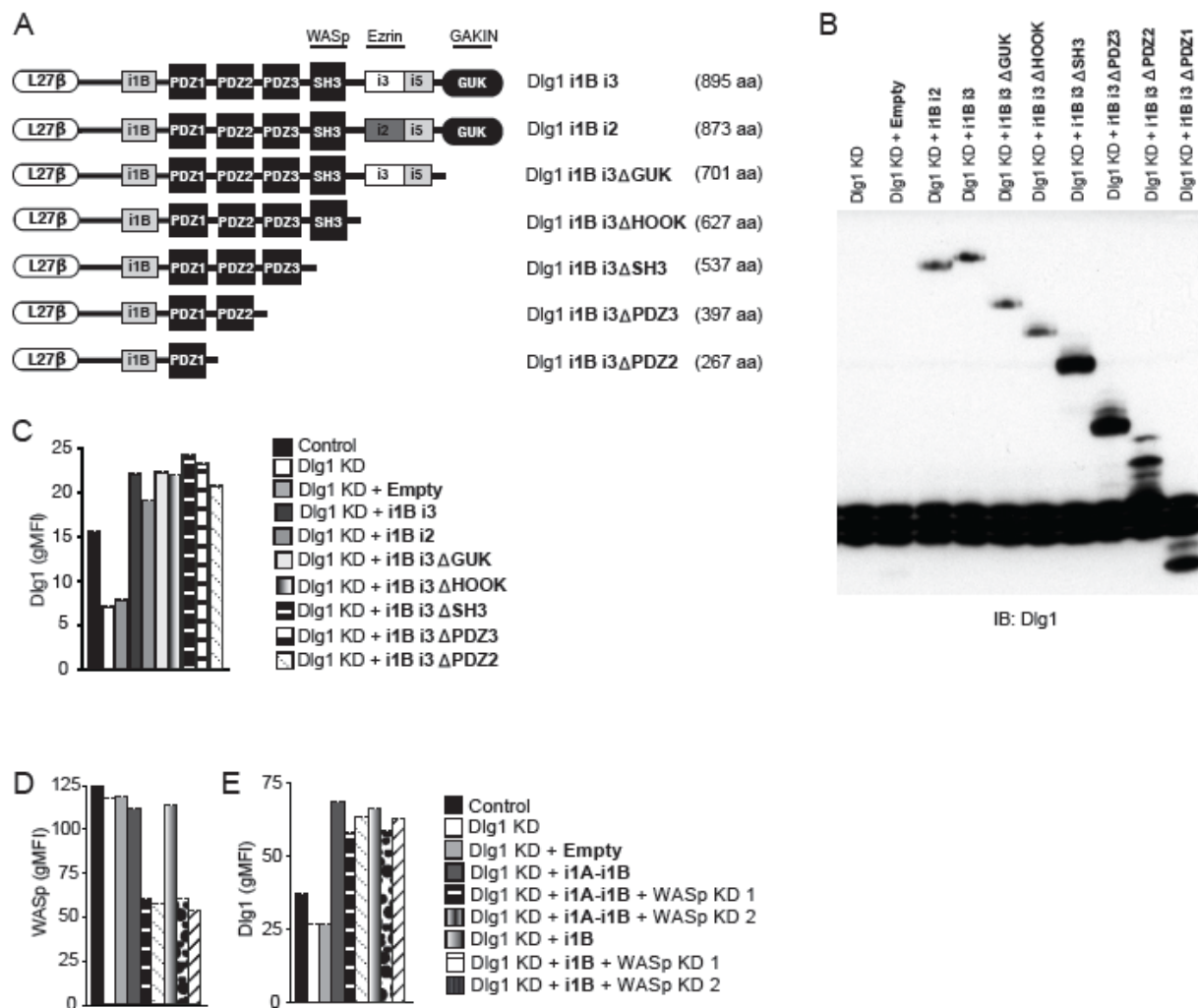


Figure 2-9: Dlg1B truncations and WASp knockdown OT-1 hybridoma T cell lines. (A) Schematic representation of Dlg1 i1B truncations. (B-E) OT-1 hybridoma T cells were infected with the indicated Dlg1 knockdown (KD) and/or re-expression (bold) viruses. The Dlg1 knockdown (Dlg1 KD) construct targets the 3UTR of *dlg1* allowing for re-expression of specific Dlg1 variants. (B) Cells were analyzed via SDS-PAGE and immunoblotted for Dlg1 to visualize Dlg1 i1B truncations/variants. (C-E) The indicated cells were analyzed for intracellular Dlg1 (C, E) or WASp (D) protein levels via flow cytometry; geometric mean fluorescent intensities (gMFIs) are graphed.

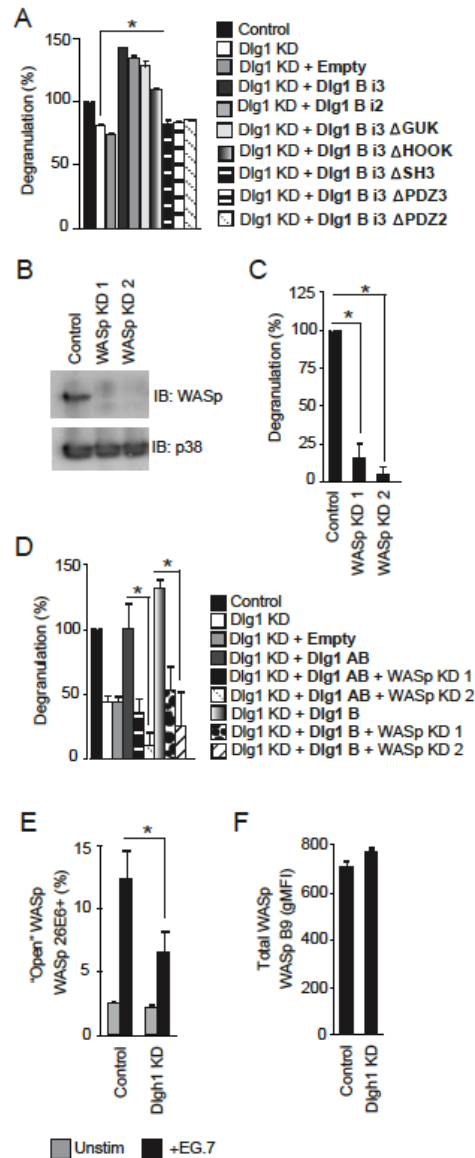


Figure 2-10: Dlg1-SH3 controls WASp activation to mediate degranulation. (A-F). OT-1 hybridoma CD8⁺ T cells were infected with re-expression (bold) and/or knockdown (KD) constructs. (A, C, D) Cells were stimulated with EG.7 cells in the presence of anti-CD107a. Relative degranulation was measured by setting the percentage of CD8⁺CD107a⁺ in the miR-control stimulated condition to 100%. Error bars represent SD of means from three independent experiments; **p* < 0.05. (B) Protein lysates from control and WASp knockdown cells were analyzed via SDS-PAGE and immunoblotting to assess WASp knockdown; p38 was used as a loading control (E) Cells were left unstimulated (grey) or stimulated with EG.7 cells for 30 mins (black) and intracellularly stained with anti-WASp 26E6 (which recognizes “open” WASp). Error bars represent SD of means from three independent experiments. **p* < 0.05. (F) Cells were stimulated with EG.7 cells for 30 mins (black) and intracellularly stained for total WASp protein levels. Error bars represent SD of samples analyzed in triplicate. Data are representative of at least three independent experiments.

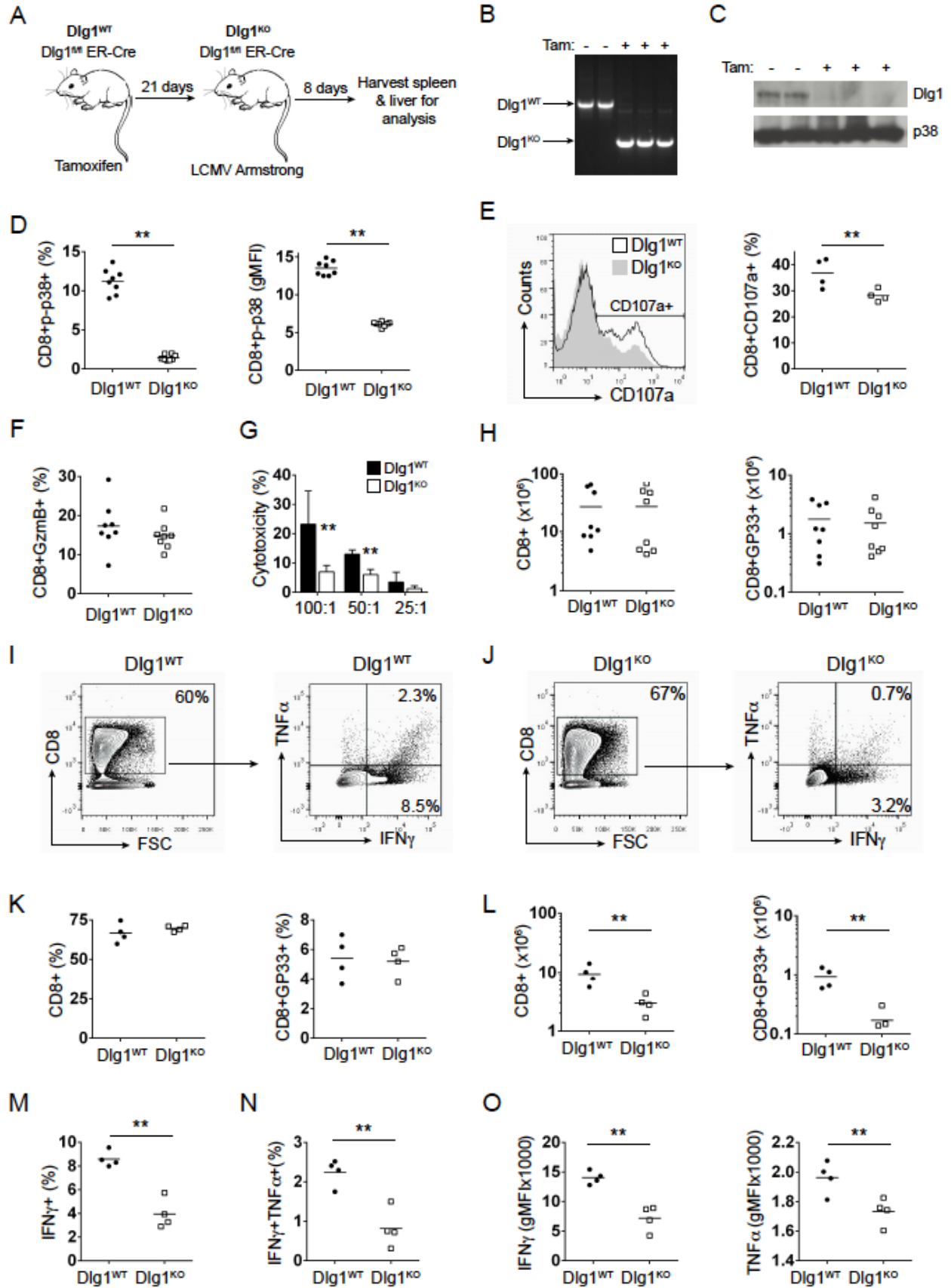


Figure 2-11: Dlg1 knockout decreases p38 activation, proinflammatory cytokine production and CTL killing in CD8+ T cells from LCMV-infected mice. (A) *Dlg1^{fl/fl}* ER-Cre mice were injected with tamoxifen or mock solution followed by LCMV Armstrong infection; livers and spleens were harvested day 8 post-infection. (B) PCR of splenic gDNA assessing *dlg1* recombination (C) SDS-PAGE of splenic protein lysate assessing Dlg1 knockout. (D) Quantitation of splenocytes stained with CD8 and p-p38 (T180/Y182) shown as both mean fluorescence intensity (left) and percent positive (right). (E, F) Analysis of splenocytes stimulated with LCMV-GP₃₃₋₄₁ peptide for 6hrs and stained with CD8 and CD107a (E) or granzyme B (F); representative histograms (E, left) and combined analysis (E, right, F) are shown. (G) Splenocytes were incubated with EL-4 cells pulsed with LCMV-GP₃₃₋₄₁ peptide at the indicated effector to target ratios for 4hrs and percent cytotoxicity quantified via LDH assay; the average cytotoxicity for all mice in each group is shown; error bars represent the SD between mice. (H) CD8+ (left) and CD8+GP33+ (right) splenocytes represented as total numbers. (I-O) Lymphocytes were isolated from the liver and stained as indicated. (I-J) Representative flow plots from Dlg1WT and Dlg1KO mice for cytokine analysis from liver lymphocytes. (K-L) Quantitation of CD8+ lymphocytes in the liver represented as total percent CD8+ (K, left), percent CD8+GP33+ (K, right), total CD8+ (L, left) or total CD8+GP33+ (L, right). (M-O) Analysis of liver lymphocytes represented as percent IFN γ + (M), percent IFN γ +TNF α + (N) or MFI of IFN γ +TNF α + cells (O). Splenocytes: n=8 Dlg1WT, n=8 Dlg1KO. Liver: n=4 Dlg1WT, n=4 Dlg1KO. **p<0.05.

Table 2-1: Knockdown sequences cloned into MGP or MRP.

Construct	Anti-Sense Sequence
miR-control	GTCTCCACGCGCAGTACATTT
miR-L27β	TTCCATAGAGCGGGTTATTAA
miR-i1A	CCAGTCCCTGCTGAGAGTACT
miR-i1A*	TCCCTGCTGAGAGTACTGTGC
miR-i1B	AGCTTAGAGACACCAACTTAT
miR-i3	AAGAACCTCTTTTCCCGAAAA
miR-i3*	GAACCTCTTTTCCCGAAAATT
Dlg1 KD (targets 3'UTR of <i>Dlg1</i>)	GTCCTCCACACTGACACAGAT
WASp KD1	TGTGTGCTTCGTGAAGGATA
WASp KD 2	ACCCTCAGAAGTCCTACTTCA

Table 2-2: RT-PCR Primers

RT-PCR Primer	Sequence
Forward i1A/i1B	CGGTATCAGGATGAAGAGGTA
Reverse i1A/i1B	CCCCTTTCAAGTGTGATTTCC
Forward i2/i3/i4/i5	CAGGCAGGTCACCCAGA
Reverse i2/i3/i4/i5	GGTCCTAATATGATGACTGGTCGGG
Forward Dlg1 exon 8	TAGATAGACACTTGTGAGGCTAAG
Reverse Dlg1 exon 8	AGGTAGAACATCAGGCTTTAAAATGTG

Table 2-3: qPCR Primers

qPCR Primer	Sequence
Forward NFATc1	GCCTCGTATCAGTGGGCGAAG
Reverse NFATc1	CGAAGCTCGTATGGACCA
Forward IκBα	CTGCAGGCCACCAACTACAA
Reverse IκBα	CAGCACCCAAAGTCACCAAGT
Forward IFNγ	GTCAACAACCCACAGGTCCAG
Reverse IFNγ	CCTTTTCCGCTTCCTGAGG
Forward TNFα	AATGGCCTCCCTCTCATCAGT
Reverse TNFα	GCTACAGGCTTGTCACTCGAATT
Forward IL-2	CCTGAGCAGGATGGAGAATTACA
Reverse IL-2	TCCAGAACATGCCGCAGAG
Forward Granzyme B	AAACGTGCTTCCTTTCTGGG
Reverse Granzyme B	GAAACTATGCCTGCAGCCACT
Forward Dlg1 (Total)	AGATCGCATCATATCGGTGAA
Reverse Dlg1 (Total)	TCAAACGACTGTACTCTTCGG
Forward Dlg1 AB	CGCACCACAGGCAAA
Forward Dlg1 B	CTCATATCTACCAATAAGGCAAA
Reverse Dlg1 AB/B	TACTTGAGTCATCTCCAATGTGTG
Forward L32	AAGCGAAACTGGCGGAAAC
Reverse L32	TAACCGATGTTGGGCATCAG

REFERENCES

1. Newell EW, Sigal N, Bendall SC, Nolan GP, Davis MM. 2012. Cytometry by time-of-flight shows combinatorial cytokine expression and virus-specific cell niches within a continuum of CD8+ T cell phenotypes. *Immunity* 36: 142-52
2. Hufford MM, Kim TS, Sun J, Braciale TJ. 2011. Antiviral CD8+ T cell effector activities in situ are regulated by target cell type. *J Exp Med* 208: 167-80
3. Rebeaud F, Hailfinger S, Thome M. 2007. Dlg1 and Carma1 MAGUK proteins contribute to signal specificity downstream of TCR activation. *Trends Immunol* 28: 196-200
4. Round JL, Tomassian T, Zhang M, Patel V, Schoenberger SP, Miceli MC. 2005. Dlg1 coordinates actin polymerization, synaptic T cell receptor and lipid raft aggregation, and effector function in T cells. *J Exp Med* 201: 419-30
5. Xavier R, Rabizadeh S, Ishiguro K, Andre N, Ortiz JB, Wachtel H, Morris DG, Lopez-Illasaca M, Shaw AC, Swat W, Seed B. 2004. Discs large (Dlg1) complexes in lymphocyte activation. *J Cell Biol* 166: 173-8
6. Mittelstadt PR, Yamaguchi H, Appella E, Ashwell JD. 2009. T Cell Receptor-Mediated Activation of p38 α by Mono-phosphorylation of the Activation Loop Results in Altered Substrate Specificity. *J Biol Chem* 284: 15469-74
7. Round JL, Humphries LA, Tomassian T, Mittelstadt P, Zhang M, Miceli MC. 2007. Scaffold protein Dlg1 coordinates alternative p38 kinase activation, directing T cell receptor signals toward NFAT but not NF-kappaB transcription factors. *Nat Immunol* 8: 154-61
8. Lue RA, Brandin E, Chan EP, Branton D. 1996. Two independent domains of hDlg are sufficient for subcellular targeting: the PDZ1-2 conformational unit and an alternatively spliced domain. *J Cell Biol* 135: 1125-37
9. Lasserre R, Charrin S, Cuche C, Danckaert A, Thoulouze M-I, de Chaumont F, Duong T, Perrault N, Varin-Blank N, Olivo-Marin J-C, Etienne-Manneville S, Arpin M, di Bartolo V, Alcover A. 2010. Ezrin tunes T-cell activation by controlling Dlg1 and microtubule positioning at the immunological synapse. *EMBO J* 29: 2301-14
10. Humphries LA, Shaffer MH, Sacirbegovic F, Tomassian T, McMahon KA, Humbert PO, Silva O, Round JL, Takamiya K, Haganir RL, Burkhardt JK, Russell SM, Miceli MC. 2012. Characterization of in vivo Dlg1 deletion on T cell development and function. *PLoS One* 7: e45276
11. Adachi K, Davis MM. 2011. T-cell receptor ligation induces distinct signaling pathways in naive vs. antigen-experienced T cells. *Proc Natl Acad Sci U S A* 108: 1549-54
12. Zanin-Zhorov A, Lin J, Scher J, Kumari S, Blair D, Hippen KL, Blazar BR, Abramson SB, Lafaille JJ, Dustin ML. 2012. Scaffold protein Disc large homolog 1 is required for T-cell receptor-induced activation of regulatory T-cell function. *Proc Natl Acad Sci U S A* 109: 1625-30

13. Gmyrek GB, Graham DB, Sandoval GJ, Blaufuss GS, Akilesh HM, Fujikawa K, Xavier RJ, Swat W. 2013. Polarity gene discs large homolog 1 regulates the generation of memory T cells. *Eur J Immunol* 43: 1185-94
14. Klocker N, Bunn RC, Schnell E, Caruana G, Bernstein A, Nicoll RA, Bredt DS. 2002. Synaptic glutamate receptor clustering in mice lacking the SH3 and GK domains of SAP97. *Eur J Neurosci* 16: 1517-22
15. Hanada T, Lin L, Chandy KG, Oh SS, Chishti AH. 1998. Human Homologue of the Drosophila Discs Large Tumor Suppressor Binds to p56lck Tyrosine Kinase and Shaker Type Kv1.3 Potassium Channel in T Lymphocytes. *Journal of Biological Chemistry* 272: 26899-904
16. Cavatorta AL, Facciuto F, Valdano MB, Marziali F, Giri AA, Banks L, Gardiol D. 2011. Regulation of translational efficiency by different splice variants of the Disc large 1 oncosuppressor 5UTR. *FEBS J* 278: 2596-608
17. Schlüter OM, Xu W, Malenka RC. 2006. Alternative N-terminal domains of PSD-95 and SAP97 govern activity-dependent regulation of synaptic AMPA receptor function. *Neuron* 51: 99-111
18. McLaughlin M, Hale R, Ellston D, Gaudet S, Lue RA, Viel A. 2002. The distribution and function of alternatively spliced insertions in hDlg. *J Biol Chem* 277: 6406-12
19. Godreau D, Vranckx R, Maguy A, Goyenville C, Hatem SN. 2003. Different isoforms of synapse-associated protein, SAP97, are expressed in the heart and have distinct effects on the voltage-gated K⁺ channel Kv1.5. *J Biol Chem* 278: 47046-52
20. Roberts S, Calautti E, Vanderweil S, Nguyen HO, Foley A, Baden HP, Viel A. 2007. Changes in localization of human discs large (hDlg) during keratinocyte differentiation are associated with expression of alternatively spliced hDlg variants. *Exp Cell Res* 313: 2521-30
21. Yamada KH, Hanada T, Chishti AH. 2007. The effector domain of human Dlg tumor suppressor acts as a switch that relieves autoinhibition of kinesin-3 motor GAKIN/ KIF13B. *Biochemistry* 46: 10039-45
22. Hanada T, Lin L, Chandy KG, Oh SS, Chishti AH. 1997. Human homologue of the Drosophila discs large tumor suppressor binds to p56lck tyrosine kinase and Shaker type Kv1.3 potassium channel in T lymphocytes. *J Biol Chem* 272: 26899-904
23. Salvador JM, Mittelstadt PR, Guszczynski T, Copeland TD, Yamaguchi H, Appella E, Fornace AJ, Ashwell JD. 2005. Alternative p38 activation pathway mediated by T cell receptor-proximal tyrosine kinases. *Nat Immunol* 6: 390-5
24. Huse M, Quann EJ, Davis MM. 2008. Shouts, whispers and the kiss of death: directional secretion in T cells. *Nat Immunol* 9: 1105-11
25. Hanada T, Lin L, Tibaldi EV, Reinherz EL, Chishti AH. 2000. GAKIN, a novel kinesin-like protein associates with the human homologue of the Drosophila discs large tumor suppressor in T lymphocytes. *J Biol Chem* 275: 28774-84

26. Nikolov NP, Shimizu M, Cleland S, Bailey D, Aoki J, Strom T, Schwartzberg PL, Candotti F, Siegel RM. 2010. Systemic autoimmunity and defective Fas ligand secretion in the absence of the Wiskott-Aldrich syndrome protein. *Blood* 116: 740-7
27. Padrick SB, Cheng H-C, Ismail AM, Panchal SC, Doolittle LK, Kim S, Skehan BM, Umetani J, Brautigam CA, Leong JM, Rosen MK. 2008. Hierarchical regulation of WASP/WAVE proteins. *Molecular Cell* 32: 426-38
28. Labno CM, Lewis CM, You D, Leung DW, Takesono A, Kamberos N, Seth A, Finkelstein LD, Rosen MK, Schwartzberg PL, Burkhardt JK. 2003. Itk Functions to Control Actin Polymerization at the Immune Synapse through Localized Activation of Cdc42 and WASP. *Current Biology* 13: 1619-24
29. Schluter OM, Xu W, Malenka RC. 2006. Alternative N-terminal domains of PSD-95 and SAP97 govern activity-dependent regulation of synaptic AMPA receptor function. *Neuron* 51: 99-111
30. Zhou W, Zhang L, Guoxiang X, Mojsilovic-Petrovic J, Takamaya K, Sattler R, Huganir R, Kalb R. 2008. GluR1 controls dendrite growth through its binding partner, SAP97. *J Neurosci* 28: 10220-33
31. Stinchcombe J, Griffiths G. 2007. Secretory mechanisms in cell-mediated cytotoxicity. *Annu Rev Cell Dev Biol* 23: 495-517
32. Orange JS, Ramesh N, Remold-O'Neil E, Sasahara Y, Koopman L, Byrne M, Bonilla FA, Rosen FS, Geha RS, Strominger JL. 2002. Wiskott-Aldrich syndrome protein is required for NK cell cytotoxicity and colocalizes with actin to NK cell-activating immunologic synapses. *J Clin Invest* 110: 1135-46
33. Ludford-Menting MJ, Oliaro J, Sacirbegovic F, Cheah ET-Y, Pedersen N, Thomas SJ, Pasam A, Iazzolino R, Dow LE, Waterhouse NJ, Murphy A, Ellis S, Smyth MJ, Kershaw MH, Darcy PK, Humbert PO, Russell SM. 2005. A network of PDZ-containing proteins regulates T cell polarity and morphology during migration and immunological synapse formation. *Immunity* 22: 737-48
34. De Meester J, Calvez R, Valitutti S, Dupré L. 2010. The Wiskott-Aldrich syndrome protein regulates CTL cytotoxicity and is required for efficient killing of B cell lymphoma targets. *J Leukoc Biol* 88: 1031-40
35. Calvez R, Lafouresse F, De Meester J, Galy A, Valitutti S, Dupré L. 2011. The Wiskott-Aldrich syndrome protein permits assembly of a focused immunological synapse enabling sustained T-cell receptor signaling. *Haematologica* 96: 1415-23
36. Feng W, Long J-F, Fan J-S, Suetake T, Zhang M. 2004. The tetrameric L27 domain complex as an organization platform for supramolecular assemblies. *Nat Struct Mol Biol* 11: 475-80
37. Nakagawa T, Futai K, Lashuel HA, Lo I, Okamoto K, Walz T, Hayashi Y, Sheng M. 2004. Quaternary structure, protein dynamics, and synaptic function of SAP97 controlled by L27 domain interactions. *Neuron* 44: 453-67
38. Serfling E, Berberich-Siebelt F, Avots A. 2007. NFAT in lymphocytes: a factor for all events? *Sci STKE* 2007: pe42

39. Huang C, Bi E, Hu Y, Deng W, Tian Z, Dong C, Hu Y, Sun B. 2006. A novel NF-kappaB binding site controls human granzyme B gene transcription. *Journal of immunology (Baltimore, Md : 1950)* 176: 4173-81
40. Hodge MR, Ranger AM, Charles de la Brousse F, Hoey T, Grusby MJ, Glimcher LH. 1996. Hyperproliferation and dysregulation of IL-4 expression in NF-ATp-deficient mice. *Immunity* 4: 397-405
41. Peng SL, Gerth AJ, Ranger AM, Glimcher LH. 2001. NFATc1 and NFATc2 together control both T and B cell activation and differentiation. *Immunity* 14: 13-20
42. Kaminuma O, Kitamura F, Kitamura N, Hiroi T, Miyoshi H, Miyawaki A, Miyatake S. 2008. Differential contribution of NFATc2 and NFATc1 to TNF-alpha gene expression in T cells. *J Immunol* 180: 319-26
43. Martinez NM, Pan Q, Cole BS, Yarosh CA, Babcock GA, Heyd F, Zhu W, Ajith S, Blencowe BJ, Lynch KW. 2012. Alternative splicing networks regulated by signaling in human T cells. *RNA* 18: 1029-40
44. Jirmanova L, Giardino Torchia ML, Sarma ND, Mittelstadt PR, Ashwell JD. 2011. Lack of the T cell-specific alternative p38 activation pathway reduces autoimmunity and inflammation. *Blood* 118: 3280-9
45. Trifari S, Sitia G, Aiuti A, Scaramuzza S, Marangoni F, Guidotti LG, Martino S, Saracco P, Notarangelo LD, Roncarolo M-G, Dupré L. 2006. Defective Th1 cytokine gene transcription in CD4+ and CD8+ T cells from Wiskott-Aldrich syndrome patients. *J Immunol* 177: 7451-61
46. Hogquist KA, Jameson SC, Heath WR, Howard JL, Bevan MJ, Carbone FR. 1994. T cell receptor antagonist peptides induce positive selection. *Cell* 76: 17-27
47. Moore MW, Carbone FR, Bevan MJ. 1988. Introduction of soluble protein into the class I pathway of antigen processing and presentation. *Cell* 54: 777-85
48. Brooks DG, Teyton L, Oldstone MB, McGavern DB. 2005. Intrinsic functional dysregulation of CD4 T cells occurs rapidly following persistent viral infection. *J Virol* 79: 10514-27
49. Brooks DG, McGavern DB, Oldstone MB. 2006. Reprogramming of antiviral T cells prevents inactivation and restores T cell activity during persistent viral infection. *J Clin Invest* 116: 1675-85

CHAPTER THREE

Phosphorylation of Discs Large Homolog 1 (Dlg1) by Lck is critical for p38 activation and pro-inflammatory cytokine gene expression in T cells

ABSTRACT

CD8⁺ T cells respond to TCR stimulation by producing pro-inflammatory cytokines and by destroying infected or malignant cells through the release of cytotoxic granules. Scaffold protein Discs large homolog 1 (Dlg1) specifies TCR-dependent functions by channeling proximal signals toward the activation of p38-dependent transcriptional events and p38-independent cytoskeletal events. Here, we show that TCR-induced tyrosine phosphorylation of Dlg1 plays a vital role in regulating p38-dependent functions in CD8⁺ T cells. We demonstrate that Dlg1 is tyrosine phosphorylated in response to TCR stimulation, and that this phosphorylation occurs specifically on the Dlg1AB splice variant. Further, we identify tyrosine 222 (Y222), in the N-terminal linker region between the i1B and PDZ1 domains, as a major site of Lck-mediated Dlg1 phosphorylation. Functional assessment of T cells expressing wild type or Y222F Dlg1 shows that phosphorylation of Dlg1 at Y222 is essential for p38 activation and NFAT-dependent transcription of pro-inflammatory cytokines, but not for degranulation and target cell killing. Finally, we extend these findings by showing that p38 phosphorylation, pro-inflammatory cytokine production and degranulation are impaired in an acute Dlg1 knockout model. Our results identify Dlg1 Y222 as a key point of control downstream of the TCR, and propose targeting of Dlg1 Y222 phosphorylation as a novel mechanism to prevent overt pro-inflammatory cytokine production.

INTRODUCTION

Activation of CD8⁺ CTLs is essential for maintaining adaptive immunity to intracellular pathogens. In response to TCR stimulation, CTLs produce and release pro-inflammatory cytokines and destroy infected cells through release of cytotoxic granules. TCR engagement is coupled to these effector functions through the recruitment and activation of TCR proximal tyrosine kinases (PTKs) Lck and Zap70. These early events initiate signaling networks including MAPKs ERK, JNK and p38, which regulate the activation of transcription factors including NFAT and NFκB. These transcription factors control gene expression levels that guide the magnitude and scope of TCR-dependent events including: proliferation, differentiation and effector responses (1, 2). Recent studies suggest that CD8⁺ T cells are capable of a vast spectrum of functional diversity (3). However, the fidelity of biological responses suggest that this diversity is not random, but instead an ordered series of events that channel TCR proximal signals toward a discrete response(s).

Scaffold proteins have emerged as key points of control that couple extracellular signals to intracellular signaling networks and downstream functions, through the formation of multi-component signaling complexes. One such scaffold protein, Discs Large Homolog 1 (Dlg1), is present at cell:cell junctions in epithelial, neuronal and immunological cells; including the junction between T cells and antigen presenting cells known as the immunological synapse where it regulates antigen-dependent cytoskeletal and signaling events (4-9). The ability of Dlg1 to regulate cellular functions is attributed to its ability to juxtapose numerous cytoskeletal regulators and signal transducers including: Lck, Zap70, p38, WASp and Ezrin. However, the mechanism(s) by which distinct Dlg1 signaling complexes are formed in response to T cell stimulation is just now being elucidated.

The MAPK p38 is expressed in all eukaryotic cells and is primarily activated through a three tiered kinase cascade, culminating in direct phosphorylation of p38 at T180 and Y182 by MKK3 or MKK6, which enhances p38 kinase activity on specific downstream substrates (10). In contrast to this canonical p38 pathway, the alternative p38 pathway is MKK-independent, is

initiated downstream of the TCR and requires Lck and Zap70 kinase activity (11). TCR engagement leads to Lck-dependent phosphorylation and activation of Zap70, which then phosphorylates p38 at Y323 followed by p38 auto-phosphorylation at T180 up regulating kinase activity (11, 12). A vital downstream target of alternatively activated p38 is transcription factor NFATc2 (NFAT1), which when phosphorylated at S54 up regulates NFATc1 (NFAT2) through an auto-regulatory loop (13). Individually, and together NFATc1 and NFATc2 regulate numerous T cell effector functions including cytokine production (14). The significance of the alternative pathway is demonstrated in GADD45 α knockout mice. In these mice the alternative p38 pathway is constitutively active, resulting in the development of spontaneous lupus-like autoimmunity (15, 16). Recent reports extended these findings by demonstrating that resting T cells in the peripheral blood of patients with active rheumatoid arthritis have increased alternative p38 and NFAT activation compared to patients in remission or controls (17). Thus, it seems that the alternative p38 pathway plays an important role in initiation and maintenance of autoimmunity. A better understanding of the molecular mechanisms that underlie this pathway could identify novel therapeutic targets.

We and others have demonstrated that Dlg1 is required for coordination of the alternative p38 pathway downstream of the TCR (5, 7, 18). Loss of the alternative pathway through Dlg1 knockdown, p38 Y323F knock-in or addition of p38 inhibitors leads to decreased NFAT-dependent transcription and production of IFN γ . Interestingly, NF κ B-dependent transcription and expression of IL-2 are not diminished with loss of Dlg1 or the alternative p38 pathway demonstrating that Dlg1-dependent p38 activation specifies proximal TCR signals toward activation of p38, NFAT and IFN γ (5, 19, 20). Dlg1 is thought to facilitate the alternative p38 pathway by juxtaposing Lck, Zap70 and p38; however, the mechanism(s) by which this signal complex is formed and regulated are just now being investigated.

Structurally, Dlg1 consists of several modular domains common to all MAGUK family members including: three PDZ domains, an SH3 domain and a catalytically inactive guanylate kinase domain (GUK). In addition, Dlg1 contains a L27 β oligomerization domain, an N-terminal

proline rich region and a C-terminal HOOK domain, which are unique among MAGUK family members. Despite having no inherent enzymatic activity, Dlg1 is dynamically regulated by alternative splicing and intramolecular interactions that induce changes in binding partners and are therefore thought to guide Dlg1 function (21-25). Recently, we have demonstrated that at least two forms of Dlg1 are present in T cells: Dlg1AB and Dlg1B. These variants are produced through alternative splicing and differ only in the inclusion or exclusion of the proline-rich i1A region, which mediates the interaction between Dlg1 and Lck that is required for p38 activation (Chapter 2). Serine phosphorylation is known to regulate Dlg1 localization, stability and binding partners in neuronal and epithelial cells (26-28). However, the role of Dlg1 phosphorylation in guiding cellular activation and function in T cells has yet to be examined.

Here we report that Dlg1 is phosphorylated on several tyrosine residues in response to TCR stimulation. This phosphorylation is mediated by Dlg1-associated Lck, and occurs in a splice variant-specific manner where Dlg1AB, but not Dlg1B, is phosphorylated. We demonstrate that tyrosine 222 (Y222) is a major site of TCR-induced Dlg1 phosphorylation. Importantly, mutation of Y222 to phenylalanine (Y222F) significantly inhibited Dlg1AB-mediated functions including p38 activation and subsequent activation of NFAT-dependent genes IFN γ and TNF α . However, Y222 phosphorylation is not required for p38-independent functions such as degranulation and target cell killing. Additionally, we demonstrate that p38 activation, pro-inflammatory cytokine production and degranulation are defective in Dlg1 knockout CTLs. Together our data demonstrate that Dlg1 phosphorylation is a key point of control required for Dlg1-mediated p38-dependent events including IFN γ production, but not for p38-independent degranulation. Our data also confirm the importance of Dlg1 in T cell signaling through the characterization of CD8+ CTL function in an acute *in vitro* Dlg1 knockout system.

RESULTS

Dlg1AB is tyrosine phosphorylated by a bound kinase in response to TCR stimulation

Dlg1 is known to associate with several tyrosine kinases; therefore we considered the possibility that Dlg1 may be tyrosine phosphorylated, and that tyrosine phosphorylation may

regulate Dlg1-mediated signaling. In order to determine if Dlg1 can be phosphorylated in T cells, we initially performed *in vitro* kinase assays. GST-tagged Dlg1AB (GST-Dlg1AB) or Dlg1B (GST-Dlg1B), the two known Dlg1 splice variants expressed in T cells (Chapter 2), were incubated with T cell lysates in order to form Dlg1 complexes with T cell-specific ligands. In the absence of ATP, Dlg1 was not phosphorylated. However, upon addition of ATP we observed robust tyrosine phosphorylation of Dlg1AB, but not Dlg1B (pY-Dlg1)(Figure 3-1). These results indicated that Dlg1AB, but not Dlg1B associates with and is phosphorylated by at least one tyrosine kinase found in T cell lysates. In order to determine if Dlg1AB phosphorylation was TCR-induced, Dlg1 complexes were immunoprecipitated from resting or TCR-stimulated T cells and the level of pY-Dlg1 was assessed. An increase in pY-Dlg1 was observed in TCR-stimulated samples compared to resting samples suggesting that Dlg1 tyrosine phosphorylation was absent in resting cells, and induced via TCR stimulation (Figure 3-1). Further, this phosphorylation was specific to Dlg1AB, which we previously demonstrated corresponds to the top 130kDa band on SDS-PAGE (Figure 3-1). Based on these data we conclude that Dlg1AB, but not Dlg1B is phosphorylated by at least one bound tyrosine kinase in response to TCR stimulation.

Tyrosine 222 is a major site of TCR-induced Dlg1 phosphorylation

The Dlg1AB protein contains 927 amino acids, 29 of which are tyrosines (GenBank: AAH57118.1) (Figure 3-2). In order to narrow our search for specific sites of Dlg1 tyrosine phosphorylation, we utilized the ScanSite algorithm to determine the most likely candidate tyrosine residues (30). Tyrosine 222 (Y222) was identified as the most likely site of tyrosine phosphorylation using high stringency search criteria. Y222 is located in the N-terminal region of Dlg1, in the flexible linker region between the i1B and PDZ1 domains. Additionally, Y222 is part of a highly conserved Tyr-Glu-Glu-Iso (YEEI) motif that is a predicted target of known Dlg1-associated tyrosine kinases Lck and Zap70 (5, 31, 32) (<http://ppsp.biocuckoo.org>, Figure 3-2).

In order to determine if this candidate tyrosine was a site of phosphorylation, we created GST-Dlg1 fusion proteins in which Y222 was mutated to phenylalanine (Y222F) to disrupt phosphorylation at Y222. *In vitro* kinase assays utilizing Dlg1AB (WT) or Y222F GST-Dlg1 consistently demonstrated a 40% decrease in tyrosine phosphorylation signal in Dlg1 Y222F compared to WT; demonstrating that Y222 was a major site of Dlg1 phosphorylation (Figure 3-2).

Dlg1 tyrosine phosphorylation is mediated by Dlg1-associated Lck

Y222 is part of a YEEI motif predicted to be targeted by Src and/or Syk family kinases (Figure 3-2). In T cells, Dlg1 associates with Src family member Lck and Syk family member Zap70. To identify a possible role for Lck and Zap70 in Dlg1 phosphorylation, we first *in vitro* phosphorylated GST-Dlg1 WT complexes in the presence or absence of Src kinase family inhibitor PP2. Dlg1 tyrosine phosphorylation was completely blocked by the addition of PP2 demonstrating that Lck kinase activity is required for Dlg1 phosphorylation (Figure 3-2). However, since Lck kinase activity regulates Zap70 activation, these data did not rule out a role for Zap70 in Dlg1 phosphorylation. Thus, we incubated WT or Y222F GST-Dlg1 proteins with recombinant Lck or Zap70 to determine the ability of each kinase to directly phosphorylate Dlg1. We found that rLck, but not rZap70 directly phosphorylated Dlg1 *in vitro*. Further, phosphorylation of Y222F GST-Dlg1 by rLck was significantly reduced compared to WT GST-Dlg1 demonstrating that Lck is likely responsible for Y222 phosphorylation (Figure 3-2). While rZap70 did not phosphorylate Dlg1, it did phosphorylate our positive control (GST-LAT) demonstrating that the rZap70 was active in our system (Figure 3-2). Collectively, our data identify Lck, but not Zap70 as the kinase responsible for phosphorylation of Dlg1 at several tyrosines including Y222.

Dlg1 Y222 phosphorylation is required for TCR-induced alternative p38 activation in CD8+ T cells

Phosphorylation of scaffold proteins is known to regulate function by inducing structural changes and/or creating new ligand binding sites (33-35). To determine the requirement of Dlg1 Y222 in coordinating Dlg1-mediated alternative p38 activation we assessed the ability of GST-Dlg1 WT and Dlg1 Y222F to facilitate phosphorylation of associated p38. Both Dlg1 WT and Dlg1 Y222F were able to associate with p38; however upon the addition of ATP to the complexes, Dlg1 Y222F demonstrated a significant reduction in p38 phosphorylation (pY-p38) compared to WT, providing evidence that Y222 is required to facilitate phosphorylation of Dlg1-bound p38 (Figure 3-3).

To determine if Dlg1 Y222 was required for TCR-triggered p38 activation we created stable cell lines expressing WT or Y222F Dlg1. In these cells, endogenous Dlg1 was knocked down in T cells using a miRNA-based retroviral construct specific for the 3' untranslated region (3'UTR) of Dlg1, yielding stable cell lines that expressed less than 10% of endogenous Dlg1 protein. Dlg1 was re-expressed in these cells using an MSCV-based retrovirus expressing Dlg1AB, Dlg1 Y222F or a control vector. The resulting T cells expressed comparable amounts of Dlg1AB or Dlg1 Y222F (Figure 3-3). Control cells expressing endogenous Dlg1 or Dlg1AB- or Dlg1 Y222F-expressing cells were stimulated through their TCR and the amount of Dlg1-associated p-p38 was assessed. TCR-inducible p38 phosphorylation was present in the control cells, which was significantly enhanced in cells expressing Dlg1AB, but not in cells expressing Dlg1 Y222F (Figure 3-3). The low level of p38 phosphorylation in Y222F cells is likely due to a small amount of endogenous Dlg1AB. In primary CD8+ CTLs we demonstrate that over expression of Dlg1AB caused a significant enhancement of TCR-induced total cellular p38 phosphorylation compared to control cells, while Dlg1 Y222F did not (Figure 3-3). Together our results highlight an essential role for Dlg1 Y222 phosphorylation in the regulation of TCR-induced alternative p38 activation in T cells.

Loss of Dlg1 Y222 phosphorylation results in decreased NFAT-, but not NFκB-dependent expression

Previous studies from our group and others have demonstrated that Dlg1-mediated alternative p38 activation induces NFAT-, but not NFκB-dependent gene transcription (5, 7, 18). Recently we have demonstrated that Dlg1AB, but not Dlg1B is able to facilitate p38-dependent NFAT activation (Chapter 2). To determine if Dlg1 Y222 plays a role in TCR-induced NFAT or NFκB activation, a panel of Dlg1 knockdown and Dlg1 re-expressing T cell lines were stimulated through their TCR and level of *Nfatc1* (NFAT-dependent gene) and *Iκba* (NFκB-dependent gene) gene expression was measured via quantitative PCR. T cells lacking Dlg1 demonstrated impaired induction of *Nfatc1* upon TCR stimulation compared to control cells (Figure 3-4). Re-expression of Dlg1AB in knockdown cells was able to rescue *Nfatc1* expression while re-expression of Dlg1 Y222F or Dlg1B further attenuated *Nfatc1* expression (Figure 3-4). Alterations in Dlg1 expression had no significant effect on the level of *Iκba* induction upon TCR stimulation (Figure 3-4). We further interrogated these findings in primary CD8⁺ T cells where expression of Dlg1AB, but not Dlg1 Y222F or Dlg1B was able to enhance TCR-dependent *Nfatc1* transcription, while Dlg1 expression levels had no significant effect on *Iκba* transcription (Figure 3-4).

Dlg1 Y222 is required for optimal IFNγ and TNFα, but not IL-2 production

Dlg1AB-mediated alternative p38 activation has been implicated in selective up regulation of pro-inflammatory cytokines IFNγ and TNFα, but not IL-2 in response to TCR stimulation (5, 13, 14, 19, 20). In order to examine the requirement of Dlg1 Y222 in TCR-induced cytokine production, a panel of Dlg1 knockdown and re-expressing T cells were stimulated and their ability to induce cytokine gene transcription was measured. Dlg1-deficient T cells had impaired induction of IFNγ and TNFα, but not IL-2 transcription compared to control cells (Figure 3-4). Expression of Dlg1AB was able to rescue the defect in IFNγ and TNFα transcription while introduction of Dlg1 Y222F or Dlg1B showed no significant increase in

cytokine gene expression, demonstrating that Dlg1 Y222 is required for Dlg1AB-mediated cytokine production. Re-expression of Dlg1AB, Dlg1B or Dlg1 Y222F had no significant effect on the level of IL-2 transcription (Figure 3-4). In primary CD8⁺ CTLs over expression of Dlg1AB, but not Dlg1B or Dlg1 Y222F was able to enhance IFN γ and TNF α gene expression, while Dlg1 expression had had a significant effect on IL-2 gene expression (Figure 3-4). In fact, cells over expressing Dlg1 Y222F demonstrated lower levels of pro-inflammatory cytokine gene expression than control cells suggesting Dlg1 Y222F might act as a dominant negative in this system. Together our results support a model where phosphorylation Dlg1 Y222 selectively up regulates NFAT-dependent gene transcription including the production of pro-inflammatory cytokines IFN γ and TNF α .

Dlg1 Y222 is not required for Dlg1-mediated cytotoxic degranulation

Dlg1 is known to regulate cytoskeletal events in epithelial, neuronal and immunologic systems (4, 7, 36, 37). In particular, Dlg1 association with WASp and ezrin is implicated in TCR-dependent positioning of the microtubule-organizing complex (MTOC), leading to the release of cytotoxic granules required for target cell cytolysis (Chapter 2). To test the requirement of Dlg1 Y222 in release of cytotoxic granules (degranulation) we incubated a panel of T cells with antigen presenting cells and tracked the expression of CD107a on the surface of the T cells. Total Dlg1 knockdown resulted in significantly impaired antigen-dependent degranulation. Surprisingly, both Dlg1AB and Dlg1 Y222F were able to rescue and enhance antigen-dependent degranulation to a similar level (Figure 3-5). Additionally, over expression of Dlg1AB, Dlg1B or Dlg1 Y222F in primary CD8⁺ CTLs enhanced antigen-dependent degranulation to a similar level compared to control cells (Figure 3-5). These data suggest that phosphorylation of Dlg1 Y222 is not required for Dlg1-mediated degranulation in response to antigen.

Acute Dlg1 knockout prevents TCR-dependent p38 activation, NFAT-dependent transcription and target cell killing

We and others have demonstrated that Dlg1 plays a vital role in mediating TCR-dependent effector functions utilizing numerous Dlg1 knockdown systems (4, 5, 7, 9, 18, 36). Despite this body of evidence, Dlg1 knockout models do not show striking functional differences due to compensation from other Dlg1 family members (38, 39). In support of the importance of our mechanistic findings, we used an acute Dlg1 knockout system to examine the requirement for Dlg1 in TCR-dependent effector functions. CD8⁺ T cells isolated from the spleens of mice with loxP sites flanking exon 8 of *dlg1* (*Dlg1^{fllox/fllox}*) were expanded *in vitro* before infection with retroviral cre recombinase (*Dlg1^{KO}*) or control vector (*Dlg1^{WT}*) (39) (Figure 3-6). This system yielded CD8⁺ CTLs with robust and reproducible Dlg1 knockout on both the gDNA and protein level (Figure 3-6). Upon TCR stimulation *Dlg1^{KO}* cells showed a 50% reduction in total cellular p38 phosphorylation (Figure 3-6). Further, *Dlg1^{KO}* cells had a severe and selective impairment in NFAT-, but not NFκB-dependent transcription including NFATc1 and pro-inflammatory cytokines IFNγ and TNFα, but not IL-2 (Figure 3-6). These data are consistent with previous reports that Dlg1-independent activation of NFATc1 may be sufficient to support TCR-dependent gene expression of IL-2, but not TNFα (14) (Chapter 2). We also interrogated the requirement of Dlg1 for TCR-induced release of cytotoxic granules and target cell lysis. Additionally, Dlg1 knockout significantly impaired antigen-dependent degranulation and target cell killing, but not granzyme B gene expression (Figure 3-6). These data support our previous findings and suggest a system where Dlg1 is required for the release of cytotoxic granules, but not the production of granule elements. Together results from our acute Dlg1 knockout system establish Dlg1 as a vital tool that guides specific TCR-dependent signaling and cytoskeletal events, and support the hypothesis that compensation by other Dlg1 family members may have masked phenotypic differences in non-acute knockout models used in previous studies.

DISCUSSION

CD8⁺ T cells produce a spectrum of effector functions in response to antigen recognition that dictate productive and destructive immune responses (3). Therefore it is essential to understand the molecular mechanisms that individually regulate CD8⁺ T cell effector functions in order to better understand events that underlie normal and aberrant responses (40, 41). Here, we identified a previously uncharacterized requirement for Dlg1 phosphorylation in the selective regulation of TCR-induced expression of pro-inflammatory cytokines, IFN γ and TNF α (Figure 3-7). We found that Dlg1 is tyrosine phosphorylated in response to TCR stimulation in a splice variant dependent manner where Dlg1AB, but not Dlg1B was phosphorylated. We determined that Y222 is a phosphorylation site targeted by Dlg1-associated Lck. Further, the loss of Y222 phosphorylation impaired TCR-induced p38 activation and NFAT-dependent gene expression of pro-inflammatory cytokines IFN γ and TNF α , but not Dlg1-mediated degranulation. These data highlight the role of Dlg1 Y222 phosphorylation as a molecular switch required for the activation of a subset of Dlg1-mediated effector functions downstream of the TCR. In support of the importance of Dlg1 in regulating T cell function, we demonstrated that acute knockout of Dlg1 in CD8⁺ CTLs resulted in selective impairment of TCR-induced p38 activation, NFAT-dependent transcription, pro-inflammatory cytokine gene expression and antigen-dependent degranulation. Our results indicate that Dlg1 plays an important role in specifying T cell function, and that Lck-mediated phosphorylation of Y222 is an inducible post-translation modification required to authorize p38-dependent Dlg1-mediated functions.

At least two Dlg1 protein variants are expressed in CD8⁺ T cells through alternative splicing that differ in the inclusion or exclusion of the proline-rich i1A region: Dlg1AB and Dlg1B (Chapter 2). The inclusion of the i1A region allows Dlg1AB to associate with tyrosine kinase Lck, and facilitate p38 activation and NFAT-dependent transcription of pro-inflammatory cytokine genes in response to TCR stimulation. In contrast, both Dlg1AB and Dlg1B are equally capable of mediating antigen-dependent degranulation suggesting that direct association with Lck is not required for coordinating these functions (Chapter 2). Here, we showed that Dlg1AB, but not

Dlg1B is phosphorylated in response to TCR stimulation, and that this phosphorylation is dependent on Dlg1-associated Lck. We also identify Y222 as an Lck-dependent phosphorylation site required for TCR-induced p38 activation and downstream transcriptional activation, but not antigen-dependent degranulation. Therefore, we propose that the differential functionality of the two known Dlg1 splice variants is regulated, at least in part, by differential ability to be phosphorylated on tyrosine residues, including Y222.

Scaffold protein structure, and therefore function, is often regulated through a series of phosphorylation and/or ligand-dependent binding events that lead to the gradual unfolding of the scaffold into an active conformation (35, 42, 43). These phosphorylation events are hypothesized to provide molecular memory by creating a primed scaffold capable of binding new ligands; endowing the scaffold with novel and/or heightened functionality upon secondary stimulation. For example, MAGUK family scaffold CARMA1 exists in an auto-inhibited closed conformation in resting T cells. Upon TCR stimulation CARMA1 undergoes a series of PKC θ -mediated phosphorylation events that relieve auto-inhibition, facilitating association with Bcl10 and MALT1 leading to activation of MAPK JNK and transcription factor NF κ B (34, 35, 44). Like CARMA1, Dlg1 forms intramolecular interactions yielding at least two distinct closed conformations hypothesized to impact Dlg1 function by masking ligand-binding sites or affecting the juxtaposition of bound ligands (22, 23). Here we show that tyrosine phosphorylation of Dlg1 in the N-terminal linker region is required for TCR-induced p38 activation. It is likely that phosphorylation at Dlg1 Y222 causes a conformational change required for proper association of Dlg1 with ligands such as Zap70. Alternatively, structural changes could affect the positioning of Dlg1-associated proteins relative to each other, disrupting signal propagation on the scaffold even in the presence of all required ligands.

Utilizing knockdown methodologies several groups have demonstrated a role for Dlg1 in regulating functionality and differentiation in both CD4 and CD8 T cells (4, 5, 7, 18) (Chapter 2). Despite growing evidence for Dlg1 in specifying signal transduction downstream of the TCR, recent attempts by numerous groups to extend these studies to knockout models have been

inconsistent and largely unavailing (38, 45, 46). The mild phenotype seen in these models is attributed to compensation by other Dlg1 family members; such as PSD-95, which is known to have functional redundancy with Dlg1 in neurons (39). Here, we have described an acute Dlg1 knockout system where knockout is induced by expressing cre recombinase in CD8⁺ CTLs from Dlg1^{flox/flox} mice, and TCR-dependent functions are assessed 72hr later. In this system we demonstrate that TCR-triggered p38 activation, NFAT activation, induction of IFN γ and TNF α gene expression and degranulation are impaired in the Dlg1^{KO} cells compared Dlg1^{WT}. We have previously utilized this system to demonstrate that acute Dlg1 knockout impairs T cell function in response to LCMV infection *in vivo* (Chapter 2).

In summary, Dlg1 acts as a key signaling and cytoskeletal regulator downstream of the TCR. Our study reveals a Dlg1 tyrosine phosphorylation as a previously unappreciated mechanism of Dlg1-mediated p38 activation downstream of the TCR. We found that the Dlg1AB splice variant is a direct target of Lck, and that preventing Dlg1AB tyrosine phosphorylation at Y222 leads to a specific loss of p38 activation and up regulation of IFN γ and TNF α genes. Recent studies have demonstrated that both qualitative and quantitative differences in the strength of the TCR interaction with antigen peptide::MHC complex can influence events downstream of the TCR (47). TCR signal strength has been shown to translate into functional differences in mouse model of rheumatoid arthritis (RA) where 'optimal' TCR signal strength leads to increased frequency and severity of disease (48). Additionally, high levels of alternative p38 activation and IFN γ and TNF α production in T cells have been correlated with increased severity of RA and other autoimmune disorders in humans (17). Given these data, it is interesting to imagine that TCR-induced phosphorylation of Dlg1 occurs at times of high antigenic stimulation, acting as a molecular switch turning on p38 dependent functions including pro-inflammatory cytokine production, while low antigenic stimulation would be sufficient to trigger degranulation but not p38 phosphorylation. Given the dependence of autoimmune disorders on the production of pro-inflammatory cytokines, particularly IFN γ and TNF α ,

pharmacologic inhibition of Dlg1 phosphorylation is an intriguing targetable option for more specific treatment of these diseases in the future.

METHODS

Mice

Generation of Dlg1^{flox/flox} mice has been previously described (49). These mice were crossed with C57BL/6 mice expressing the OT-1 TCR. All mice were maintained and used in accordance with the University of California Los Angeles Chancellor's Animal Research Committee.

In vitro kinase assays

OT-1 hybridoma cells (40x10⁶) were lysed using IP Lysis buffer (Pierce) in the presence of protease and phosphatase inhibitors (Pierce). Lysates were cleared by centrifugation and incubated with WT or Y222F GST-Dlg1 fusion proteins bound to glutathione sepharose beads, then washed twice with kinase buffer (Cell Signaling). Resulting bead complexes were incubated at 30°C for 20 minutes in 50µl kinase buffer in the presence or absence of ATP (Cell Signaling). Alternatively, WT or Y222F GST-Dlg1 fusion proteins were bound to glutathione sepharose beads and incubated with recombinant Lck or Zap70 (Active Motif) in 50µl kinase buffer in the presence or absence of ATP at 30°C for 20 minutes.

Dlg1 knockdown and re-expression

Stable Dlg1 knockdown lines were created in both OT-1 hybridomas using a miR-155-based retroviral knockdown vector (29). Sense and anti-sense sequences specific for the 3'UTR region of Dlg1 (5'-GTCCTCCACACTGACACAGAT-3') were cloned in to the miR-155-based knockdown vector. Virus was produced by transfecting 293T cells with 25µg of knockdown vector and 25µg of pCL-Eco vector (Mirus). Resulting virus was used to spin infect OT-1 hybridomas for 90min at 1250g on two consecutive days. Cells were allowed to rest for a day

then assessed for Dlg1 knockdown. Dlg1 was re-introduced into these cell lines using an MSCV-based retroviral vector expressing Dlg1 variants/mutants.

Flow Cytometry

For quantification of intracellular Dlg1: 1×10^6 cells were fixed and permeabilized using FoxP3 staining buffer set (eBioscience 00-5523-00) according to the manufacturer's instructions. Dlg1 was detected using α Dlg1 antibody (BD Biosciences 610875) at 1:1000 followed by Alexa Fluor 647-conjugated donkey anti-mouse IgG F(ab')₂ (Jackson ImmunoResearch 715-606-150) at 1:1000. For measurement of p38 phosphorylation: expanded primary CD8⁺ T cells were harvested, counted and placed in fresh media at a concentration of 2×10^6 cells per ml. Cells were allowed to rest for 4hrs at 37°C in 6-well dishes at volume of 2mls per well and were transferred to 12-well plates coated with 5 μ g anti-CD3 (clone 145-2C11; BD 553057) and 5 μ g anti-CD28 (clone 37.51; BD 553295) with a final volume of 1ml per well (2×10^6 cells) and incubated for 5min or 15min at 37°C to stimulate. Cells were fixed in paraformaldehyde (4% final concentration) for 30min followed by permeabilization using the FoxP3 staining buffer set (eBioscience 00-5523-00) according to manufacturer's instructions. Phosphorylated p38 T180/Y182 was detected using Alexa Fluor 647 conjugated p-p38 antibody (T180/Y182; BD Phosflow 612595) at 1:20. For CD107a staining: primary 1×10^5 CD8⁺ T cells were incubated with EG.7 thymoma cells at indicated concentrations for 2-4hrs in the presence of GolgiPlug, GolgiStop and CD107a-APC antibody (BD 560646). Cells were surface stained using CD8a-PE and fixed. Events were collected using a FACSCalibur (BD Biosciences) and analyzed using FlowJo software.

Immunoprecipitation and immunoblotting

For immunoprecipitation: T cell lysates were first pre-cleared by incubating with 20 μ l 50% (v/v) protein G sepharose beads (GE Healthcare 17-5132-01) for 2hrs at 4°C. Sepharose beads were removed and lysates were incubated with 2 μ g Dlg1 antibody (BD Biosciences 610875) or IgG1k

control antibody (BD Pharmingen 554121) for 1hr at 4°C, then 40µl 50% protein G sepharose beads in PBS were added and incubated over night (~12hrs) at 4°C. Beads were washed and boiled with Laemmle buffer. Blotting was performed using antibodies directed against Dlg1 (BD Biosciences 610875), phosphotyrosine (Millipore, clone 4G10), p38 (clone C20; Santa Cruz SC535), GST (Cell Signaling 2625) or phosphorylated p38 (T180/Y182 clone D3F9; Cell Signaling 4511). Blots were imaged using ECL Plus Western Blotting Substrate (Pierce 32132) or the LiCor Odyssey Imaging System.

Quantitative PCR

RNA was isolated using TriZol reagent as previously described (5). 2µg RNA was reverse-transcribed using Superscript II reverse transcriptase (Invitrogen) according to the manufacturer's instructions using random hexamer and oligo(dT)₂₀ as primers. The iCycler thermocycler was used for quantitative PCR analysis according to manufacturer's instructions (BioRad). A final volume of 25µl was used for each quantitative PCR reactions as previously described(5). The following gene-specific primers were used for amplification: L32(F)-5'-AAG CGAAACTGGCGGAAAC-3', L32(R)-5'-TAACCGATGTTGGGCATCAG-3', NFATc1(F)-5'-GCCTCGTATCAGTGGGCGAAG-3', NFATc1(R)-5'-CGAAGCTCGTATGGACCA-3', IκBα(F)-5'-CTGCAGGCCACCAACTACAA-3', IκBα(R)-5'-CAGCACCCAAAGTCACCAAGT-3', IFNγ(F)-5'-GTCAACAACCCACAGGTCCAG-3', IFNγ(R)-5'-CCTTTTCCGCTTCCTGAGG-3', TNFα(F)-5'-AATGGCCTCCCTCTCATCAGT-3', TNFα(R)-5'-GCTACAGGCTTGCTCACTCGAATT-3', IL-2(F)-5'-CCTGAGCAGGATGGAGAATTACA-3', IL-2(R)-5'-TCCAGAACATGCCGCAGAG-3'. All quantitative PCR products were normalized to ribosomal L32.

Dlg1 Knockout

CD8+T cells were sorted from the spleens of Dlg1^{flox/flox} mice using negative selection (Miltenyi), and expanded on CD3 and CD28 antibody for 72hrs followed by transduction with Cre-expressing retrovirus. Cellular function was tested 5 days after retroviral transduction.

Cytotoxicity

T cell cytotoxicity was determined using the Cyto96 non-radioactive assay (Promega). 10,000 EG.7 thymoma cells were incubated with OT-1 CD8⁺ CTLs at indicated concentrations for 4hrs followed by analysis according to manufacturer's instructions.

gDNA Isolation and Amplification

Genomic DNA was isolated from total splenocytes using a DNeasy Blood and Tissue Kit (Qiagen). PCR amplification of genomic DNA was performed using primers to amplify *dIg1* exon 8.

Statistical methods

Standard deviation was calculated using Microsoft Excel. Statistical significance was obtained with a two-sided student t-test assuming equal variances.

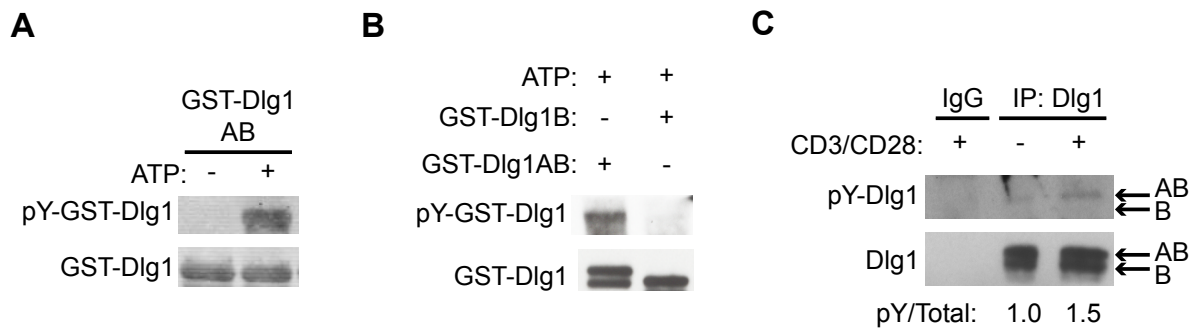


Figure 3-1: A Dlg1-associated kinase phosphorylates Dlg1AB in response to TCR stimulation. (A,B) *In vitro* kinase assay where (A,B) GST-Dlg1AB or (B) GST-Dlg1B fusion proteins were bound to glutathione sepharose beads, and incubated with T cell lysates, centrifuged, washed and incubated with 10mM ATP for 20min at 30°C. Protein complexes were boiled off beads and subjected SDS-PAGE, and blotted using 4G10 (pY-Dlg1) and GST (GST-Dlg1). (B) OT-1 hybridomas were stimulated using 5g/ml CD3 and 5g/ml CD28 followed by cross-linking with donkey anti-armerian hamster antibody for 15min at 37C followed by lysis. Dlg1 was immunoprecipitated from resulting lysates and subjected to SDS-PAGE then blotted using 4G10 (pY-Dlg1) and Dlg1. Blot was quantified using Image J software. Arrows refer to the Dlg1AB and Dlg1B variants.

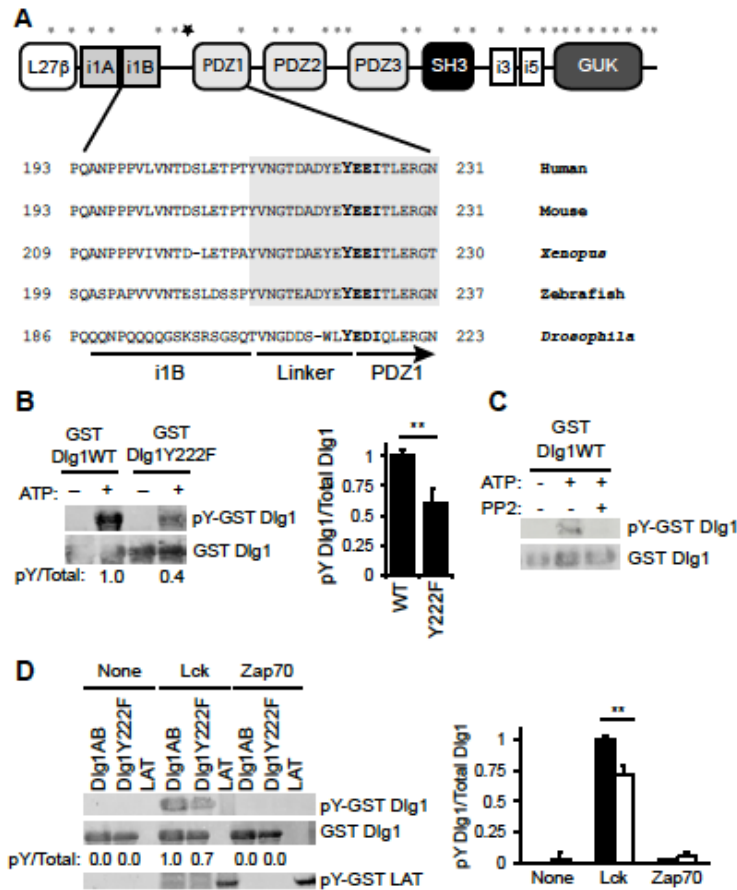


Figure 3-2: Dlg1-associated Lck phosphorylates Dlg1 at position 222. (A) Domain structure of Dlg1. Asterisks indicate the location of the 29 tyrosine residues along the Dlg1 sequence, the bold asterisk indicates the location of Y222. (A, inset) Amino acid sequence alignment of the region of Dlg1 surrounding Y222 from various all species listed in the National Center for Biotechnology Information Database. Shaded region indicates conserved linker region of Dlg1. (B) *In vitro* kinase assays using GST-Dlg1AB WT (wild type) or GST-Dlg1 Y222F (Tyr to Phe mutation) fusion proteins bound to glutathione sepharose beads, and incubated with T cell lysates, centrifuged, washed and incubated with ATP. Protein complexes subjected SDS-PAGE, and blotted using 4G10 (pY-Dlg1) and GST (GST-Dlg1). (C) *In vitro* kinase assay using GST-Dlg1AB fusion proteins bound to glutathione sepharose beads, and incubated with T cell lysates, centrifuged, washed and incubated with ATP in the presence or absence of 10M PP2 inhibitor. Protein complexes were subjected SDS-PAGE, and blotted using 4G10 (pY-Dlg1) and GST (GST-Dlg1). (D) GST-Dlg1AB WT or Y222F fusion proteins were bound to glutathione sepharose beads and incubated with ATP and rLck, rZap70 or buffer only (none). Proteins were subjected to SDS-PAGE and blotted for 4G10 (pY-GST-Dlg1, pY-GST-LAT) or GST (GST-Dlg1). (B right, D right) Blots were quantitated using Li-Cor Odyssey software. pY-Dlg1 was normalized to total Dlg1 for each lane and WT phosphorylation was set to 1.0; error bars represent the standard deviation of four independent experiments, ** p<0.05.

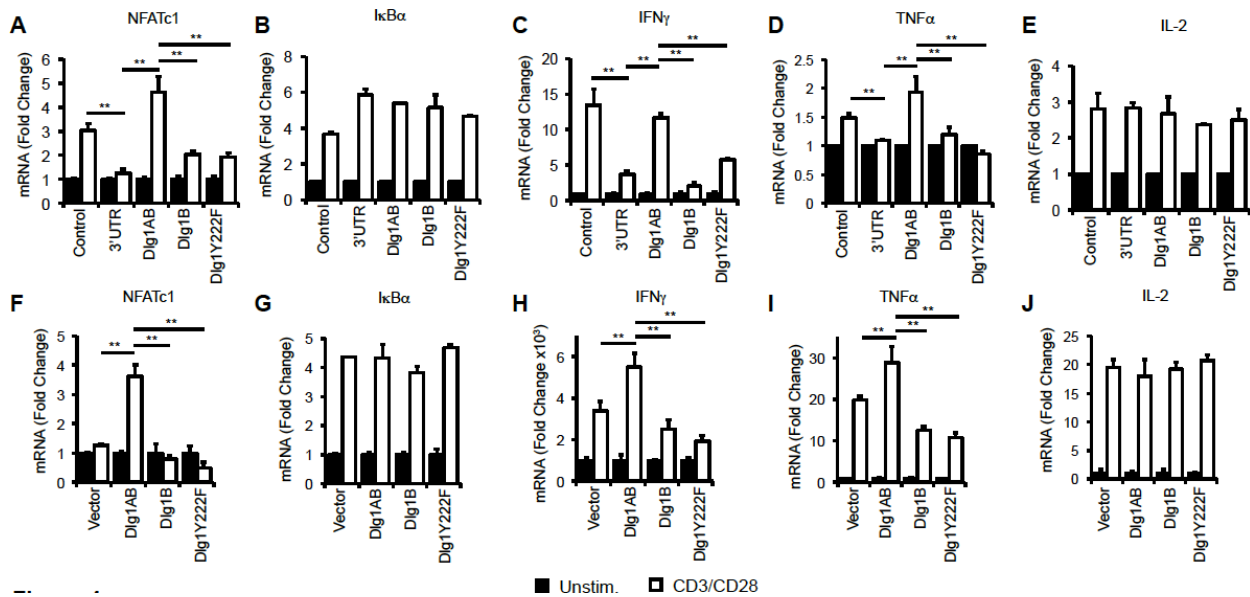


Figure 3-4: Dlg1 Y222 is required for selective induction of TCR-triggered NFAT-, but not NFκB-dependent genes including pro-inflammatory cytokines IFN γ and TNF α . (A-E) Control, Dlg1 deficient OT-1 hybridomas (3'UTR) re-expressing Dlg1AB, Dlg1B, or Dlg1AB Y222F (Dlg1 Y222F). (F-J) CD8+ T cells were isolated from the spleens of OT-1 mice and expanded on plate-bound CD3 and CD28 antibody for 72hrs followed by over expression of Dlg1AB, Dlg1B, Dlg1 Y222F or empty vector (control). (A-J) Cells were stimulated with CD3 and CD28 antibody for 2hrs or 6hrs followed by mRNA isolation, reverse transcription and qPCR analysis using primers for NFATc1 (A,F), IkB α (B,G), IFN γ (C,H), TNF α (D,I) or IL-2 (E,J). All values were normalized to L32 and unstimulated values set to 1.0. Error bars represent stand deviation of triplicates; data is representative of three independent experiments. **p<0.05.

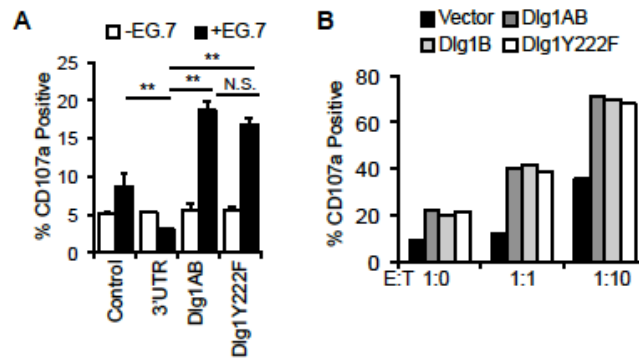


Figure 3-5: Dlg1 Y222 phosphorylation is not required for antigen-dependent CTL degranulation. (A-B) Control, Dlg1 deficient OT-1 hybridomas (3'UTR) re-expressing vector only (3'UTR+Vector), Dlg1AB (3'UTR+Dlg1AB) or Dlg1AB Y222F (3'UTR+Dlg1 Y222F) (A) or CD8+ T cells were isolated from the spleens of OT-1 mice and expanded on plate-bound CD3 and CD28 antibody for 72hrs followed by over expression of Dlg1AB, Dlg1B, Dlg1 Y222F or empty vector (control) cells (B) were incubated with EG.7 thymoma target cells at indicated effector:target (E:T) ratios for 2hrs in the presence of CD107a (LAMP1) antibody. CD107a was assessed by flow cytometry where control cells at E:T of 1:0 was set to 5%. Data is representative of three experiments.

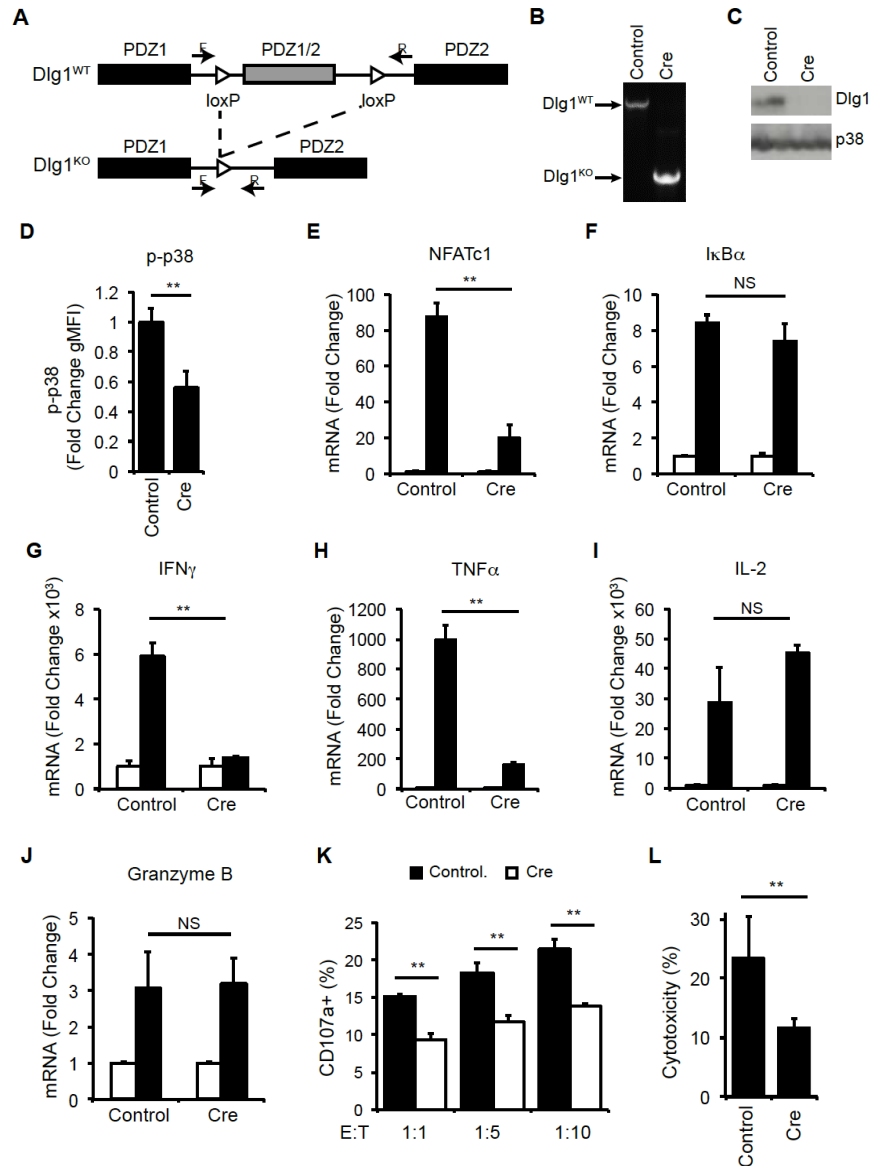


Figure 3-6: Acute Dlg1 KO impairs p38 activation, NFAT-dependent pro-inflammatory cytokines gene expression and target cell lysis in response to TCR stimulation. (A) Genomic organization of Dlg1^{fllox/fllox} mice as previously described (49). F and R refer to the location of the forward and reverse primers for gDNA analysis (B-L) CD8+ T cells isolated from OT-1 Dlg1^{fllox/fllox} splenocytes and expanded on plate-bound CD3 and CD28 antibody for 48-72hrs followed by infection with cre recombinase or vector control. (B) gDNA was isolated and PCR analysis was performed. (C) Whole cell lysates were subjected to SDS-PAGE and blotted for Dlg1 or p38. (D) Cells were stimulated with CD3 and CD28 antibody for 15min followed by staining for p-p38 180/182. Error bars represent standard deviation of three independent experiments. (E-J) Cells were left unstimulated or stimulated with plate-bound CD3 and CD28 for 2hrs (E,F) or 6hrs (G-J) followed by mRNA isolation, reverse transcription and qPCR analysis using primers specific for (E) NFATc1 (F) IκBα (G) IFNγ (H) TNFα (I) IL-2 or (J) granzyme B. All values were normalized to L32 and unstimulated values set to 1.0. Error bars represent stand deviation of triplicates; data is representative of four independent experiments. (K-L) Cells were incubated with EG.7 thymoma cells at indicated ratios for 2hrs followed (K) surface staining for CD107a or (L) LDH cytotoxicity assay. **p<0.05.

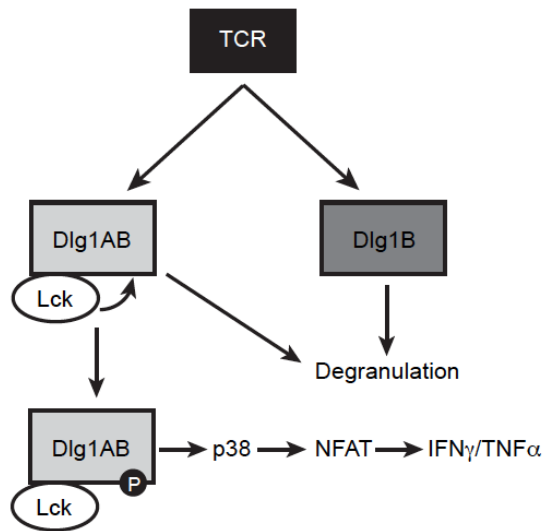


Figure 3-7: Model of Dlg1-dependent signaling downstream of the TCR. In response to TCR engagement Dlg1-bound Lck phosphorylates Dlg1AB at several tyrosine residues including Y222. This phosphorylation event empowers Dlg1 to enhance p38 activation and NFAT-dependent transcription of IFN γ and TNF α . Dlg1AB or Dlg1B are able to facilitate antigen-induced degranulation and target cell killing in a phosphorylation independent manner.

REFERENCES

1. Peng SL, Gerth AJ, Ranger AM, Glimcher LH. 2001. NFATc1 and NFATc2 Together Control Both T and B Cell Activation and Differentiation. *Immunity* 14: 13-20
2. Rutishauser RL, Kaech SM. 2010. Generating diversity: transcriptional regulation of effector and memory CD8+ T-cell differentiation. *Immunological Reviews* 235: 219-33
3. Newell EW, Sigal N, Bendall SC, Nolan GP, Davis MM. 2012. Cytometry by time-of-flight shows combinatorial cytokine expression and virus-specific cell niches within a continuum of CD8+ T cell phenotypes. *Immunity* 36: 142-52
4. Round JL, Tomassian T, Zhang M, Patel V, Schoenberger SP, Miceli MC. 2005. Dlg1 coordinates actin polymerization, synaptic T cell receptor and lipid raft aggregation, and effector function in T cells. *J Exp Med* 201: 419-30
5. Round JL, Humphries LA, Tomassian T, Mittelstadt P, Zhang M, Miceli MC. 2007. Scaffold protein Dlg1 coordinates alternative p38 kinase activation, directing T cell receptor signals toward NFAT but not NF-kappaB transcription factors. *Nat Immunol* 8: 154-61
6. Wang D, You Y, Case SM, McAllister-Lucas LM, Wang L, DiStefano PS, Nunez G, Bertin J, Lin X. 2002. A requirement for CARMA1 in TCR-induced NF-kappa B activation. *Nat Immunol* 3: 830-5
7. Lasserre R, Charrin S, Cuche C, Danckaert A, Thoulouze MI, de Chaumont F, Duong T, Perrault N, Varin-Blank N, Olivo-Marin JC, Etienne-Manneville S, Arpin M, Di Bartolo V, Alcover A. 2010. Ezrin tunes T-cell activation by controlling Dlg1 and microtubule positioning at the immunological synapse. *EMBO J* 29: 2301-14
8. Hanada T, Lin L, Tibaldi EV, Reinherz EL, Chishti AH. 2000. GAKIN, a novel kinesin-like protein associates with the human homologue of the Drosophila discs large tumor suppressor in T lymphocytes. *J Biol Chem* 275: 28774-84
9. Xavier R, Rabizadeh S, Ishiguro K, Andre N, Ortiz JB, Wachtel H, Morris DG, Lopez-Illasaca M, Shaw AC, Swat W, Seed B. 2004. Discs large (Dlg1) complexes in lymphocyte activation. *J Cell Biol* 166: 173-8
10. Ashwell JD. 2006. The many paths to p38 mitogen-activated protein kinase activation in the immune system. *Nat Rev Immunol* 6: 532-40
11. Salvador JM, Mittelstadt PR, Guszczynski T, Copeland TD, Yamaguchi H, Appella E, Fornace AJ, Jr., Ashwell JD. 2005. Alternative p38 activation pathway mediated by T cell receptor-proximal tyrosine kinases. *Nat Immunol* 6: 390-5
12. Mittelstadt PR, Yamaguchi H, Appella E, Ashwell JD. 2009. T cell receptor-mediated activation of p38{alpha} by mono-phosphorylation of the activation loop results in altered substrate specificity. *J Biol Chem* 284: 15469-74
13. Macian F. 2005. NFAT proteins: key regulators of T-cell development and function. *Nat Rev Immunol* 5: 472-84

14. Kaminuma O, Kitamura F, Kitamura N, Hiroi T, Miyoshi H, Miyawaki A, Miyatake S. 2008. Differential Contribution of NFATc2 and NFATc1 to TNF- α Gene Expression in T cells. *Journal of Immunology* 180: 319-26
15. Salvador JM, Hollander MC, Nguyen AT, Kopp JB, Barisoni L, Moore JK, Ashwell JD, Jr AJF. 2002. Mice Lacking the p53-Effector Gene Gadd45a Develop a Lupus-Like Syndrome. *Immunity* 16: 499-508
16. Salvador JM, Mittelstadt PR, Belova GI, Fornace AJ, Jr., Ashwell JD. 2005. The autoimmune suppressor Gadd45 α inhibits the T cell alternative p38 activation pathway. *Nat Immunol* 6: 396-402
17. Lopez-Santalla M, Salvador-Bernaldez M, Gonzalez-Alvaro I, Castaneda S, Ortiz AM, Garcia-Garcia MI, Kremer L, Roncal F, Mulero J, Martinez AC, Salvador JM. 2011. Tyr323-dependent p38 activation is associated with rheumatoid arthritis and correlates with disease activity. *Arthritis Rheum* 63: 1833-42
18. Zanin-Zhorov A, Lin J, Scher J, Kumari S, Blair D, Hippen KL, Blazar BR, Abramson SB, Lafaille JJ, Dustin ML. 2012. Scaffold protein Disc large homolog 1 is required for T-cell receptor-induced activation of regulatory T-cell function. *Proc Natl Acad Sci U S A* 109: 1625-30
19. Jirmanova L, Sarma DN, Jankovic D, Mittelstadt PR, Ashwell JD. 2009. Genetic disruption of p38 α Tyr323 phosphorylation prevents T-cell receptor-mediated p38 α activation and impairs interferon- γ production. *Blood* 113: 2229-37
20. Jirmanova L, Giardino Torchia ML, Sarma ND, Mittelstadt PR, Ashwell JD. 2011. Lack of the T cell-specific alternative p38 activation pathway reduces autoimmunity and inflammation. *Blood* 118: 3280-9
21. Martinez NM, Pan Q, Cole BS, Yarosh CA, Babcock GA, Heyd F, Zhu W, Ajith S, Blencowe BJ, Lynch KW. 2012. Alternative splicing networks regulated by signaling in human T cells. *RNA* 18: 1029-40
22. Tully MD, Grossmann JG, Phelan M, Pandelaneni S, Leyland M, Lian LY. 2012. Conformational characterization of synapse-associated protein 97 by nuclear magnetic resonance and small-angle X-ray scattering shows compact and elongated forms. *Biochemistry* 51: 899-908
23. Wu H, Reissner C, Kuhlendahl S, Coblenz B, Reuver S, Kindler S, Gundelfinger ED, Garner CC. 2000. Intramolecular interactions regulate SAP97 binding to GKAP. *EMBO J* 19: 574-5751
24. Hanada T, Lin L, Chandy KG, Oh SS, Chishti AH. 1997. Human Homologue of the Drosophila Discs Large Tumor Suppressor Binds to p56lck Tyrosine Kinase and Shaker Type Kv1.3 Potassium Channel in T Lymphocytes. *Journal of Biological Chemistry* 272: 26899-904
25. Sabio G, Simon J, Arthur C, Kuma Y, Peggle M, Carr J, Murray-Tait V, Centeno F, Goesdert M, Morrice NA, Cuenda A. 2005. p38 γ regulates the localisation of SAP97 in the cytoskeleton by modulating its interaction with GKAP. *EMBO J* 24: 1134-45

26. Gardoni F, Mauceri D, Fiorentini C, Bellone C, Missale C, Cattabeni F, Di Luca M. 2003. CaMKII-dependent phosphorylation regulates SAP97/NR2A interaction. *J Biol Chem* 278: 44745-52
27. Mantovani F, Banks L. 2003. Regulation of the discs large tumor suppressor by a phosphorylation-dependent interaction with the beta-TrCP ubiquitin ligase receptor. *J Biol Chem* 278: 42477-86
28. Narayan N, Massimi P, Banks L. 2009. CDK phosphorylation of the discs large tumour suppressor controls its localisation and stability. *Journal of Cell Science* 122: 65-74
29. O'Connell RM, Chaudhuri AA, Rao DS, Baltimore D. 2009. Inositol phosphatase SHIP1 is a primary target of miR-155. *Proc Natl Acad Sci U S A* 106: 7113-8
30. Obenauer JC. 2003. Scansite 2.0: proteome-wide prediction of cell signaling interactions using short sequence motifs. *Nucleic Acids Research* 31: 3635-41
31. Granum S, Andersen TC, Sorlie M, Jorgensen M, Koll L, Berge T, Lea T, Fleckenstein B, Spurkland A, Sundvold-Gjerstad V. 2008. Modulation of Lck function through multisite docking to T cell-specific adapter protein. *J Biol Chem* 283: 21909-19
32. Isakov N, Wange RL, Burgess WH, Watts JD, Aebersold R, Samelson LE. 1995. ZAP-70 Binding Specificity to T Cell Receptor Tyrosine-based Activation Motifs: The Tandem SH2 Domains of ZAP-70 Bind Distinct Tyrosine-based Activation Motifs with Varying Affinity. *Journal of Experimental Medicine* 181: 375-80
33. Yaffe MB. 2002. Phosphotyrosine-binding domains in signal transduction. *Nat Rev Mol Cell Biol* 3: 177-86
34. Matsumoto R, Wang D, Blonska M, Li H, Kobayashi M, Pappu B, Chen Y, Wang D, Lin X. 2005. Phosphorylation of CARMA1 plays a critical role in T Cell receptor-mediated NF-kappaB activation. *Immunity* 23: 575-85
35. Sommer K, Guo B, Pomerantz JL, Bandaranayake AD, Moreno-Garcia ME, Ovechkina YL, Rawlings DJ. 2005. Phosphorylation of the CARMA1 linker controls NF-kappaB activation. *Immunity* 23: 561-74
36. Lue RA, Brandin E, Chan EP, Branton D. 1996. Two independent domains of hDlg are sufficient for subcellular targeting: the PDZ1-2 conformational unit and an alternatively spliced domain. *J Cell Biol* 135: 1125-37
37. Funke L, Dakoji S, Bredt DS. 2005. Membrane-associated guanylate kinases regulate adhesion and plasticity at cell junctions. *Annu Rev Biochem* 74: 219-45
38. Humphries LA, Shaffer MH, Sacirbegovic F, Tomassian T, McMahon KA, Humbert PO, Silva O, Round JL, Takamiya K, Haganir RL, Burkhardt JK, Russell SM, Miceli MC. 2012. Characterization of in vivo Dlg1 deletion on T cell development and function. *PLoS One* 7: e45276
39. Schluter OM, Xu W, Malenka RC. 2006. Alternative N-terminal domains of PSD-95 and SAP97 govern activity-dependent regulation of synaptic AMPA receptor function. *Neuron* 51: 99-111

40. Walter U, Santamaria P. 2005. CD8+ T cells in autoimmunity. *Curr Opin Immunol* 17: 624-31
41. Shin H, Wherry EJ. 2007. CD8 T cell dysfunction during chronic viral infection. *Curr Opin Immunol* 19: 408-15
42. Torres E, Rosen MK. 2003. Contingent Phosphorylation/Dephosphorylation Provides a Mechanism of Molecular Memory in WASP. *Molecular Cell* 11: 1215-27
43. Brenner D, Brechmann M, Rohling S, Tapernoux M, Mock T, Winter D, Lehmann WD, Kiefer F, Thome M, Krammer PH, Arnold R. 2009. Phosphorylation of CARMA1 by HPK1 is critical for NF-kappaB activation in T cells. *Proc Natl Acad Sci U S A* 106: 14508-13
44. Rawlings DJ, Sommer K, Moreno-Garcia ME. 2006. The CARMA1 signalosome links the signalling machinery of adaptive and innate immunity in lymphocytes. *Nat Rev Immunol* 6: 799-812
45. Stephenson LM, Sammut B, Graham DB, Chan-Wang J, Brim KL, Huett AS, Miletic AV, Kloepfel T, Landry A, Xavier R, Swat W. 2007. DLG1 is a negative regulator of T-lymphocyte proliferation. *Mol Cell Biol* 27: 7574-81
46. Gmyrek GB, Graham DB, Sandoval GJ, Blaufuss GS, Akilesh HM, Fujikawa K, Xavier RJ, Swat W. 2013. Polarity gene discs large homolog 1 regulates the generation of memory T cells. *Eur J Immunol* 43: 1185-94
47. Corse E, Gottschalk RA, Allison JP. 2011. Strength of TCR-peptide/MHC interactions and in vivo T cell responses. *J Immunol* 186: 5039-45
48. Olasz K, Boldizsar F, Kis-Toth K, Tarjanyi O, Hegyi A, van Eden W, Rauch TA, Mikecz K, Glant TT. 2012. T cell receptor (TCR) signal strength controls arthritis severity in proteoglycan-specific TCR transgenic mice. *Clin Exp Immunol* 167: 346-55
49. Zhou W, Zhang L, Guoxiang X, Mojsilovic-Petrovic J, Takamaya K, Sattler R, Haganir R, Kalb R. 2008. GluR1 controls dendrite growth through its binding partner, SAP97. *J Neurosci* 28: 10220-33

CHAPTER FOUR

The Scaffolding Protein Synapse-Associated Protein 97 (SAP97/DLG1) is required for
Enhanced Signaling Through Isotype-Switched IgG Memory B cell Receptors

ABSTRACT

After their first encounter with a foreign antigen, naïve B cells that have immunoglobulin M (IgM) B cell receptors (BCRs) trigger the primary antibody response and the generation of memory B cells with IgG BCRs. When these memory B cells reencounter the same antigen, the cell surface IgG BCRs stimulate their rapid differentiation into plasma cells that release large amounts of IgG antibodies. We showed that the conserved cytoplasmic tail of the IgG BCR, which contains a putative PDZ (postsynaptic density 95/disc large/zona occludens 1)–binding motif, associated with synapse-associated protein 97 (SAP97/Dlg1), a PDZ domain–containing scaffolding molecule that is involved in controlling receptor density and signal strength at neuronal synapses. SAP97 accumulated and bound to IgG BCRs in the immunological synapses that formed in response to B cell engagement with antigen. Knocking down SAP97 in IgG+ B cells or mutating the putative PDZ-binding motif in the BCR tail impaired formation of the immunological synapse, initiation of IgG BCR signaling, and downstream activation of the mitogen-activated protein kinase p38. Thus, heightened B cell memory responses are encoded, in part, by a mechanism that involves SAP97 serving as a scaffolding protein in the IgG BCR immunological synapse.

INTRODUCTION

Memory responses are characterized by the rapid production of high-affinity, class-switched antibodies, which are predominantly of immunoglobulin G (IgG) subclasses. Antibody memory is encoded, in part, in memory B cells that are generated during an individual's first encounter with an antigen and have high-affinity IgG B cell receptors (BCRs). In contrast, naïve B cells, which give rise to primary antibody responses upon the first encounter with antigen, have IgM and IgD BCRs (1). It has long been suspected that differences in the signaling capacities of IgM and IgG BCRs might account for the accelerated, high-titer antibody memory responses compared to primary responses. However, IgM and IgG BCRs are both composed of a membrane-bound form of Ig (mIg) that associates in a 1:1 molar ratio with a heterodimer of Ig α and Ig β , which contain immunoreceptor tyrosine-based activation motifs (ITAMs) in their cytoplasmic domains that are phosphorylated upon antigen binding to initiate signaling (2). Thus, differences in the signaling capacities of IgM and IgG BCRs must reflect functional differences in mIgM and mIgG. Indeed, in addition to differences in the extracellular domains of mIgM and mIgG, mIgM has no cytoplasmic tail, with just 3 amino acids predicted to face the cytoplasm; in contrast, all mIgG subtypes have highly conserved cytoplasmic tails consisting of 28 amino acids. Early studies *in vivo* with transgenic mouse models demonstrated that the cytoplasmic tail of mIgG was both necessary and sufficient for enhanced IgG memory antibody responses (3, 4). Biochemical studies suggested that the mIgG tail served to enhance Ca²⁺ responses in BCR signaling relative to that induced by mIgM (5–7). Comparing antigen-induced gene transcription profiles, Horikawa et al. showed that gene activation in mIgG-expressing (IgG+) B cells was qualitatively different from that in mIgM-expressing (IgM+) B cells (5), with most of the gene expression induced in IgM+ B cells being diminished in IgG+ B cells. However, the molecular mechanism by which the mIgG cytoplasmic tail enhances the response of IgG BCR-expressing B cells is incompletely understood.

Waisman et al. (6) showed that the cytoplasmic tail of mIgG was able to partially replace the requirement for the Ig α and Ig β heterodimer during B cell development, which suggested the

possibility that the cytoplasmic tail of mIgG independently interacted with cytoplasmic BCR signaling-related molecules. The first evidence for a direct interaction between the cytoplasmic tail of IgG and a component of the BCR signaling cascade came from Engels et al. (8), who showed that a conserved Ig tail tyrosine (ITT) motif in the cytoplasmic domain of both mIgG and mIgE was phosphorylated upon cross-linking of IgG BCRs, which resulted in the recruitment of the adaptor protein Grb2 and the enhancement of Ca^{2+} responses and B cell proliferation. This result indicated that once BCR signaling was initiated, the mIgG cytoplasmic tail functioned to enhance downstream signaling, raising the question of whether the mIgG cytoplasmic tail played a fundamental role in initiating signaling and forming the immunological synapse in IgG+ memory B cells.

Our understanding of the molecular events that initiate antigen-driven BCR signaling that lead to the formation of an immunological synapse has advanced markedly with the use of total internal reflection fluorescence (TIRF) microscopy to image B cells as they first encounter antigen incorporated into lipid bilayers (9, 10). These studies provided evidence for an ordered series of events beginning with BCR oligomerization and microcluster formation, which triggered a dynamic spreading of the B cell over the bilayer and the formation of new microclusters, which was ultimately followed by a contraction event that concentrated the BCRs in an ordered immunological synapse. We previously compared the initiation of BCR signaling for IgM and IgG BCRs, and provided evidence that compared to IgM BCRs, IgG BCRs were enhanced in their ability to oligomerize and form active signaling BCR clusters and immunological synapses (11). We further showed that the enhanced antigen-induced clustering of IgG BCRs was dependent on the membrane-proximal 15 amino acid residues of the mIgG cytoplasmic tail, a region that does not overlap with the ITT motif described by Engels et al. (8) and had not been previously implicated in IgG BCR signaling. Here, we report that a member of the membrane-associated guanylate kinase (MAGUK) family, synapse-associated protein 97 (SAP97), is a binding partner of the membrane-proximal region of the cytoplasmic tail of mIgG and functions to enhance the

accumulation of IgG BCRs in the B cell immunological synapse, which results in heightened signaling by IgG⁺ memory B cells.

RESULTS

The cytoplasmic tail of mIgG binds to SAP97

We recently determined that the 15–amino acid membrane-proximal region of the mouse mIgG tail (Figure 4-1) was both necessary and sufficient for the enhanced microclustering and signaling of IgG BCRs at the immunological synapse compared to that of IgM BCRs (11). We noted that this membrane-proximal region contained the evolutionarily conserved sequence SSVV, which is a putative type I postsynaptic density 95 (PSD95)/disc large (Dlg)/zona occludens 1 (PDZ) domain–binding motif (X-S/T-X-V) (12, 13). PDZ domains are protein interaction domains often found in multidomain scaffolding proteins that serve to assemble specific proteins into large complexes at defined locations in the cell. The SSVV sequence is conserved in all mIgG subtypes in both humans and mice and in all known mammalian IgG cytoplasmic tail sequences, including platypus mIgG2 (Figure 4-1). Even the lizard mIgY contains a sequence that fits the PDZ domain–binding motif. We also examined the sequences of the cytoplasmic tails of mouse mIgA and mIgE, both of which can be expressed as BCRs; however, neither tail shares sequence similarity with the mIgG tails nor contains a putative PDZ domain–binding motif.

To search for potential PDZ domain–containing binding partners for the mIgG tail, we performed immunoprecipitations of lysates of J558L cells (a mouse B cell myeloma cell line) with either a biotin-conjugated, membrane-proximal 15–amino acid peptide that contained the SSVV motif (N15SSVV) bound to streptavidin beads or a control biotin-conjugated peptide in which SSVV was changed to GGGG (N15GGGG). N15SSVV immunoprecipitated a 130-kD protein, which was absent in N15GGGG immunoprecipitates, that was recognized by a monoclonal antibody (mAb) that broadly recognizes members of the PDZ domain–containing MAGUK family (anti–PAN-MAGUK) (12) (Figure 4-2). The anti–PAN-MAGUK mAb itself

immunoprecipitated a 130-kD protein from mouse B cell lysates that was identified as SAP97 by liquid chromatography–mass spectrometry (LC-MS) sequencing (Figure 4-2). A SAP97-specific mAb recognized the 130-kD protein in the N15SSVV immunoprecipitate from lysates of A20 II1.6 cells (a mouse B cell line), which was absent in the samples immunoprecipitated with N15GGGG (Figure 4-2). Collectively, these results suggested that SAP97 was a binding partner for the 15–amino acid, membrane-proximal peptide within the cytoplasmic tail of mIgG. SAP97 is a member of a subfamily of MAGUK proteins that consists of four proteins, PSD95, PSD93, SAP102, and SAP97. Of these, B cells have predominantly SAP97, as determined by quantitative real-time polymerase chain reaction (PCR) analysis of mouse B cell lines and primary splenic B cells (Figure 4-3).

SAP97 and other members of the MAGUK family have been best characterized in neurons, where they play an essential role as synaptic scaffolding proteins in controlling the density, localization, and clustering of glutamate receptors and ion channels at the synapse, and by so doing control excitatory synaptic transmission (12, 13). SAP97 contains an N-terminal L27 domain and a proline (P)–, glutamic acid (E)–, serine (S)–, and threonine (T)–rich (PEST) domain, three PDZ domains, and a C-terminal Src homology 3 (SH3)–GUK domain (Figure 4-4) (12, 13). To characterize the binding of SAP97 to the mIgG tail, we generated full-length SAP97 (FL-SAP97) as well as the three PDZ domains (PDZ123) and the C-terminal (CT) SH3-GUK domain of SAP97 as glutathione S-transferase (GST) fusion proteins (Figure 4-4). By enzyme-linked immunosorbent assay (ELISA) in which N12SSVV or N12GGGG was coated onto the assay plates, we observed that both FL-SAP97 and the PDZ123 construct bound selectively to N12SSVV (Figure 4-4). The extent of binding of FL-SAP97 to N12SSVV was weaker than that of the PDZ123 domains of SAP97, which may be because of incomplete folding of the FL-SAP97 expressed in *E. coli*. Indeed, the PSD95 subfamily of PDZ scaffold proteins fold into compact structures and form N-terminal head-to-head multimers that may be essential to their function (12, 13). Such folding may not be achieved in proteins produced in *E. coli*. Neither the C-terminal SH3-GUK domain nor the GST control bound to either peptide (Figure 4-4). We also

performed GST pull-down assays from detergent lysates of A20 II1.6 cells with GST, GST-PDZ123, GST-CT, and GST-FL-SAP97 constructs (Figure 4-4). When 10 to 20 μ l of the pull-down eluates were used, we observed selective binding of Ig to GST-PDZ123 compared to GST alone (Figure 4-4). In separate experiments, we observed selective binding of Ig to GST-FL-SAP97 compared to GST alone, but only by loading larger amounts of the pull-down eluates for SDS-polyacrylamide gel electrophoresis (SDS-PAGE) (Figure 4-4), consistent with the weak binding of GST-FL-SAP97 to the N15SSVV peptide as determined by ELISA (Figure 4-4).

IgG BCRs induce increased accumulation of SAP97 in the immunological synapse

We determined the subcellular location of the BCR and SAP97 by confocal microscopic analysis of B cells placed on fluid lipid bilayers that either did or did not contain antigen (Figure 4-5). After 10 min on the bilayers, cells were fixed, permeabilized, and stained with fluorescently tagged antibodies specific for the BCR or SAP97. In the absence of antigen, the BCRs were dispersed over the B cell surface (Figure 4-5). SAP97 was located at the plasma membrane, but, in contrast to the BCR, SAP97 showed a clear polarization toward the interface of the B cell and the bilayer (Figure 4-5). In the presence of antigen in the bilayer, the BCRs accumulated in the immunological synapse at the interface with the bilayer, as previously described (14, 15), and SAP97 appeared to show an increased accumulation in the immunological synapse.

We used TIRF microscopy to quantify the accumulation of the BCR and SAP97 in the B cell immunological synapse (Figure 4-5). We imaged a series of J558L cell lines expressing either wild-type mIgG-BCR (IgG wild type), a mutant mIgG-BCR in which the mIgG tail was composed of only the membrane-proximal 15 amino acids (IgG-N15), a mutant mIgG-BCR that contained the cytoplasmic tail of mIgM (IgG-CytoM), or wild-type mIgM-BCR (IgM wild type). All four cell lines showed similar amounts of cell surface BCR as measured by flow cytometric analysis of the binding of the antigen NP16-BSA (bovine serum albumin) to the BCR (Figure 4-3). When placed on membrane lipid bilayers that did not contain antigen, there was no obvious accumulation of the BCR at the interface of the B cell and the bilayer for any of the B

cell lines (Figure 4-5). In contrast, a portion of SAP97 was present at the interface of the B cell and the bilayer in similar amounts in all of the B cell lines (Figure 4-5). When placed on antigen-containing bilayers, BCRs rapidly accumulated at the immunological synapse, and B cells expressing BCRs containing mIgG tails (either IgG wild type or IgG-N15) showed the accumulation of substantially increased amounts of BCR at the immunological synapse than did B cells expressing BCRs containing mIgM cytoplasmic tails (either IgM wild type or IgG-CytoM) (Figure 4-5), as previously reported (11). The amount of SAP97 in the immunological synapse was also substantially increased with BCR antigen engagement, but only in B cells expressing BCRs with mIgG cytoplasmic tails (IgG wild type) or BCRs with the mIgG membrane-proximal 15–amino acid tails (IgG-N15) (Figure 4-5). Collectively, these results provide evidence that SAP97 is associated with the plasma membrane in resting B cells and that it polarizes toward the region of contact between the cell and the bilayer in an antigen-independent manner. Upon BCR-antigen engagement and immunological synapse formation, SAP97 further accumulated in the immunological synapse in B cells expressing BCRs containing the membrane-proximal region of the mIgG cytoplasmic tail.

The observation that engagement of the IgG BCR with antigen resulted in increased accumulation of SAP97 in the immunological synapse raised the question of whether SAP97 and IgG BCRs were colocalized or possibly in contact in the immunological synapse. A Pearson's correlation analysis of two-color TIRF images showed a greater degree of colocalization of the IgG wild type BCR and IgG-N15 BCR with SAP97 than that of IgM wild type BCRs and IgG-CytoM BCRs with SAP97 (Figure 4-6). To determine whether the IgG BCRs were in contact with SAP97, we used fluorescence resonance energy transfer (FRET) combined with fluorescence lifetime imaging microscopy (FLIM), taking advantage of the feature that FRET measured by FLIM is independent of changes in donor or receptor concentration, excitation intensity, and other factors that limit sensitized fluorescence intensity-based measurements (16). To do so, we generated J558L cells that expressed yellow fluorescent protein (YFP)-tagged SAP97 (YFP-SAP97) and cyan fluorescent protein (CFP)-tagged mIgG

(mIgG-CFP) by cotransfecting J558L B cells that stably expressed endogenous Ig β and Ig λ light chain and a plasmid containing Ig α with plasmids containing YFP-SAP97 and mIgG-CFP. The fluorescence lifetime of the CFP molecule was measured with a Becker & Hickl time-correlated single-photon counting device linked to a confocal fluorescence microscope equipped with a two-photon-pulsed laser. Upon antigen binding, the lifetime of CFP fluorescence was substantially reduced, indicating that BCR clustering and immunological synapse formation induced the close molecular proximity of YFP-SAP97 and mIgG-CFP (Figure 4-6), supporting the conclusion that SAP97 binds to the tail of antigen-engaged IgG BCRs in living B cells. In control experiments, J558L B cells stably expressing Ig β , Ig α , and Ig λ light chains that were transfected with plasmid encoding mIgG-CFP alone showed no substantial reduction in the lifetime of CFP fluorescence upon antigen engagement (Figure 4-6), indicating that the reduced fluorescence lifetime was not a result of quenching of clustered BCRs.

We also imaged the spatial distribution and colocalization of the BCR and SAP97 in primary human IgM⁺ and IgG⁺ B cells isolated from the peripheral blood of healthy donors by negative selection. We found that SAP97 protein was similarly abundant in human IgM⁺ and IgG⁺ B cells (Figure 4-3). We recently showed, with F(ab')₂ antibodies specific for human IgG and IgM (H + L) F(ab')₂ anti-Ig or for human κ light chain to cross-link the BCRs, that human IgG⁺ memory B cells are more robust than naïve B cells at each step in the initiation of B cell activation, including the accumulation of BCR in the synapse and the recruitment and activation of signaling-associated kinases (17). Here, we labeled B cells with fluorescently tagged Fab goat antibodies specific for human IgM or IgG and placed them for 10 min on fluid lipid bilayers that did or did not contain F(ab')₂ anti-Ig to cross-link the BCRs. The cells were permeabilized and stained with fluorescently labeled anti-PAN-MAGUK mAb and imaged by TIRF microscopy (Figure 4-7). In the absence of BCR cross-linking, little BCR, either IgM or IgG, accumulated at the interface of the B cells and the bilayer (Figure 4-7). BCR cross-linking resulted in the accumulation of BCRs in the immunological synapse, with the IgG BCR substantially more abundant than the IgM BCR (Figure 4-7), as shown previously (17). In the absence of BCR

cross-linking, similar amounts of SAP97 were present at the interface between either IgM- and IgG-expressing cells and the bilayer (Figure 4-7). BCR cross-linking induced an increase in the amount of SAP97 in the immunological synapse, but only in IgG-expressing B cells (Figure 4-7). In resting B cells, IgM BCRs and IgG BCRs showed low but similar extents of colocalization with SAP97 (Figure 4-7). Upon BCR cross-linking, the colocalization increased in both cases; however, the extent of colocalization of IgG BCRs with SAP97 was substantially greater than that of IgM BCRs (Figure 4-7). Thus, consistent with the earlier experiment with mouse J558L cell lines, in the context of human primary and isotype-switched memory B cells, SAP97 accumulated in the immunological synapse after cross-linking of IgG BCRs to a substantially greater degree and showed enhanced colocalization with IgG BCRs than with IgM BCRs.

The enhanced initiation of IgG-BCR signaling is SAP97-dependent

To determine whether SAP97 was necessary for the enhanced accumulation of IgG BCRs into the B cell immunological synapse, we knocked down SAP97 by short interfering RNA (siRNA) in IgG+ A20 II1.6 B cells. The abundance of SAP97 protein was decreased by >60% after transfection with a Thermal ON-TARGETplus SMARTpool siRNA SAP97 construct compared to that in cells transfected with a control, nontargeted siRNA construct (Figures 4-8 & 4-9), although both sets of cells maintained comparable amounts of surface IgG BCRs, as assessed by flow cytometry (Figure 4-8). Cells were placed on lipid bilayers containing F(ab')₂ anti-IgG to cross-link the BCRs, and the accumulation of IgG BCRs and phosphorylated Syk (pSyk), one of the earliest kinases recruited to BCR microclusters, in the immunological synapse was imaged by TIRF microscopy. We observed a marked reduction in the amounts of IgG BCRs and pSyk recruited to the immunological synapse of B cells in which SAP97 was knocked down compared to those of the control cells (Figure 4-8). Through correlation analyses, we determined that within the immunological synapse, the mean fluorescence intensity (MFI) of IgG BCRs was substantially positively correlated with the MFI of SAP97 (Figure 4-9).

We obtained similar results investigating the SAP97 dependence of the enhanced accumulation of IgG-BCRs into the immunological synapse in J558L cells stably expressing the reconstructed IgG-BCR (IgG wild type BCR) containing the B1-8-High heavy chain that binds to the small hapten, nitrophenol (NP) with high affinity (11). With a pSuper plasmid construct targeting SAP97 (18), we generated two stable sublines (clones 13 and 24) in which the abundance of SAP97 was decreased by more than 80% compared to that of control cells expressing nontargeting, scrambled siRNAs (Figure 4-10). Both sublines showed equivalent binding to the antigen NP16-BSA by flow cytometry (Figure 4-10), indicating similar cell surface abundances of the BCR. We found a marked impairment in the accumulation of IgG-BCRs and pSyk in the immunological synapse in clone 13 and 24 cells compared to that of control cells (Figure 4-10).

To ensure that the observed reduction in the accumulation of the BCR in cells with decreased abundance was specific to IgG BCRs, we initially transfected mouse CH27 B cells expressing phosphocholine (PC)-specific IgM BCRs with the Thermal ON-TARGETplus SMARTpool siRNA SAP97 construct. However, we found that SAP97 abundance was reduced by only about 40%, probably as a result of the relatively low transfection efficiency of CH27 cells. Thus, we used the pSuper plasmid construct, which specifically interferes with the translation of SAP97 mRNA (18). After puromycin screening and selection, we obtained a cell line in which SAP97 protein abundance was reduced by >70% compared to that in CH27 cells transfected with the control scrambled siRNA (Figure 4-9), although both lines maintained similar amounts of cell surface BCR as assessed by flow cytometry (Figure 4-9). We imaged the accumulation of IgM BCRs, SAP97, and pSyk in the immunological synapse of SAP97 knockdown CH27 B cells (SAP97 KD cells) placed on lipid bilayers containing the antigen BSA-PC10 and observed a substantial reduction in the amount of SAP97 that accumulated in the immunological synapse compared to that of the control cells (Figure 4-9). However, we did not observe a substantial difference in the antigen-induced accumulation of IgM BCRs and pSyk in the immunological synapse of control and SAP97 KD cells (Figure 4-9).

We next determined whether the SSVV motif in the mIgG cytoplasmic tail was required for the enhanced accumulation of IgG BCRs in the immunological synapse. To do so, we cotransfected J558 cells stably expressing endogenous Ig β and Ig λ light chains and transfected with a plasmid expressing Ig α -YFP with plasmids expressing wild-type IgG, mIgG with the SSVV tail motif mutated to AAAA (IgG-SSVV/AAAA), or the IgG CytoM construct (Figure 4-11). We first determined the amount of cell surface BCR by epifluorescence imaging and subsequently switched to a TIRF mode to quantify the accumulation of IgG-BCRs in the immunological synapse (Figure 4-11). Although all three cell lines had similar amounts of BCRs on their surfaces (Figure 4-11), cells expressing either IgG-SSVV/AAAA BCRs or IgG-CytoM BCRs showed substantially reduced accumulation of SAP97 and pSyk in the immunological synapse compared to that of cells expressing IgG wild type BCRs (Figure 4-11). Moreover, cells expressing the IgG-SSVV/AAAA BCRs and SAP97 showed significantly less colocalization of the BCRs and SAP97 compared to cells expressing IgG wild type BCRs and SAP97 ($P < 0.0001$) (Figure 4-12). These findings indicate a requirement for the evolutionarily conserved SSVV motif in the mIgG tail for the colocalization of the IgG BCR with SAP97 and the enhanced immunological synapse formation of cells expressing IgG BCRs.

SAP97 is required for signaling downstream of the BCR, including activation of p38

We also wanted to determine the effect of knocking down SAP97 on signaling downstream of the BCR. Because SAP97 is required for the activation of p38 mitogen-activated protein kinase (MAPK) in activated T cells (19), we determined the effect of SAP97 deficiency on MAPK activation after cross-linking of IgG BCRs. We activated A20 II1.6 SAP97 KD cells and control cells by cross-linking their BCRs with F(ab')₂ anti-IgG F(ab')₂ in solution. Knockdown of SAP97 did not affect the phosphorylation of c-Jun N-terminal kinase (JNK) or extracellular signal-regulated kinase (ERK); however, we found that the phosphorylation of p38 MAPK at Thr180 and Tyr182, an indication of p38 MAPK activation, was substantially decreased in SAP97 KD cells compared to that in control cells (Figure 4-13). This finding is similar to that in

T cells in which knockdown of SAP97 blocked T cell receptor (TCR)–induced activation of p38 (19). In neuronal cells, members of the PSD95 subfamily of MAGUK proteins regulate the activity of membrane proteins by influencing their surface abundance and endocytosis (13). Consequently, we also characterized the internalization of the BCR after cross-linking of the BCR in A20 II1.6 SAP97 KD cells and control cells. Knockdown of SAP97 accelerated the rate of cross-linking–induced BCR internalization (Figure 4-13), which suggested that SAP97 might function to retain BCR-antigen signaling complexes at the plasma membrane.

DISCUSSION

Here, we provide evidence that SAP97 associates with the membrane-proximal region of the cytoplasmic tail of mIgG and that through this interaction it acts to enhance the initiation of early signaling and immunological synapse formation in class-switched IgG⁺ B cells, which led to enhanced signaling. These results place isotype switching at a critical tipping point in B cell activation that ensures the enhanced initiation of IgG⁺ B cell responses through SAP97. The importance of the interaction of the mIgG tail and SAP97 for the biology of IgG⁺ B cells is reflected in the degree of conservation of the membrane-proximal region of the IgG tail and the PDZ-binding motif among all known mammalian mIgGs and lizard mIgY-BCRs. The functions of SAP97 and other members of the family of MAGUK scaffold proteins are best understood in neuronal cells, in which SAP97 plays an essential role in controlling the density, localization, and clustering of glutamate receptors and ion channels at the synapse and by doing so controls the size and transmission strength of excitatory synapses (12, 13, 20). Our results suggest a similar role for SAP97 in the immunological synapse of IgG⁺ memory B cells. In experiments with knockout mice, several SAP family members have been demonstrated to be of key importance in the establishment of learning and memory (13, 21–24). The observation that SAP97 also functions in immunological memory adds to the long-standing analogies drawn between neurological and immunological synapses and memory.

The markedly impaired phenotype in antigen recall responses of transgenic mice lacking the cytoplasmic tail of mIgG strongly suggested the possibility that the mIgG cytoplasmic tail directly connected to the B cell signaling apparatus to enhance B cell activation (5–7). Engels et al. (8) provided the first evidence for such an association by showing that a conserved ITT motif present in both mIgG and mIgE is phosphorylated upon BCR cross-linking, which results in the recruitment of the adaptor protein Grb2 and enhanced Ca²⁺ responses and subsequent increased B cell proliferation. The results presented here, that the ITT motif was not required for the enhanced ability of IgG BCRs to cluster and initiate signaling, places the function of the ITT motif as an important amplifier downstream of the initiating events in BCR signaling.

We provided evidence from FLIM that the association of SAP97 and the mIgG tail was greatly enhanced upon antigen-induced clustering of IgG BCRs, which raised the question of how the interaction between SAP97 and IgG BCRs is restricted to clustered BCRs. The binding of PDZ-binding motifs to PDZ domains is weak in the low micromolar range (1 to 10 μ M) when measured by solution-based methods (25–27). Thus, individual IgG BCRs may not be able to stably associate with SAP97, but when clustered by antigen, the avidity of the interactions of the clustered tails with the PDZ domains of SAP97 may be sufficient to stabilize the interaction. Alternatively, the mIgG tail may not be available for binding to SAP97 in resting B cells. Consistent with this possibility, we previously showed with FRET microscopy that the IgG BCR tail and the Ig α and Ig β tails initially come into close molecular proximity upon antigen binding to the BCR but then rapidly come apart to an "open" state (28). The antigen-induced open form of the BCR may enable the binding of SAP97. It is also possible that SAP97 is brought into close molecular proximity with the clustered IgG BCRs by a mechanism similar to that which brings the first kinase in the BCR signaling cascade, Lyn, into proximity with clustered BCRs. We previously showed that BCR clustering perturbs its local lipid microenvironment, congealing raft lipids around the BCR cluster (29). Lyn, which is myristoylated and palmitoylated and associates with lipid rafts, is first brought into proximity with clustered BCRs transiently through lipid-lipid interactions, and then, through protein-protein interactions between Lyn and the Ig α and Ig β

tails, Lyn becomes stably associated with the BCR. SAP97 is palmitoylated at its N terminus and is predicted to associate with the saturated lipids in lipid rafts in the inner leaflet of the plasma membrane (30, 31); thus, it may similarly be brought into close molecular proximity with clustered BCRs. Such a mechanism for the association between SAP97 and IgG BCRs may also explain why IgM BCRs that perturb the local lipid environment but lack the ability to bind to SAP97 do not stably associate with SAP97.

We do not yet know the mechanisms by which SAP97 contributes to the enhanced initiation of signaling. SAP97, acting as a scaffold, could enhance the stability of early BCR oligomers, driving these toward the growth of larger clusters. Consistent with this possibility, we previously observed that a portion of IgG BCRs, but not IgM BCRs, were recruited to growing BCR clusters in an antigen-independent fashion (11). Even the weak interaction between SAP97 and IgG BCRs could serve to amplify signaling. SAP97 interacts with the Src family kinase, Lck, and with ZAP70 in T cells (32–34), suggesting that SAP97 might serve to concentrate early kinases around the clustered BCR. Once engaged, SAP97 could also enhance the activation of IgG⁺ B cells by enhancing the coordination of BCR microclusters with the cytoskeleton. Studies have highlighted the substantial role of cortical actin and ezrin-radixin-moesin (ERM) in regulating both tonic and antigen-driven BCR signaling (35–37). It has been reported in other cell types that ezrin interacts with SAP97 through its N-terminal FERM domain (38, 39). It is possible that through SAP97, the IgG BCRs more efficiently interact with the cytoskeleton to promote signaling.

Here, we also provided evidence that activation of p38 MAPK by IgG BCRs was substantially decreased in cells in which SAP97 was knocked down. This result mirrors reported results showing that cross-linking of TCRs on antigen-experienced T cells, but not naïve T cells, results in the association of SAP97 and p38 and the phosphorylation of p38 (40). Regulatory T cells (Tregs) were also recently reported to require SAP97 for the phosphorylation of p38 at Thr180 and Tyr182 and for the activation of nuclear factor of activated T cells c1 (NFATc1), which is necessary for Treg function (41). Earlier results showed that SAP97 mutants that

cannot bind to p38 fail to trigger downstream signaling in T cells (19). Together, these results indicated an important function of SAP97 in the activation of p38 in memory B cells and antigen-experienced T cells, as well as in Tregs. The findings presented here indicate that once having switched from expressing mlgM BCRs to expressing mlgG BCRs, the B cell is endowed with an enhanced ability to initiate and transduce signaling that may enable IgG+ B cells to outcompete IgM+ B cells in immune responses. The discovery that the binding of the conserved IgG tail to SAP97 is required for enhanced signaling may provide new targets for therapies to block enhanced BCR activation in autoimmune disease and in some B cell tumors.

METHODS

Cells, antibodies, antigens, plasmids, and transfections

J558L, A20 II1.6, and CH27 mouse cell lines were maintained as previously reported (14, 15). B cells were purified from peripheral blood mononuclear cells from healthy, anonymous, adult blood bank donors [collected for research purposes at the National Institutes of Health (NIH) Department of Transfusion Medicine under an NIH Institutional Review Board–approved protocol with informed consent] by negative selection magnetic cell separation with a human B Cell Isolation Kit II (Miltenyi). Anti–PAN MAGUK antibody (clone K28/86) and anti-SAP97 antibody (clone K64/15) were purchased from the University of California Davis/NIH NeuroMab Facility. Anti–human SAP97 antibody (clone 2D11) was purchased from Santa Cruz Biotechnology. Anti–pZAP70 (pY319)–Syk (pY352) antibody was purchased from Cell Signaling. Isotype-matched mouse IgG1 antibody was purchased from Invitrogen. Horseradish peroxidase (HRP)–conjugated antibodies against mouse or rabbit IgG were purchased from GE. HRP-conjugated anti-GST antibody was purchased from Sigma. HRP-conjugated anti-mouse light-chain antibody was purchased from Jackson ImmunoResearch. Purified unconjugated Fab goat anti-mouse Fc μ 5 IgM (anti-IgM), biotin-conjugated F(ab')₂ goat anti-mouse or anti-human IgM + IgG F(ab')₂, and goat anti-mouse or anti-human IgG Fc were purchased from Jackson ImmunoResearch. Fab anti-mouse or anti-human IgG Fc (anti-IgG) was prepared with a Fab

micro preparation kit (Pierce) as previously reported (11). Antibodies against IgM and IgG were conjugated to Alexa fluorophores with Alexa Fluor mAb labeling kits (Invitrogen) as previously reported (15). F(ab')₂ anti-IgG F(ab')₂ were biotinylated with an EZ-Link Biotinylation kit (Pierce). Antibodies against the following targets were purchased from Cell Signaling: pERK, phospho-p44/42 MAPK (ERK1/2) (Thr202/Tyr204) (197G2); pJNK, phospho-SAPK/JNK (Thr183/Tyr185); and pp38 MAPK (Thr180/Tyr182). Anti- γ -tubulin antibody was purchased from Sigma. Anti-actin antibody was purchased from Santa Cruz Biotechnology (C-11). HRP-conjugated donkey anti-goat IgG was purchased from Santa Cruz Biotechnology, and ECL anti-mouse IgG was from GE. Real-time PCR primers specific for Dlg1 (SAP97), Dlg2 (PSD93), Dlg3 (SAP102), Dlg4 (PSD95), and internal control ribosomal RNA (rRNA) were purchased from Qiagen. Plasmids expressing μ -B1-8 or γ 1-B1-8 fused at the C terminus with CFP and plasmid expressing Ig α fused at the C terminus with YFP through the linker peptide GGGAAS were constructed as previously described (28). Plasmids expressing γ 1-wild type, γ 1-Cyto N15 γ 1, and γ 1-Cyto μ were constructed as previously reported (11). Plasmid expressing SAP97 fused at the N terminus with YFP and the pSuper plasmid expressing short hairpin RNA specific for SAP97 (pSuper-puromycin-SAP97) were constructed as previously reported (18) and were provided as gifts from R. T. Javier (Baylor College of Medicine). The sequence of the hairpin used in scrambled control plasmids was reported in the literature (42). Plasmids expressing FL-SAP97 or the SH3-GUK domain of SAP97 fused at the N terminus with GST (GST-SAP97-FL or GST-SAP97-SH3-GUK) were constructed as previously reported (19) and were provided as gifts by M. C. Miceli (University of California, Los Angeles). On the basis of the GST-SAP-FL plasmid, a plasmid expressing the PDZ123 of SAP97 fused at the N terminus with GST (GST-SAP97-PDZ123) was generated by standard subcloning. ON-TARGETplus SMARTpool against mouse SAP97 (cat. no. L-042037-00) and nontargeting control (cat. no. D-001810-10-05) were purchased from Thermal Dharmacon. The hapten 4-hydroxy-3-iodo-5-nitrophenyl (NIP) conjugated to the peptide ASTGKTASACTSGASSTGSHis12 (NIP1-His12), N15 SSVV peptide conjugated at the N terminus with biotin (biotin-GG-KVKWIFSSVVELKQT), and the biotin-

conjugated mutant form N15GGGG (biotin-GG-KVKWIFGGGGELKQT) were purchased from Anaspec and California Peptides. All peptides were purified by high-performance liquid chromatography (HPLC) and verified by MS with >90% purity. BSA-conjugated 1:16 with phosphorylcholine (PC16-BSA) was purchased from Biosearch Technologies. Transient transfections were performed with Amaxa transfection kits, and the transfected B cells were imaged after overnight culture.

Preparation of antigen-containing planar fluid lipid bilayers

Planar fluid lipid bilayers were prepared as described previously (11). Ni-NTA (nickel–nitrilotriacetic acid)–containing lipid bilayers were prepared by mixing 1,2-dioleoyl-sn-glycero-3-phosphocholine (DOPC) and 1,2-dioleoyl-sn-glycero-3-[N(5-amino-1-carboxypentyl)iminodiacetic acid]-succinyl (nickel salt) (DOGS-Ni-NTA; Avanti Polar Lipids) in a mixture of 90% DOPC and 10% DOGS-Ni-NTA. Biotin-containing planar lipid bilayers were prepared with DOPC and 1,2-dioleoyl-sn-glycero-3-phosphoethanolamine-cap-biotin (DOPE-cap-biotin, Avanti Polar Lipids) in a mixture of 99% DOPC and 1% DOPE-cap-biotin. Ni-NTA–containing or biotin-containing unilamellar vesicles were formed by sonication of the mixed lipids and were clarified by ultracentrifugation and filtering as described previously (15). Glass coverslips were cleaned with Nano-Strip (Cyantek) and dried. Lipid bilayers were prepared from 0.1 mM lipid unilamellar vesicles on freshly cleaned glass coverslips. NIP1-His12 hapten antigen was attached to the Ni-NTA–containing lipid bilayer by incubating NIP1-His12 with the bilayer for 20 min at room temperature. The antigen-containing lipid bilayers were washed and then used in TIRF imaging. The amount of antigen bound to the bilayer was quantified as described previously (15). Incubation of the planar lipid bilayers with 10 nM NIP1-His12 peptide solutions resulted in bilayers containing about 25 molecules/ μm^2 , as previously reported (15). For biotin-containing lipid bilayers, biotinylated intercellular adhesion molecule–1 (ICAM-1) and PC16-BSA or biotin-conjugated F(ab')₂ goat anti–mouse or anti–human IgM + IgG F(ab')₂ were attached through streptavidin as reported previously (29). Briefly, 50 nM streptavidin was incubated with biotin-

containing lipid bilayers for 10 min. After washing, 10 nM biotinylated ICAM-1 and 10 nM PC16-BSA or 10 nM biotin-conjugated F(ab')₂ goat anti-mouse or anti-human IgM + IgG F(ab')₂ were bound to the planar lipid bilayer.

Imaging BCR, SAP97, and pSyk microclusters by two-color TIRF microscopy

Cells were placed on planar fluid lipid bilayers lacking or containing antigens. TIRF images were acquired at 37°C on a heated stage by an Olympus IX-81 microscope supported by a TIRF port, Cascade II 512 x 512 electron-multiplying charge-coupled device (CCD) camera (Roper Scientific) with Olympus 100x 1.45 numerical aperture (NA) and Zeiss 100x 1.4 NA objective lenses. The acquisition was controlled by MetaMorph software (Molecular Devices). The exposure time was 100 ms unless otherwise indicated. Three types of lasers were used: a 442-nm solid-state laser, a 488- and 514-nm argon gas laser, and a 568- and 647-nm red krypton and argon gas laser. When indicated, B cells were labeled with Fab anti-Ig as specified in each figure, washed twice, and placed on lipid bilayers. B cells were then fixed 10 min after being placed on antigen-containing lipid bilayers. The fixed cells were permeabilized with 0.1% Triton X-100 in phosphate-buffered saline and then incubated in blocking buffer. The cells were incubated with rabbit antibody against pZAP70 (pY319)–Syk (pY352), washed three times, and then incubated with Alexa Fluor 488– or Alexa Fluor 647–conjugated F(ab')₂ goat antibodies specific for rabbit IgG (Invitrogen). BCR and pSyk images were acquired by two-color TIRF microscopy through multidimensional acquisition mode controlled by MetaMorph software. YFP, Alexa Fluor 568, and Alexa Fluor 647 were excited by the 488-, 568-, and 647-nm lasers, respectively. YFP, Alexa Fluor 568, and Alexa Fluor 647 emission fluorescences were collected by 550 ± 40 ET band-pass (BP), 605 ± 40 BP, and 665 long-pass (LP) emission filters through a 488, 568, and 647 dichroic wheel filter cube. Intracellular staining for SAP97 with Alexa Fluor 647–conjugated Fab anti-SAP97 antibody was by the procedure described for the intracellular staining of pSyk. TIRF images were background-subtracted with Image-Pro Plus. The MFIs of BCR, SAP97, and pSyk microclusters within the contact area were measured with Image J.

Immunoprecipitations, purification of GST fusion proteins, and ELISA

Peptide-based immunoprecipitations were performed as described previously (8), with some modifications obtained from protocols available online (http://www.protocol-online.org/cgi-bin/prot/view_cache.cgi?ID=4089). Briefly, biotinylated N15SSVV or control biotinylated N15GGGG peptides were conjugated to streptavidin beads. B cells (107) were lysed in lysis buffer, and clear supernatants were incubated with the peptide-streptavidin beads overnight at 4°C. The beads were then washed and boiled with sample buffer to elute the associated proteins. The eluted samples were then subjected to SDS-PAGE for subsequent silver staining or Western blotting analysis. The induction of GST and SAP97 fusion protein production by isopropyl- β -D-thiogalactopyranoside (IPTG) in BI21 E. coli cells and the further purification of GST fusion proteins were performed by standard protocols. The ELISA assay was also performed according to standard protocols. Briefly, N15SSVV or N15GGGG peptides were coated onto the wells of an ELISA assay plate overnight at 4°C. The wells were then blocked and incubated with various GST-SAP97 fusion proteins for 1 hour at room temperature. The plates were then washed and incubated with HRP-conjugated anti-GST antibody and subjected to optical density measurement at 450 nm.

Quantitative reverse transcription–PCR analysis

Total cellular RNA was extracted with the RNeasy Mini Kit (Qiagen) and reverse-transcribed with the SuperScript III First-Strand Synthesis System for reverse transcription–PCR (RT-PCR) (Invitrogen). Quantitative RT-PCR was performed with iQ SYBR Green Supermix (Bio-Rad). Cycling conditions were 10 min at 95°C followed by 40 repeats of 95°C for 15 s and 60°C for 1 min. Analysis was performed by the sequence detection software supplied with the instrument (Eppendorf realplex 2). Real-time PCR primers targeting Dlg1 (SAP97), Dlg2 (PSD93), Dlg3 (SAP102), Dlg4 (PSD95), TFRC, and rRNA were purchased from Qiagen. Sequences are unavailable because of proprietary licensing, but the primers yielded bands

between 90 and 168 base pairs in length. TFRC and rRNA served as internal controls in our experiments.

FLIM analysis

Sensitized FRET measurements based on the intensities of donor or acceptor emission fluorescence are difficult to apply to intermolecular FRET experiments because the emission fluorescence intensity can often be affected by changes in the concentrations of donors or receptors or in excitation intensity (16). FLIM-linked FRET experiments can avoid these problems. FLIM is a measurement of the rate of decay of the donor emission, which will not be affected by donor concentration and excitation laser intensity. Instead, the donor fluorescence lifetime is substantially influenced by the FRET energy transferred from the donor to the acceptor. In our experiments, a femtosecond two-photon laser (~120 fs, Coherent) was used to provide the 890-nm excitation laser source for CFP in confocal fluorescence microscopy (710, Zeiss). The laser line was conditioned and steered to the confocal scanner and a Zeiss 63x 1.4 NA oil-immersion objective lens by the microscopy system manufacturer. Fluorescence life images were captured with a time-correlated single-photon counting device (Becker & Hickl). Live-cell images were initially chosen and focused by the standard procedure for CFP and YFP channels through the ZEN software package from Zeiss, and then the FLIM images were recorded and analyzed with the standard Becker & Hickl SPCM software package (version 9).

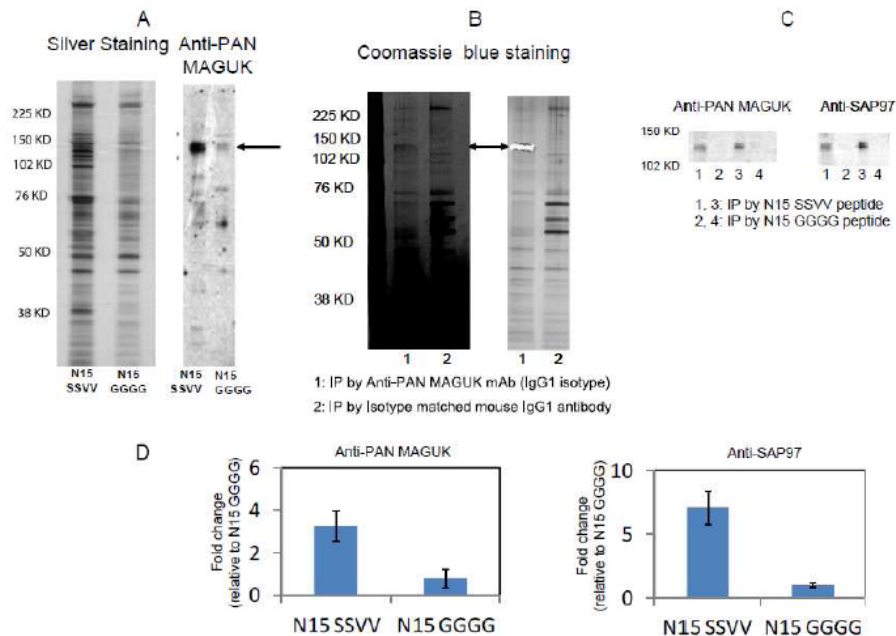


Figure 4-2: The cytoplasmic tail of mlgG binds SAP97. (A) Silver staining (left) and Western blotting analysis (right) with anti-PAN MAGUK mAb (right) of SDS-PAGE gels of samples immunoprecipitated from J558L cell lysates with a biotin-conjugated membrane-proximal 15 amino acid peptide that contained the SSVV motif (N15 SSVV) bound to streptavidin beads or with biotinylated control peptide in which SSVV was changed to GGGG (N15 GGGG) bound to streptavidin beads. The black arrow indicates the 130-kD protein recognized by the anti-PAN MAGUK antibody. (B) Coomassie blue staining of samples from immunoprecipitated from J558L cell lysates with beads conjugated to an anti-PAN MAGUK mAb or to an isotope matched control antibody. On the left is the original SDS-PAGE gel stained with coomassie blue, on the right is the gel after removal of the 130-kD protein band indicated by the black arrow that was subjected to LC-MS/MS analysis by ProtTech. (C) Western blotting analysis of samples immunoprecipitated from A20 I11.6 cell lysates with either N15 SSVV peptide or N15 GGGG control peptide were analyzed by Western blotting with either anti-PAN MAGUK mAb (left, clone K28/86) or anti-SAP97 mAb (right, clone 64/15). Immunoprecipitates (IPs) 1 and 2 and IPs 3 and 4 were from independent lysate preparations loaded onto the same SDS-PAGE gel. (D) Statistical analysis of the mean fold-change \pm SD in the intensity of the N15 SSVV bands relative to those of the N15 GGGG control samples from four independent experiments.

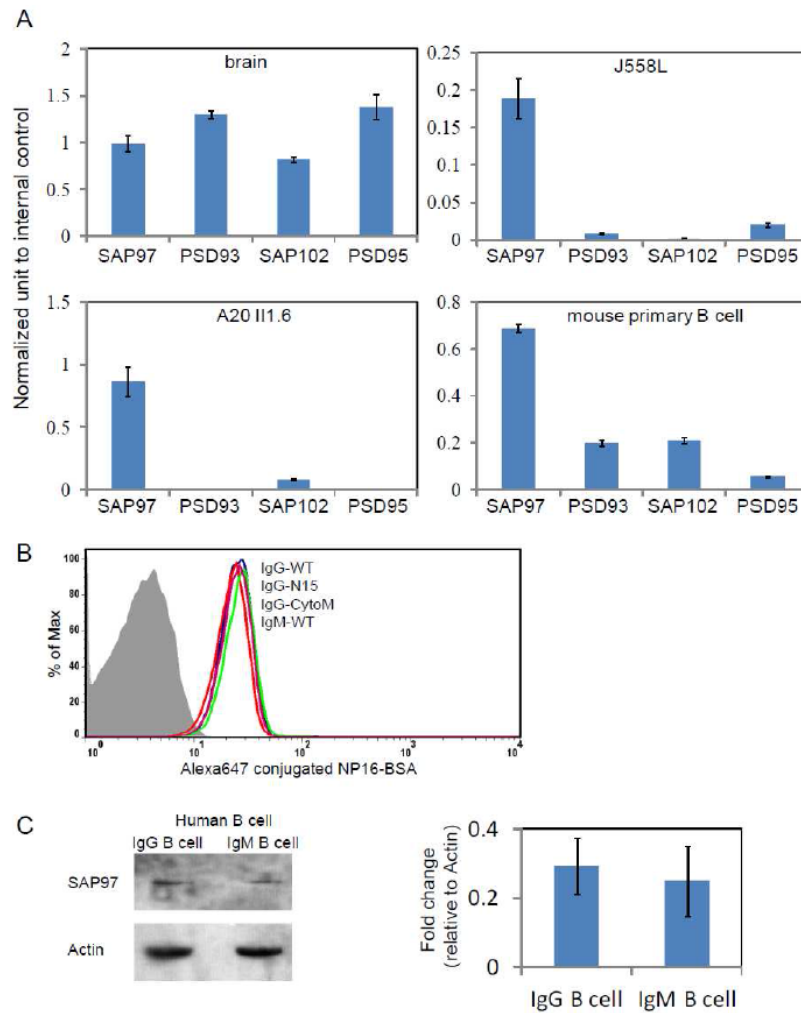


Figure 4-3: SAP97 is the most abundant SAP family protein in B cells. (A) Quantitative RT-PCR analysis of the abundances of mRNAs for the four SAP family members in brain homogenate, J558L cells, A20 II1.6 cells and freshly purified primary mouse splenic B cells. Real-time RT-PCR primers specific for Dlg1 (SAP97), Dlg2 (PSD93), Dlg3 (SAP102), Dlg4 (PSD95), and internal control were purchased from Qiagen and were used according to the manufacturer's instructions. Arbitrary units for the abundance of the mRNA for each SAP family member normalized to that of the internal control are given. Brain samples have large amounts of all four SAP family members and were therefore used as controls of primer quality and the experimental system. (B) Cell-surface abundances of nitrophenol (NP)-specific BCRs (either IgG or IgM) in J558L cells expressing IgG-WT, IgG-N15, IgG-CytoM or IgM-WT were measured by flow cytometric analysis Alexa Fluor 647-conjugated NP16-BSA staining. (C) Human IgM- and IgG-expressing B cells both express SAP97. Primary human IgM- and IgG-expressing B cells sorted from peripheral blood of healthy donors were lysed and subjected to SDS-PAGE and Western blotting analysis for human SAP97. The data represent the mean \pm SD from two independent experiments.

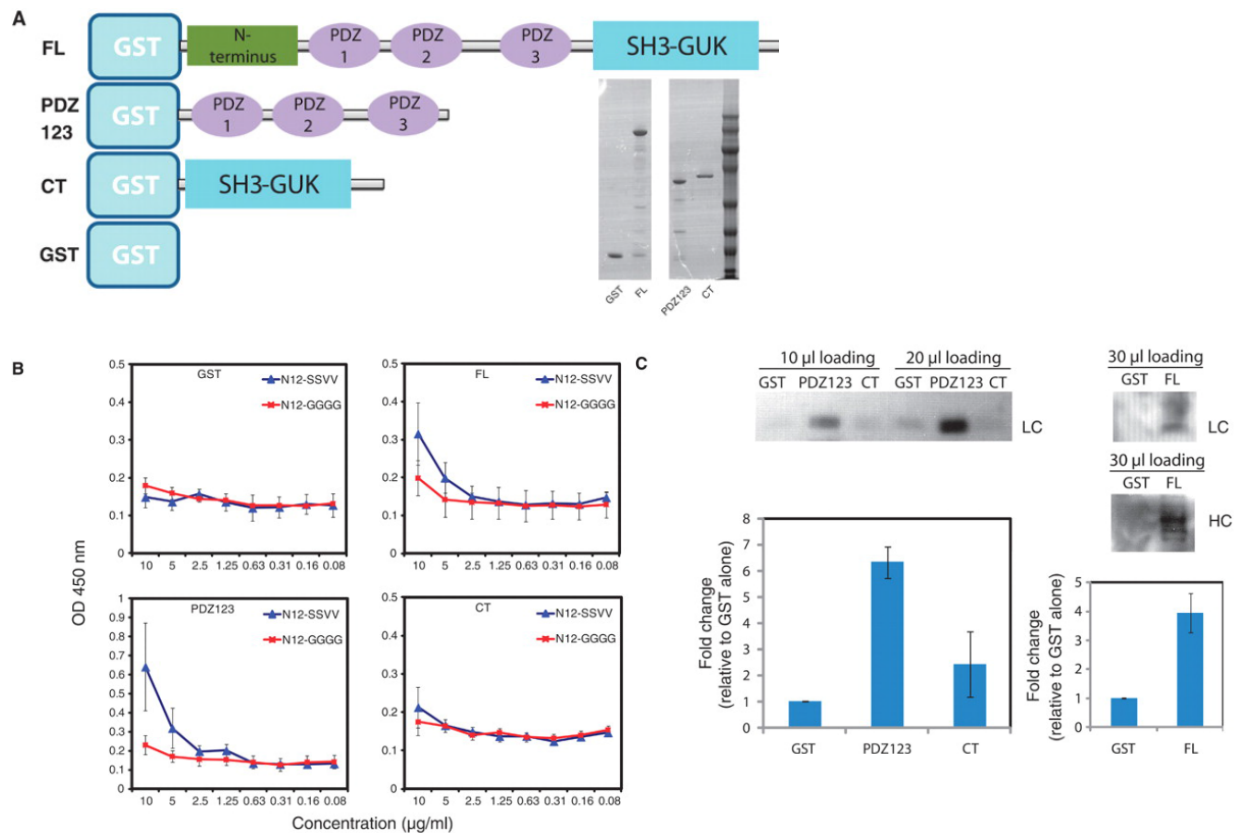


Figure 4-4. The binding of SAP97 to the cytoplasmic tail of mlgG. (A) The GST fusion proteins that were expressed and purified as described in Materials and Methods, including full-length SAP97 (FL), the three tandem PDZ domains of SAP97 (PDZ123), the C-terminal SH3-GUK domain of SAP97 (CT), and GST alone. These purified GST fusion proteins were subjected to SDS-PAGE and Coomassie blue staining as shown in the gel on the right. (B) The purified proteins were tested by ELISA for their ability to bind to the N15SSVV and N15GGGG peptides. Binding is indicated by the increased optical density (OD) at 450 nm. The data represent the means \pm SD from four independent experiments. (C) GST pull-down assays with GSH (glutathione, reduced form) beads bound to the same amounts of purified GST alone or of the FL, PDZ123, and CT fusion proteins. Beads were incubated with A20 II1.6 cell lysates, centrifuged, washed, eluted into the same volume, and subjected to SDS-PAGE. For the GST, PDZ123, and CT pull-downs, 10 and 20 μ l of the pull-down eluates were analyzed by SDS-PAGE. In separate experiments, 30 μ l of the eluates from samples containing GST alone or the FL construct was analyzed by SDS-PAGE. Western blots were analyzed with mouse IgG-specific antibodies for light chain (LC) or heavy chain (HC). Bar graphs show a statistical comparison (means \pm SD from five independent experiments) showing the fold changes in the intensity of the PDZ123, CT, or FL bands relative to those in the GST alone samples.

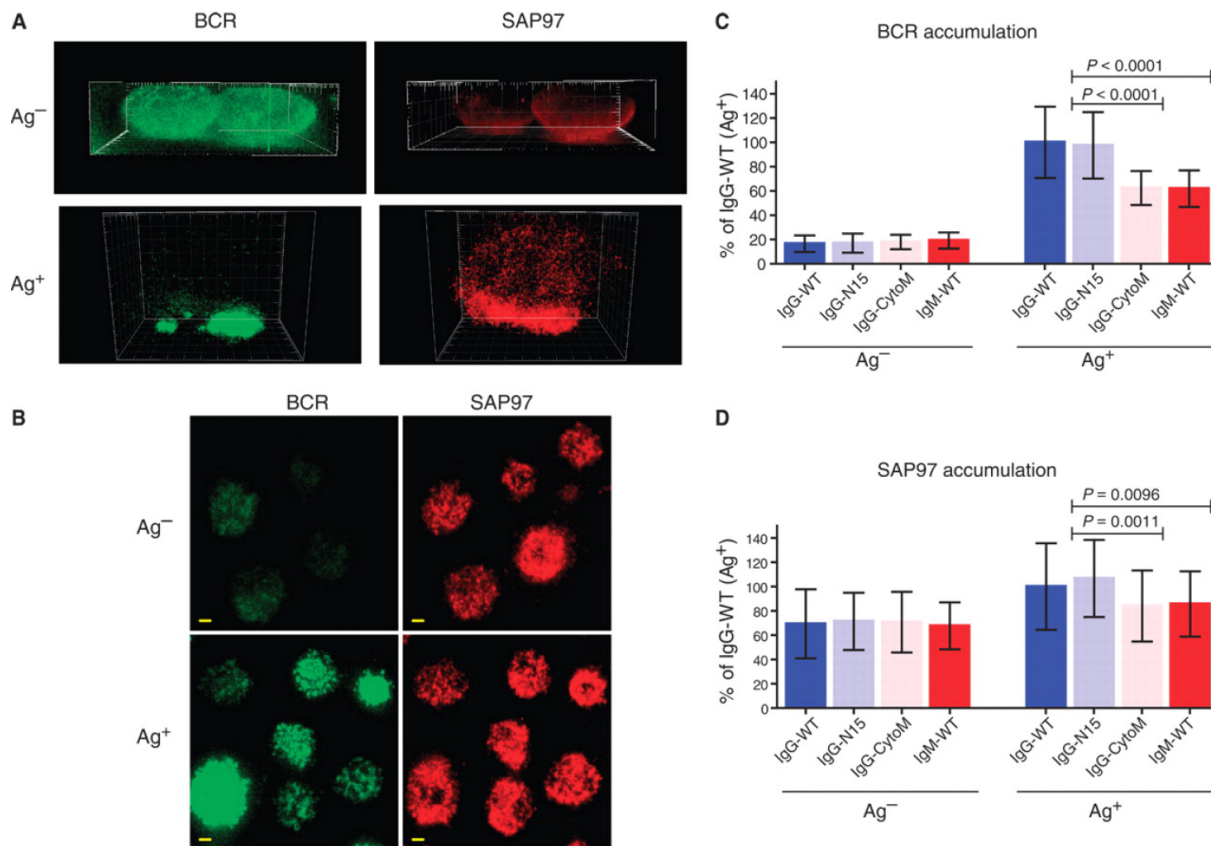


Figure 4-5: IgG BCRs enhance the accumulation of SAP97 in the immunological synapse. (A and B) Representative (A) two-color three-dimensional (3D) images and (B) TIRF images of the BCR and SAP97 in J558L cells expressing reconstructed NIP-specific BCRs. Cells were placed on planar lipid bilayers containing either no antigen or the antigen NIP-H12 for 10 min. Cells were then fixed, permeabilized, and incubated with fluorescently tagged antibodies specific for the BCR or for SAP97. (A) The 3D images are shown in side view (see movies S1 to S4 for 360° full views). (B) For the original 16-bit gray scale TIRF images, the display range was set from 0 to 500 for both BCR and SAP97 images to enable direct evaluation of the accumulated amounts of the BCR and SAP97 by comparing the MFIs. Scale bars, 1.5 μ m. (C and D) Accumulation of (C) the BCR and (D) SAP97 within the contact area of the cell with planar lipid bilayers containing either no antigen or NIP-H12 antigen for J558L cell lines expressing either wild-type B1-8-High mIgG-BCR (IgG-WT), mIgG-BCR with a mIgG tail composed of only the membrane-proximal 15 amino acids (IgG-N15), mIgG-BCR with the cytoplasmic tail of mIgM (IgG-CytoM), or wild-type mIgM-BCR (IgM-WT). The accumulation of the BCR and SAP97 into the contact interface is given as the percentage of their accumulation in IgG-WT cells placed on antigen-containing lipid bilayers. The data represent the means \pm SD of at least 20 cells from three independent experiments. Two-tailed t tests were performed for the statistical comparisons.

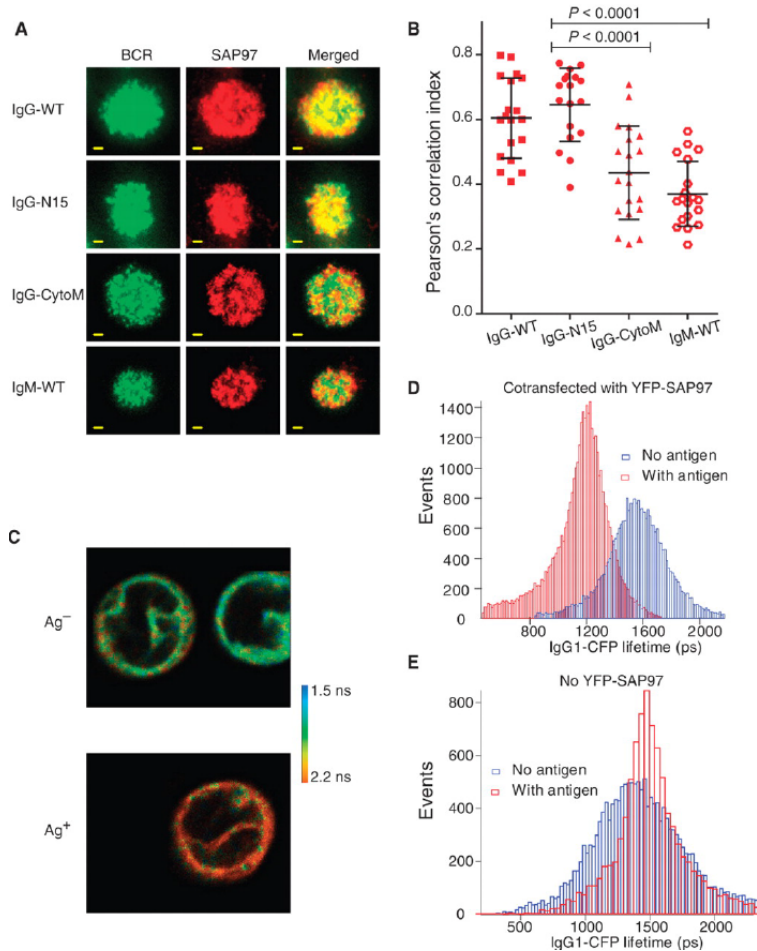


Figure 4-6: IgG BCRs and SAP97 show increased colocalization and close molecular proximity after antigen binding. (A to E) Pearson's correlation analyses of two-color (A and B) TIRF images and (C to E) FLIM analyses. (A) Two-color TIRF images of the BCR and SAP97 within the immunological synapse of J558L cells expressing BCRs containing IgG-WT, IgG-N15, IgG-CytoM, or IgM-WT. The cells were placed on planar lipid bilayers containing NIP-H12 for 10 min, fixed, permeabilized, and incubated with fluorescently tagged antibodies specific for the BCR or for SAP97. Scale bars, 1.5 μ m. (B) Pearson's correlation indexes quantifying the colocalization of BCR and SAP97 within the immunological synapse in two-color TIRF images, as represented in (A). Each dot represents one cell analyzed in three independent experiments, and bars represent the means \pm SD. Two-tailed t tests were performed for the statistical comparisons. (C to E) To assess molecular proximity between YFP-SAP97 and mIgG-CFP, we measured the fluorescence lifetime of the CFP molecules with a Becker & Hickl time-correlated, single-photon counting device linked to a confocal fluorescence microscope equipped with a two-photon-pulsed laser. (C) Representative FLIM images from at least three independent experiments for J558L B cells stably expressing Ig β , Ig α , and Ig λ light chains that were cotransfected with plasmids encoding YFP-SAP97 and mIgG-CFP and placed on planar lipid bilayers containing no antigen (top) or the antigen NIP-H12 (bottom). The FLIM images were pseudo-colored to indicate the lifetime of CFP pixel by pixel. (D) Histogram plots of the CFP lifetime values from all of the pixels in the FLIM images. (E) Histogram plots of the CFP lifetime values from all of the pixels in FLIM images of J558 B cells expressing Ig β , Ig α , Ig λ , and mIgG-CFP.

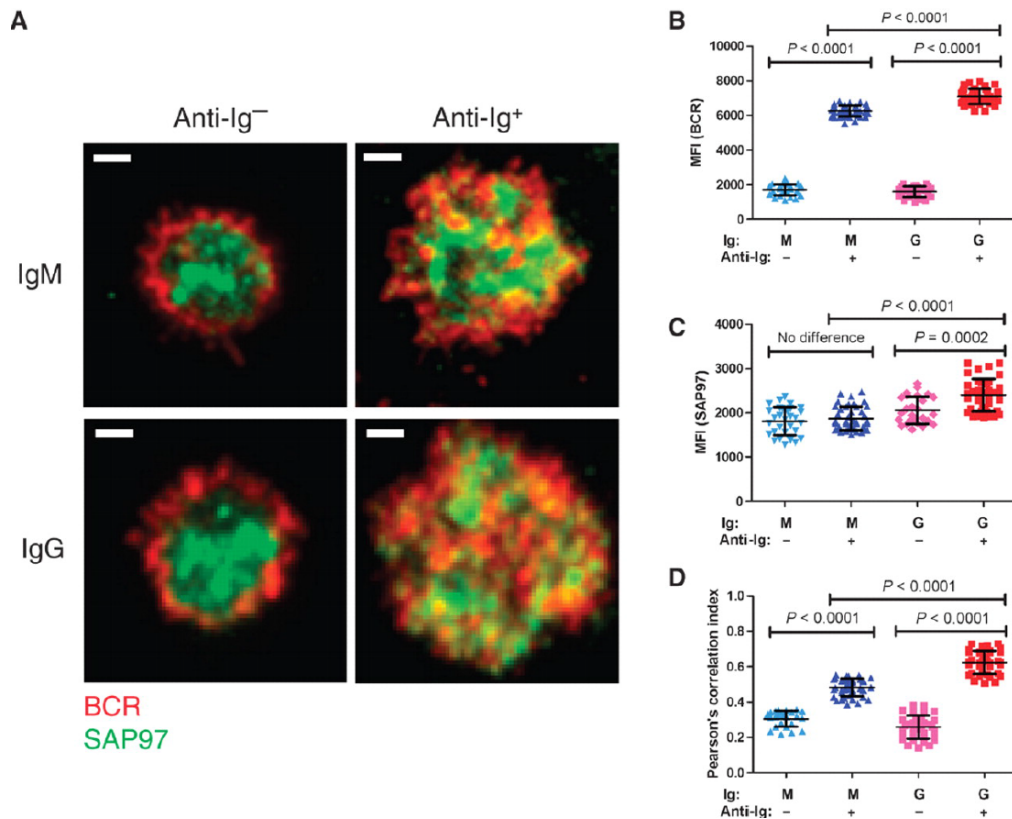


Figure 4-7: The accumulation of SAP97 at the immunological synapse and its colocalization with IgG and IgM BCRs in human B cells. (A) Two-color TIRF images showing BCR and SAP97 within the immunological synapse of IgM⁺ and IgG⁺ human peripheral blood B cells. Cells were placed on planar lipid bilayers that did or did not contain anti-Ig to cross-link the BCRs for 10 min and then were fixed, permeabilized, and incubated with fluorescently labeled antibodies specific for IgM or IgG and for SAP97. Scale bars, 1 μ m. (B and C) MFIs of (B) the BCR and (C) SAP97 in the immunological synapse. (D) Pearson's correlation analysis for the colocalization of the BCR and SAP97 in the two-color TIRF images. Each dot represents one cell analyzed in two independent experiments, and bars represent the means \pm SD. Two-tailed t tests were performed for the statistical comparisons.

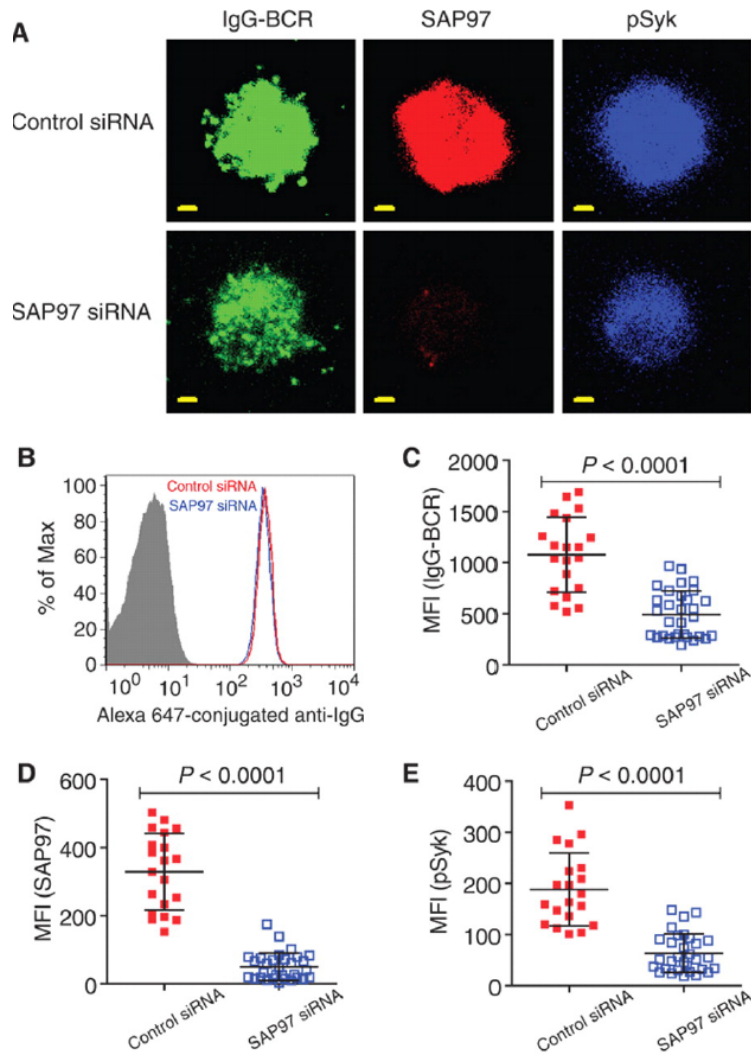


Figure 4-8: The enhanced accumulation of IgG-BCRs in the immunological synapse and the increased recruitment of pSyk is SAP97-dependent. (A) Three-color TIRF images showing the accumulation of the BCR, SAP97, and pSyk within the immunological synapse of A20 II1.6 B cells expressing a control siRNA (control) or a SAP97-specific siRNA (SAP97 KD). B cells were placed on planar lipid bilayers containing F(ab')₂ anti-IgG to cross-link the BCRs. Scale bars, 1.5 μ m. (B) Cell surface abundance of IgG BCRs in control and SAP97 KD A20 II1.6 cells as measured by flow cytometry with Alexa Fluor 647-conjugated mouse IgG-specific antibodies. (C to E) MFIs of (C) the BCR, (D) SAP97, and (E) pSyk within the immunological synapse. Each dot represents one cell analyzed in three independent experiments, and the bars represent the means \pm SD. Two-tailed t tests were performed for the statistical comparisons.

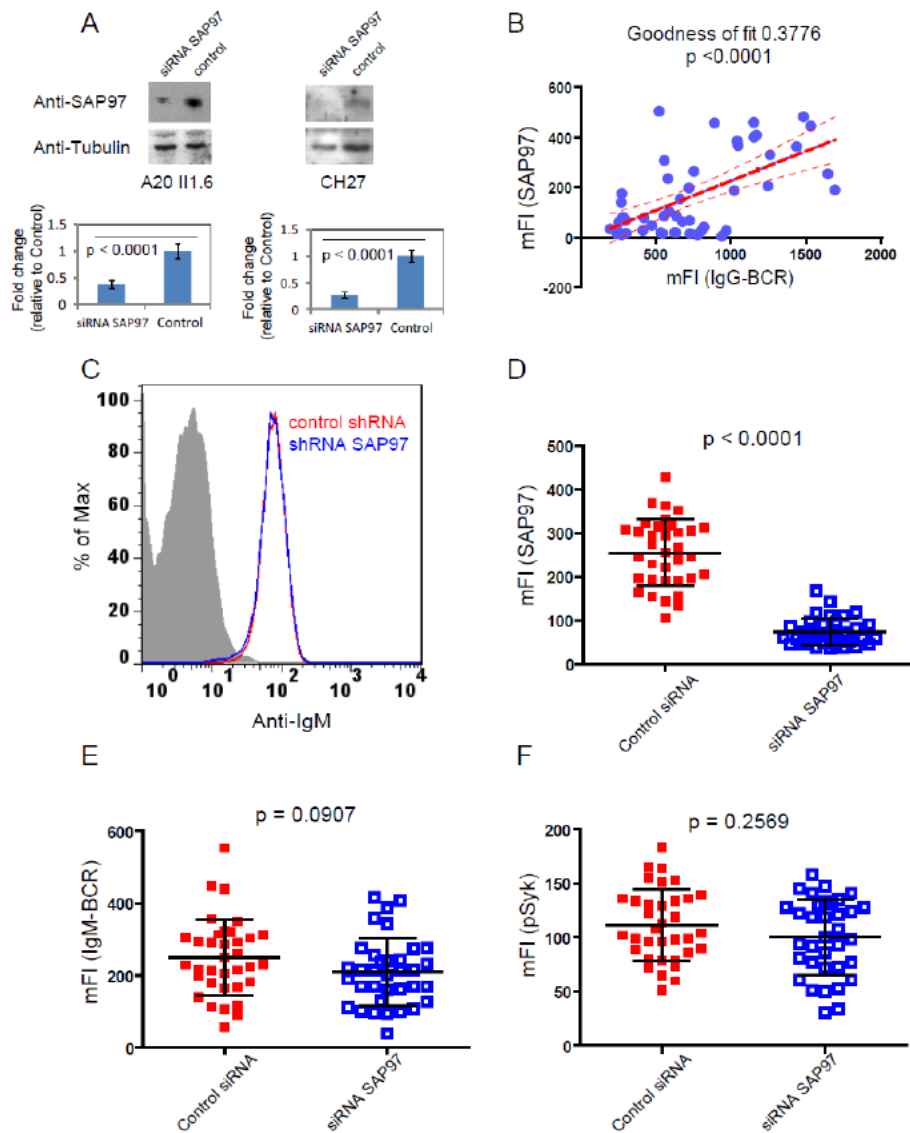


Figure 4-9: Knockdown of SAP97 has mild effects on the antigen-induced accumulation of IgM BCRs in the immunological synapse. (A) Western blotting analysis of the presence of SAP97 in A20 II1.6 cells (left) and CH27 cells (right) transfected with a thermal smart pool siRNA specific for SAP97 (left) or with pSuper-ShRNA-SAP97 (right) as well as of their corresponding control constructs. Bar graphs show the fold-change in SAP97 abundance relative to that of control cells as well as the statistical analysis. Data are means \pm SD from three independent experiments. (B) The correlation of the MFI of IgG-BCRs with that of SAP97 within the immunological synapse of IgG⁺ B cells. (C) Cell-surface abundance of IgM-BCRs in CH27 control cells or CH27 stable sub-lines in which SAP97 was knocked down were measured by flow cytometric analysis of Alexa Fluor 647-conjugated anti-mouse IgM staining. The MFIs of (D) SAP97, (E) BCR and (F) pSyk within the IS of CH27 control cells or CH27 stable sublines in which SAP97 was knocked down. Each dot represents one cell analyzed in at least three independent experiments and the bars represent means \pm SD. Two-tailed t tests were performed for the statistical comparisons.

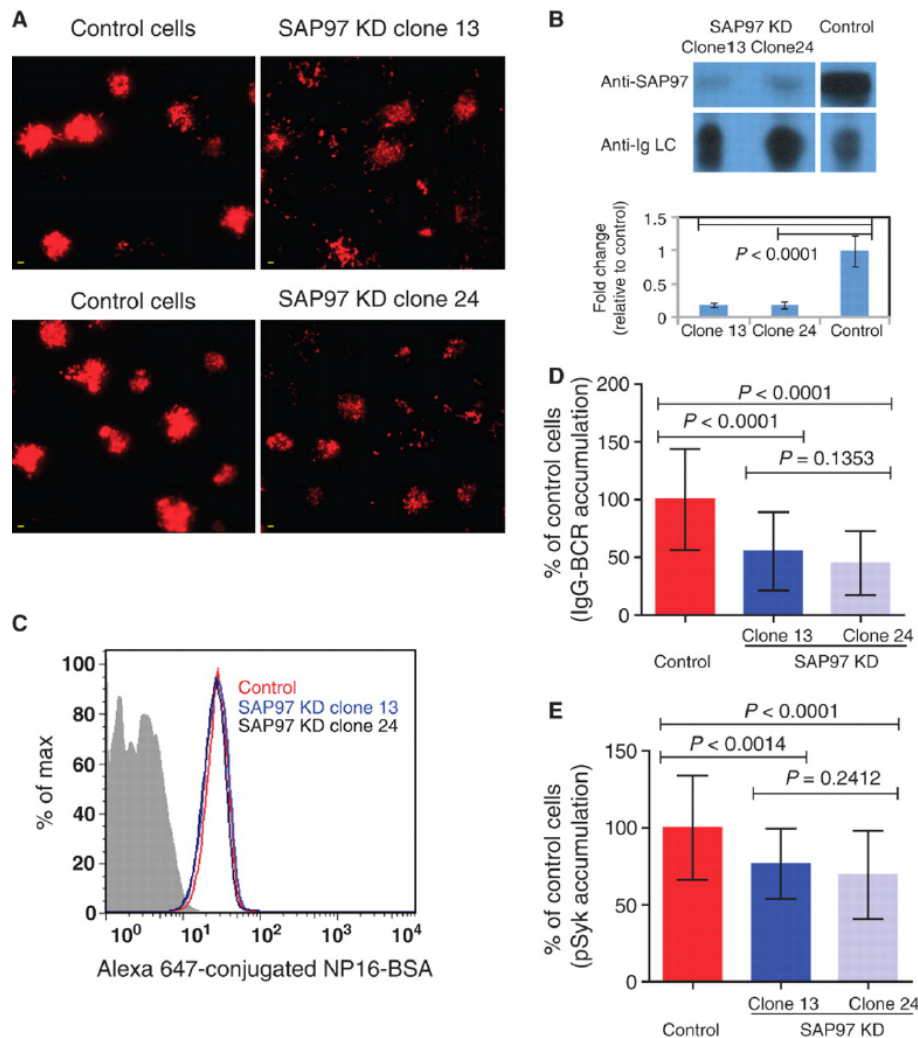


Figure 4-10: The enhanced accumulation of IgG-BCRs in the immunological synapse is SAP97-dependent. (A) TIRF images show the BCR within the immunological synapse of J558L-IgG-B1-8-High cells expressing a control siRNA and in cell lines stably expressing SAP97-specific siRNAs (SAP97 KD clone 13 and SAP97 KD clone 24). In the original 16-bit TIRF images, the display range was set from 0 to 500 to enable direct evaluation of the amount of the BCR by comparing the MFIs. Scale bars, 1.5 μ m. (B) Western blotting analysis of the lysates of J558L-IgG-B1-8-High control cells and SAP97 KD clone 13 and clone 24 cells. Bar graph shows the statistical analysis of the fold change in SAP97 abundance compared to that of control cells. Data are the means \pm SD from three independent experiments. (C) Cell surface abundance of the BCR was measured by flow cytometry with Alexa Fluor 647-conjugated NP16-BSA. (D and E) Accumulation of (D) IgG-BCR and (E) pSyk into the contact interface as a percentage of that in control cells placed on antigen-containing lipid bilayers. Data represent the means \pm SD of (D) 40 to 67 cells or (E) 29 to 43 cells from five independent experiments. Two-tailed t tests were performed for the statistical comparisons.

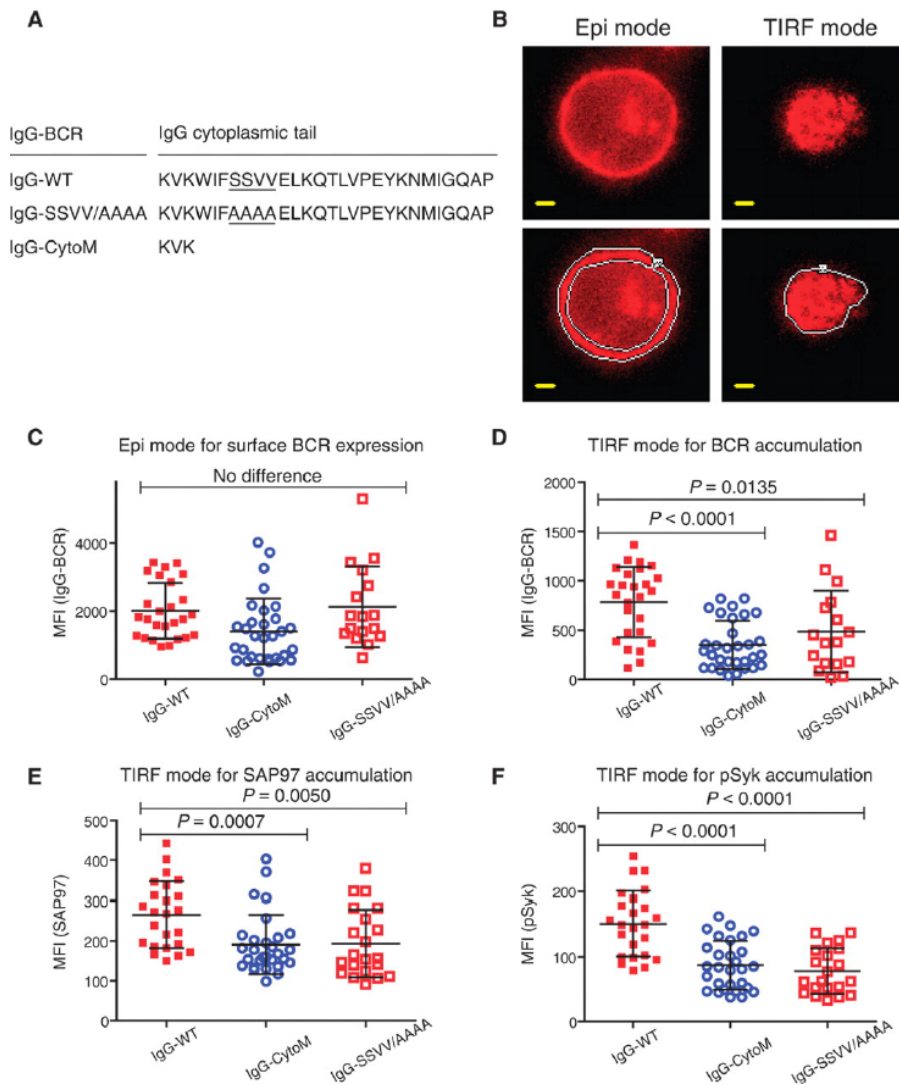


Figure 4-11: The SSVV motif in the mIgG cytoplasmic tail is required for the enhanced accumulation of IgG BCRs into the immunological synapse. (A) The cytoplasmic tail sequences of B1-8-High IgG-BCR (mIgG-WT) and mutant forms of IgG-BCRs in which the SSVV motif was changed to AAAA (underlined) or the tail was truncated. (B) Images of the same representative cell illuminated first in an epifluorescence mode (left panels) and then in TIRF mode (right panels). The area of the BCR epifluorescence image from which the MFI of cell surface BCR was acquired is outlined in white (left bottom panel). Similarly, the area of the BCR TIRF image from which the MFI of the BCRs in the immunological synapse was acquired is outlined in white (right bottom panel). Scale bars, 1.5 μ m. (C to F) The MFIs of (C) surface BCRs, (D) accumulated BCRs, (E) SAP97, and (F) pSyk in the immunological synapse are given for cells expressing BCRs containing IgG-WT, IgG-CytoM, or IgG-SSVV/AAAA. Each dot represents one cell analyzed in three independent experiments, and the bars represent the means \pm SD. Two-tailed t tests were performed for the statistical comparisons.

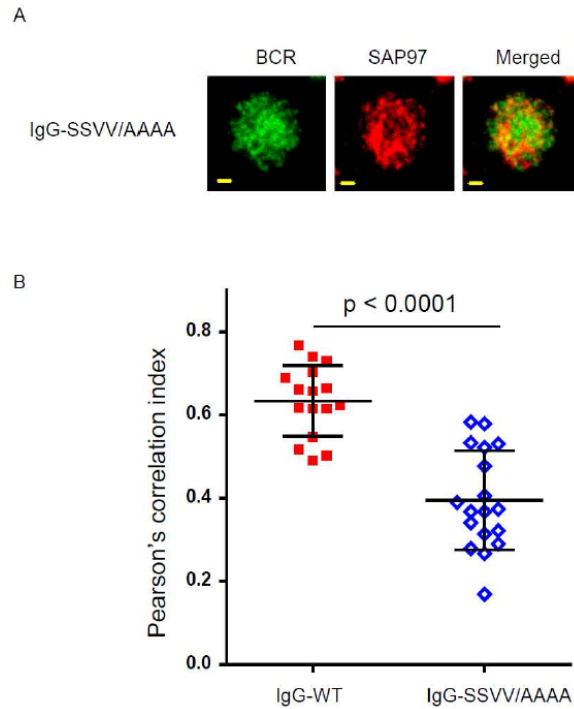


Figure 4-12: The extent of colocalization of IgG-SSVV/AAAA mutant BCRs with SAP97 upon antigen engagement is substantially reduced compared to that of IgG-WT BCRs. (A) Two-color TIRF images of the BCR and SAP97 within the immunological synapse of J558L cells expressing IgG-SSVV/AAAA BCRs. The cells were placed on planar lipid bilayers containing NIP-H12 for 10 min, fixed, permeabilized and then incubated with fluorescently tagged antibodies specific for the BCR or for SAP97. Scale bar: 1.5 μ m. (B) The Pearson, correlation index was applied to quantify the colocalization of BCR and SAP97 within the immunological synapse for cells expressing IgG-WT or IgG-SSVV/AAAA BCRs. Each dot represents one cells analyzed in two independent experiments, and bars represent means \pm SD. Two-tailed t tests were performed for the statistical comparisons.

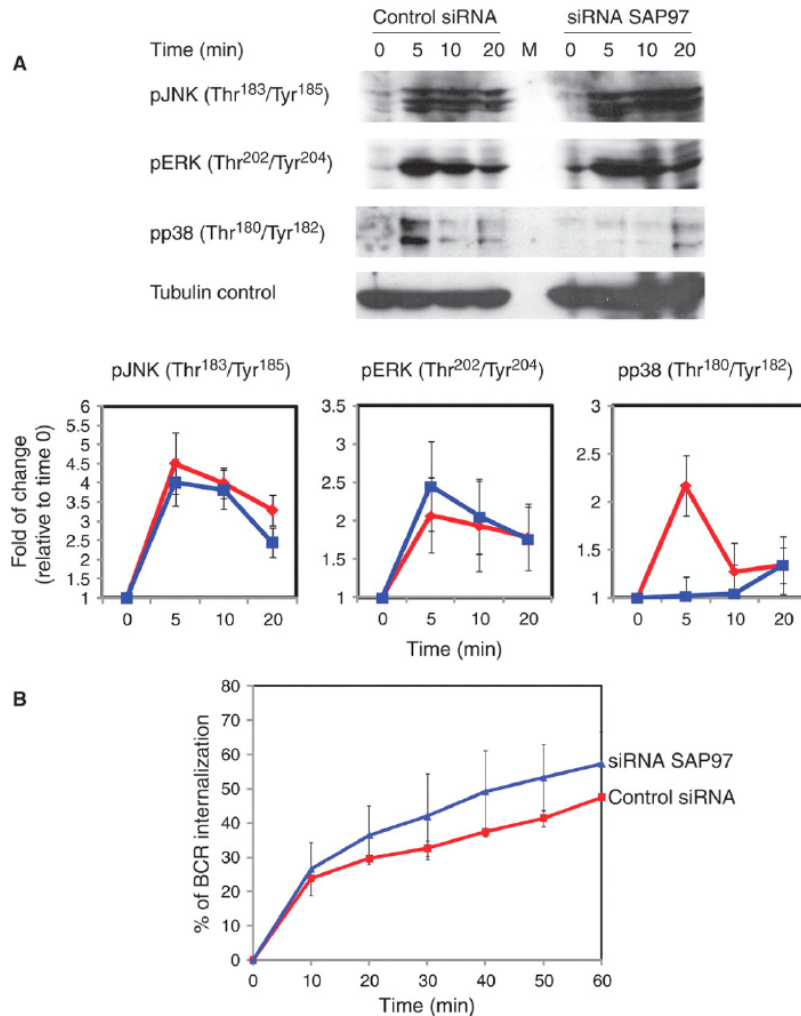


Figure 4-13: Knockdown of SAP97 substantially impairs activation of p38 MAPK.

(A) Control or SAP97 KD A20 II1.6 cells were activated by F(ab')₂ anti-mouse IgM F(ab')₂ (20 µg/ml) for the indicated times. Cells were lysed and lysates were subjected to SDS-PAGE and Western blotting analysis for pJNK, pERK, and p-p38. Bar graphs show the fold change in protein accumulation over time and the statistical comparisons. Data are means ± SD from three independent experiments. The red lines represent control cells and the blue lines represent SAP97 KD cells. (B) Internalization of IgG-BCRs in SAP97 KD versus control A20 II1.6 B cells. Cells were incubated with biotin-conjugated F(ab')₂ anti-mouse IgG F(ab')₂, washed, and incubated at 37°C for the indicated times. The amounts of cell surface IgG-BCR at each time point were measured by flow cytometry with phycoerythrin (PE)-conjugated streptavidin. Data are means ± SD from three independent experiments.

REFERENCES

1. L. J. McHeyzer-Williams, M. G. McHeyzer-Williams, Antigen-specific memory B cell development. *Annu. Rev. Immunol.* 23, 487–513 (2005)
2. M. Reth, Antigen receptors on B lymphocytes. *Annu. Rev. Immunol.* 10, 97–121 (1992).
3. T. Kaisho, F. Schwenk, K. Rajewsky, The roles of γ 1 heavy chain membrane expression and cytoplasmic tail in IgG1 responses. *Science* 276, 412–415 (1997).
4. S. W. Martin, C. C. Goodnow, Burst-enhancing role of the IgG membrane tail as a molecular determinant of memory. *Nat. Immunol.* 3, 182–188 (2002).
5. K. Horikawa, S. W. Martin, S. L. Pogue, K. Silver, K. Peng, K. Takatsu, C. C. Goodnow, Enhancement and suppression of signaling by the conserved tail of IgG memory-type B cell antigen receptors. *J. Exp. Med.* 204, 759–769 (2007).
6. A. Waisman, M. Kraus, J. Seagal, S. Ghosh, D. Melamed, J. Song, Y. Sasaki, S. Classen, C. Lutz, F. Brombacher, L. Nitschke, K. Rajewsky, IgG1 B cell receptor signaling is inhibited by CD22 and promotes the development of B cells whose survival is less dependent on Ig α / β . *J. Exp. Med.* 204, 747–758 (2007).
7. C. Wakabayashi, T. Adachi, J. Wienands, T. Tsubata, A distinct signaling pathway used by the IgG-containing B cell antigen receptor. *Science* 298, 2392–2395 (2002).
8. N. Engels, L. M. Konig, C. Heemann, J. Lutz, T. Tsubata, S. Griep, V. Schrader, J. Wienands, Recruitment of the cytoplasmic adaptor Grb2 to surface IgG and IgE provides antigen receptor–intrinsic costimulation to class-switched B cells. *Nat. Immunol.* 10, 1018–1025 (2009).
9. N. E. Harwood, F. D. Batista, Early events in B cell activation. *Annu. Rev. Immunol.* 28, 185–210 (2010).
10. S. K. Pierce, W. Liu, The tipping points in the initiation of B cell signalling: How small changes make big differences. *Nat. Rev. Immunol.* 10, 767–777 (2010).
11. W. Liu, T. Meckel, P. Tolar, H. W. Sohn, S. K. Pierce, Intrinsic properties of immunoglobulin IgG1 isotype-switched B cell receptors promote microclustering and the initiation of signaling. *Immunity* 32, 778–789 (2010).
12. M. Sheng, C. Sala, PDZ domains and the organization of supramolecular complexes. *Annu. Rev. Neurosci.* 24, 1–29 (2001).
13. E. Kim, M. Sheng, PDZ domain proteins of synapses. *Nat. Rev. Neurosci.* 5, 771–781 (2004).
14. W. Liu, H. Won Sohn, P. Tolar, T. Meckel, S. K. Pierce, Antigen-induced oligomerization of the B cell receptor is an early target of Fc γ RIIB inhibition. *J. Immunol.* 184, 1977–1989 (2010).
15. W. Liu, T. Meckel, P. Tolar, H. W. Sohn, S. K. Pierce, Antigen affinity discrimination is an intrinsic function of the B cell receptor. *J. Exp. Med.* 207, 1095–1111 (2010).

16. H. Wallrabe, A. Periasamy, Imaging protein molecules using FRET and FLIM microscopy. *Curr. Opin. Biotechnol.* 16, 19–27 (2005).
17. A. M. Davey, S. K. Pierce, Intrinsic differences in the initiation of B cell receptor signaling favor responses of human IgG⁺ memory B cells over IgM⁺ naive B cells. *J. Immunol.* 188, 3332–3341 (2012).
18. K. K. Frese, I. J. Latorre, S. H. Chung, G. Caruana, A. Bernstein, S. N. Jones, L. A. Donehower, M. J. Justice, C. C. Garner, R. T. Javier, Oncogenic function for the Dlg1 mammalian homolog of the *Drosophila* discs-large tumor suppressor. *EMBO J.* 25, 1406–1417 (2006).
19. J. L. Round, L. A. Humphries, T. Tomassian, P. Mittelstadt, M. Zhang, M. C. Miceli, Scaffold protein Dlg1 coordinates alternative p38 kinase activation, directing T cell receptor signals toward NFAT but not NF- κ B transcription factors. *Nat. Immunol.* 8, 154–161 (2007).
20. G. M. Elias, R. A. Nicoll, Synaptic trafficking of glutamate receptors by MAGUK scaffolding proteins. *Trends Cell Biol.* 17, 343–352 (2007).
21. G. Zanni, H. van Esch, A. Bensalem, Y. Saillour, K. Poirier, L. Castelnaud, H. H. Ropers, A. P. de Brouwer, F. Laumonnier, J. P. Fryns, J. Chelly, A novel mutation in the DLG3 gene encoding the synapse-associated protein 102 (SAP102) causes non-syndromic mental retardation. *Neurogenetics* 11, 251–255 (2010).
22. P. Tarpey, J. Parnau, M. Blow, H. Woffendin, G. Bignell, C. Cox, J. Cox, H. Davies, S. Edkins, S. Holden, A. Kornly, U. Mallya, J. Moon, S. O'Meara, A. Parker, P. Stephens, C. Stevens, J. Teague, A. Donnelly, M. Mangelsdorf, J. Mulley, M. Partington, G. Turner, R. Stevenson, C. Schwartz, I. Young, D. Easton, M. Bobrow, P. A. Futreal, M. R. Stratton, J. Gecz, R. Wooster, F. L. Raymond, Mutations in the DLG3 gene cause nonsyndromic X-linked mental retardation. *Am. J. Hum. Genet.* 75, 318–324 (2004).
23. M. Migaud, P. Charlesworth, M. Dempster, L. C. Webster, A. M. Watabe, M. Makhinson, Y. He, M. F. Ramsay, R. G. Morris, J. H. Morrison, T. J. O'Dell, S. G. Grant, Enhanced long-term potentiation and impaired learning in mice with mutant postsynaptic density-95 protein. *Nature* 396, 433–439 (1998).
24. W. D. Yao, R. R. Gainetdinov, M. I. Arbuckle, T. D. Sotnikova, M. Cyr, J. M. Beaulieu, G. E. Torres, S. G. Grant, M. G. Caron, Identification of PSD-95 as a regulator of dopamine-mediated synaptic and behavioral plasticity. *Neuron* 41, 625–638 (2004).
25. B. Z. Harris, W. A. Lim, Mechanism and role of PDZ domains in signaling complex assembly. *J. Cell Sci.* 114, 3219–3231 (2001).
26. M. Niethammer, J. G. Valtschanoff, T. M. Kapoor, D. W. Allison, R. J. Weinberg, A. M. Craig, M. Sheng, CRIPT, a novel postsynaptic protein that binds to the third PDZ domain of PSD-95/SAP90. *Neuron* 20, 693–707 (1998).
27. R. A. Hall, L. S. Ostedgaard, R. T. Premont, J. T. Blitzer, N. Rahman, M. J. Welsh, R. J. Lefkowitz, A C-terminal motif found in the β 2-adrenergic receptor, P2Y1 receptor and cystic fibrosis transmembrane conductance regulator determines binding to the Na⁺/H⁺ exchanger regulatory factor family of PDZ proteins. *Proc. Natl. Acad. Sci. U.S.A.* 95, 8496–8501 (1998).
28. P. Tolar, H. W. Sohn, S. K. Pierce, The initiation of antigen-induced B cell antigen receptor signaling viewed in living cells by fluorescence resonance energy transfer. *Nat. Immunol.* 6, 1168–1176 (2005).

29. H. W. Sohn, P. Tolar, S. K. Pierce, Membrane heterogeneities in the formation of B cell receptor-Lyn kinase microclusters and the immune synapse. *J. Cell Biol.* 182, 367–379 (2008).
30. C. L. Waites, C. G. Specht, K. Härtel, S. Leal-Ortiz, D. Genoux, D. Li, R. C. Drisdell, O. Jeyifous, J. E. Cheyne, W. N. Green, J. M. Montgomery, C. C. Garner, Synaptic SAP97 isoforms regulate AMPA receptor dynamics and access to presynaptic glutamate. *J. Neurosci.* 29, 4332–4345 (2009).
31. W. Zhou, L. Zhang, X. Guoxiang, J. Mojsilovic-Petrovic, K. Takamaya, R. Sattler, R. Huganir, R. Kalb, GluR1 controls dendrite growth through its binding partner, SAP97. *J. Neurosci.* 28, 10220–10233 (2008).
32. R. Xavier, S. Rabizadeh, K. Ishiguro, N. Andre, J. B. Ortiz, H. Wachtel, D. G. Morris, M. Lopez-Illasaca, A. C. Shaw, W. Swat, B. Seed, Discs large (Dlg1) complexes in lymphocyte activation. *J. Cell Biol.* 166, 173–178 (2004).
33. J. L. Round, T. Tomassian, M. Zhang, V. Patel, S. P. Schoenberger, M. C. Miceli, Dlg1 coordinates actin polymerization, synaptic T cell receptor and lipid raft aggregation, and effector function in T cells. *J. Exp. Med.* 201, 419–430 (2005).
34. M. J. Ludford-Menting, J. Oliaro, F. Sacirbegovic, E. T. Cheah, N. Pedersen, S. J. Thomas, A. Pasam, R. Iazzolino, L. E. Dow, N. J. Waterhouse, A. Murphy, S. Ellis, M. J. Smyth, M. H. Kershaw, P. K. Darcy, P. O. Humbert, S. M. Russell, A network of PDZ-containing proteins regulates T cell polarity and morphology during migration and immunological synapse formation. *Immunity* 22, 737–748 (2005).
35. B. Treanor, D. Depoil, A. Bruckbauer, F. D. Batista, Dynamic cortical actin remodeling by ERM proteins controls BCR microcluster organization and integrity. *J. Exp. Med.* 208, 1055–1068 (2011).
36. B. Treanor, D. Depoil, A. Gonzalez-Granja, P. Barral, M. Weber, O. Dushek, A. Bruckbauer, F. D. Batista, The membrane skeleton controls diffusion dynamics and signaling through the B cell receptor. *Immunity* 32, 187–199 (2010).
37. N. Parameswaran, K. Matsui, N. Gupta, Conformational switching in ezrin regulates morphological and cytoskeletal changes required for B cell chemotaxis. *J. Immunol.* 186, 4088–4097 (2011).
38. R. A. Lue, E. Brandin, E. P. Chan, D. Branton, Two independent domains of hDlg are sufficient for subcellular targeting: The PDZ1-2 conformational unit and an alternatively spliced domain. *J. Cell Biol.* 135, 1125–1137 (1996).
39. R. Lasserre, S. Charrin, C. Cuche, A. Danckaert, M. I. Thoulouze, F. de Chaumont, T. Duong, N. Perrault, N. Varin-Blank, J. C. Olivo-Marin, S. Etienne-Manneville, M. Arpin, V. Di Bartolo, A. Alcover, Ezrin tunes T-cell activation by controlling Dlg1 and microtubule positioning at the immunological synapse. *EMBO J.* 29, 2301–2314 (2010).
40. K. Adachi, M. M. Davis, T-cell receptor ligation induces distinct signaling pathways in naive vs. antigen-experienced T cells. *Proc. Natl. Acad. Sci. U.S.A.* 108, 1549–1554 (2011).
41. A. Zanin-Zhorov, J. Lin, J. Scher, S. Kumari, D. Blair, K. L. Hippen, B. R. Blazar, S. B. Abramson, J. J. Lafaille, M. L. Dustin, Scaffold protein Disc large homolog 1 is required for

T-cell receptor-induced activation of regulatory T-cell function. *Proc. Natl. Acad. Sci. U.S.A.* 109, 1625–1630 (2012).

42. D. D. Sarbassov, D. A. Guertin, S. M. Ali, D. M. Sabatini, Phosphorylation and regulation of Akt/PKB by the rictor-mTOR complex. *Science* 307, 1098–1101 (2005).

CHAPTER FIVE

Discs large homolog 1 (Dlg1) facilitates BCR-induced alternative p38 activation in IgM+ B cells

ABSTRACT

B cell receptors (BCRs) detect extracellular antigens and initiate signal transduction that influences cell survival, proliferation, differentiation and effector function. p38 is an ubiquitously expressed MAP kinase that acts as a key point of signal integration downstream of several extracellular receptors. In most cells p38 is activated in response to extracellular stress through direct phosphorylation by MKK3 and MKK6. However in T cells, an alternative activation pathway exists downstream of the TCR that requires scaffold protein Dlg1 and tyrosine kinases Lck and Zap70. Despite similarities in signal transduction downstream of the TCR and BCR, the existence of the alternative p38 pathway in B cells remains controversial. Here, we provide evidence that p38 can be activated via the alternative pathway in IgM⁺ B cells, and that this pathway requires scaffold protein Dlg1. We demonstrate that the Dlg1AB variant that facilitates activation of the alternative p38 pathway in T cells is highly expressed in naïve B cells. Dlg1AB forms a complex with Syk, Lyn and p38 in B cells that is able to coordinate phosphorylation of associated p38. In response to BCR-stimulation, we detected p38 phosphorylation at Y323, which is indicative of the alternative p38 pathway. Dlg1 knockout impaired BCR-induced p38 phosphorylation and production of p38-dependent cytokines IFN γ and IL-4. Together our results demonstrate that Dlg1 coordinates alternative p38 activation in response to BCR stimulation in IgM⁺ B cells.

INTRODUCTION

B cells play a vital role in the adaptive immune response by rapidly expanding, producing cytokines and releasing antibodies. Recognition of extracellular antigens by the B cell receptor (BCR) leads to receptor aggregation and activation of an array of intracellular effector molecules. BCR-dependent signaling is initiated by proximal tyrosine kinases Lyn and Syk, propagated by MAP kinase (MAPK) family members ERK, JNK and p38 and guided by transcription factors such as NFAT, NF κ B and Jun. These transcription factors control the expression of genes that control B cell proliferation, differentiation and effector responses. The high fidelity of B cell responses suggest that these cells do not produce a singular response to all stimuli, but instead survey their environment and make decisions based on the cues encountered (1). In fact, it is essential that these signals translate into precise biological responses as aberrant B cell responses lead to the initiation and progression of autoimmune disorders (2).

The MAPK p38 is expressed in all eukaryotic cells, and is primarily activated through a three tiered kinase cascade culminating in direct phosphorylation of p38 at Y182 and T180 by MKK3 or MKK6, which enhances p38 kinase activity on a host of downstream substrates (3, 4). Additionally, an alternative p38 activation pathway has been described in T cells that is MKK-independent and instead depends on the kinase activity of TCR proximal tyrosine kinases Lck and Zap70 (5, 6). Despite the similarities in signaling components downstream of the TCR and the BCR, initial reports suggested that alternative p38 pathway does not occur in B cells (5, 7). This difference has been attributed to expression of different Src and Syk family members in each cell type. While T cells express Src kinase Lck and Syk kinase Zap70, the major family members expressed in B cells are Lyn and Syk respectively.

In T cells, the alternative p38 pathway is coordinated by MAGUK family scaffold protein Dlg1, which forms a complex with Lck, Zap70 and p38. This complex facilitates the phosphorylation of p38 at Y323 by Zap70. Phosphorylation of p38 at Y323 is specific to the alternative pathway, and facilitates p38 auto-phosphorylation at T180 in the activation loop that

enhances p38 kinase activity (5, 7, 8). Subsequently, alternative p38 activation induces a subset of NFAT-dependent transcription through phosphorylation of NFATc2 at activating residue S54 (9). Recently, Liu et al. demonstrated a role for Dlg1 in BCR clustering, immune synapse formation and signal transduction in IgG+ B cells (10). Their study determined that Dlg1 localizes to the immune synapse in B cells by associating with the cytoplasmic tail of the IgG BCR. While at the synapse Dlg1 plays a role required for phosphorylation of Syk, and the specific activation of p38, but not ERK or JNK (10). However, the mechanism of p38 activation or the role of Dlg1 in IgM+ B cells was not investigated.

Here we provide evidence that p38 can be activated via the alternative p38 pathway downstream of the BCR in IgM+ B cells, and that Dlg1 is an essential mediator of this pathway. We demonstrate that the Dlg1 splice variant known to regulate alternative p38 activation in T cells, Dlg1AB, is expressed at high levels in B cells. We show that Dlg1 forms a complex with Lyn, Syk and p38, and that this complex can coordinate phosphorylation of Dlg1-associated p38 *in vitro*. Importantly, stimulation of IgM+ B cells through their BCR induces p38 phosphorylation at Y323, and at T180. Phosphorylation of p38 Y180 is inhibited by blocking p38 or Lyn activity, demonstrating that its phosphorylation occurred through the alternative pathway. Further, we show that acute knockout of Dlg1 in B cells impairs p38 phosphorylation as well as production of p38-dependent cytokines. Together our data provide strong evidence that Dlg1 facilitates alternative activation of p38 in IgM+ B cells in response to BCR stimulation.

RESULTS

Dlg1AB splice variant is expressed in B cells

Dlg1 is expressed in B cells; however, the existence of the alternative p38 pathway in B cells, and the ability of Dlg1 to coordinate this pathway are still under investigation. We have recently demonstrated that the Dlg1AB, but not Dlg1B splice variant can coordinate the alternative p38 pathway (Chapter 2, Chapter 3). As a first approximation of Dlg1 expression across cell types we performed quantitative RT-PCR analysis on a panel of primary and

transformed T and B cells using primers specific for total Dlg1 (Figure 5-1) or Dlg1AB (Figure 5-1). Controls were run to validate the specificity of the primers for Dlg1AB, and to optimize quantitation (data not shown). These experiments demonstrated that total Dlg1 expressed is at a similar level in naïve B cells, naïve CD8⁺ T cells and naïve CD4⁺ T cells which are known to facilitate Dlg1-dependent events. Additionally, naïve B cells express the highest proportion of the Dlg1AB splice variant, known to coordinate the alternative p38 pathway in T cells. Together our demonstrate that B cells express total Dlg1 and specifically Dlg1AB at equivalent or higher levels compared to their T cell counterparts.

Dlg1 forms an active complex with Lyn, Syk and p38 that facilitates p38 phosphorylation in vitro

In T cells association of Dlg1 with Src family member Lck and Syk family member Zap70 along with MAPK p38 is required for alternative p38 activation (9). In B cells, the major Src family member expressed is Lyn and the major Syk family member is Syk. We performed Dlg1 immunoprecipitations from WeHi B cells unstimulated or stimulated for 15 min with α lgM. In these experiments Dlg1 associated constitutively with p38 and inducibly with Lyn and Syk (Figure 5-2). To determine if the Dlg1 complex was able to facilitate p38 phosphorylation we used GST-Dlg1AB fusion proteins as bait in WeHi B cell lysates. Upon the addition of ATP, robust phosphorylation of Dlg1-associated p38 was observed (Figure 5-2). Together our results showed that Dlg1 forms a complex with Lyn, Syk and p38 in B cells similar to the Dlg1 complex formed in T cells. Additionally, this complex is active, and facilitated p38 phosphorylation *in vitro*.

Alternative p38 activation occurs in response to BCR-stimulation in IgM⁺ B cells

In T cells, the hallmarks of alternative p38 activation are TCR-dependence, p38 phosphorylation at Y323 and inhibition of p38 T180 phosphorylation by p38 or Src family kinase inhibitors (5, 6). To determine if p38 is activated via the alternative pathway in response to BCR stimulation in IgM⁺ B cells, we stimulated WeHi B cells in the presence or absence of 20 μ M p38 inhibitor. In response to BCR stimulation, p38 phosphorylation was detected with an antibody

for p-p38 T180/Y182 (Figure 5-3), and p-p38 Y323 (Figure 5-3). Additionally, p38 T180/Y182 phosphorylation was blocked by addition of p38 inhibitor (Figure 5-3). To extend our results into primary cells we isolated murine B cells and stimulated them with α IgM in the presence or absence of p38 inhibitor or Src kinase inhibitor PP2. We found that p38 phosphorylation was BCR-inducible in primary B cells, and that this phosphorylation was blocked by p38 or Src kinase inhibitors (Figure 5-3). Additionally, we found that BCR-induced NFAT, but not NF κ B-dependent transcription was p38-dependent (Figure 5-4). Together these results showed that p38 is activated via the alternative p38 pathway in IgM⁺ B cells in response to BCR stimulation, and that this pathway may specifically regulate NFAT-, but not NF κ B-dependent genes.

Acute Dlg1 knockout impairs BCR-triggered p38 phosphorylation and cytokine production

Recently we have utilized an acute Dlg1 knockout system to characterize the role of Dlg1 in CD8⁺ CTLs *in vitro* and CD8⁺ T cells *in vivo* (Chapters 2 & 3). In both cases, loss of Dlg1 has impaired TCR-induced p38 phosphorylation and expression or production of IFN γ . To determine if Dlg1 plays a role in coordinating p38 activation in B cells we treated Dlg1^{fl^{ox}/fl^{ox}} ER-cre mice with tamoxifen or mock solution. Total splenic B cells were isolated and Dlg1 knockout was confirmed via genomic DNA PCR and Western blot protein analysis (Figure 5-5). While we observed no significant changes in the total number of splenocytes or B cells in Dlg1 knockout mice, we did observe significant functional changes (Figure 5-5). Upon stimulation with α IgM, Dlg1^{KO} cells exhibited a 50% decrease in p38 phosphorylation compared Dlg1^{WT} (Figure 5-5). Additionally, Dlg1^{KO} cells produced significantly less IFN γ and IL-4 when stimulated with α IgM (Figure 5-5). Together our data demonstrate a role for Dlg1 in mediating p38 activation in B cells, and suggest that this activation is required for optimal production of cytokine IFN γ and IL-4.

DISCUSSION

In T cells, activation of p38 via the alternative pathway is mediated by scaffold protein Dlg1, and leads to specific up regulation of NFAT-dependent genes including pro-inflammatory cytokines IFN γ and TNF α , but not IL-2 (9) (Chapter 3). Dysregulation of this pathway in T cells has been linked to the initiation and progression of autoimmunity through the overproduction of pro-inflammatory cytokine and/or deterioration of FoxP3⁺ regulatory T cells (8, 11-13). Here, we identified a Dlg1-mediated mechanism of alternative p38 activation in IgM⁺ B cells. We demonstrated that Dlg1AB is highly expressed in B cells and forms a complex with Lyn, Syk and p38 that facilitated phosphorylation of bound p38 in a cell-free system. BCR stimulation led to phosphorylation of p38 at alternative residue Y323, and p38-dependent phosphorylation at T180. Further inhibition of p38 activity impaired NFAT-, but not NF κ B-dependent transcription. Finally genetic knockout of Dlg1 led to impaired p38 phosphorylation and cytokine production. Together our data demonstrate that p38 can be activated via the alternative p38 pathway in a Dlg1-dependent manner downstream of the BCR, and that this pathway may guide the production of several cytokines including IFN γ and IL-4.

Initial reports characterizing the alternative p38 pathway suggested that it occurred in T cells, but not B cells (5, 7). These reports show that p38 immunoprecipitates from B cells do not auto-phosphorylate, and that p38 immunoprecipitates from stimulated B cells are not phosphorylated at p38 Y323 (5). Additionally, they showed that p38 immunoprecipitates from p38 Y323F knock-in mice are able to phosphorylate canonical p38 substrate ATF-2 (7). In order to explain these apparent discrepancies, we suggest that alternative p38 activation may be occurring in subset of p38, which is associated with Dlg1. All of the experiments presented by Ashwell's group involve examination of total cellular p38 via p38 immunoprecipitation. In this case, the canonical pathway could mask the presence of an alternative p38 pathway occurring in a subset of p38. In contrast, many of our experiments have examined p38 phosphorylation specifically in the subset of p38 that is associated with scaffold protein Dlg1. This method could allow us to identify a pathway that is masked when examining total cellular p38. Further, while

our experiments used the same amount IgM stimulation as Ashwell's group, we added co-stimulation with CD40 antibody, which could increase the intensity of p38 alternative activation.

Recently Liu et al. has shown that Dlg1 enhances BCR-mediated signaling in IgG+ memory B cells (10). This report demonstrates that Dlg1 accumulates at the immune synapse through association with the cytoplasmic tail of the IgG BCR and that loss of Dlg1 in B cells leads to impaired BCR-clustering, immune synapse formation and Syk phosphorylation. Importantly, they also observed a specific defect in p38 phosphorylation, but not in other MAPKs JNK and ERK when Dlg1 was knocked down. These results suggest that Dlg1 is required for p38 phosphorylation downstream of the IgG BCR. However, they do not rule out the possibility that Dlg1 is facilitating p38 activation through a canonical pathway. Our work demonstrates that Dlg1 coordinates p38 phosphorylation in IgM+ B cells through an alternative p38 activation pathway similar to the one characterized in T cells, and suggests that Dlg1-mediated p38 activation in IgG+ B cells may also occur through the alternative pathway (5, 9).

In summary, our study demonstrates that p38 can be activated via the alternative p38 pathway in IgM+ B cells through a Dlg1-dependent mechanism. We found that Dlg1AB is expressed at high levels in B cells, and that it forms a complex with Lyn, Syk and p38 analogous to the complex it forms with Lck, Zap70 and p38 in T cells. The complex facilitates phosphorylation of associated p38 using a cell free system. Further, BCR-induced p38 phosphorylation occurs on Y323, which is the hallmark of alternative activation. Similarly to T cells, NFAT, but not NF κ B-dependent transcription is p38 dependent. Finally, using a Dlg1 knockout system we show that loss of Dlg1 impairs BCR-induced p38 activation and cytokine production. Together our data are the first to describe the activation of p38 via the alternative pathway in B cells.

METHODS

Mice and Dlg1 knockout

The generation of Dlg1^{flox/flox} mice has been previously described (Chapters 2 and 3). These mice have loxP sites flanking the *dlg1* exon encoding a portion of PDZ1 and PDZ2. Dlg1^{flox/flox} mice were crossed with ER-Cre transgenic mice (Jackson Lab) and offspring (ER-Cre Dlg1^{flox/+}) were crossed with Dlg1^{flox/flox} mice to generate ER-Cre Dlg1^{flox/flox} mice. For knockout, 6-to-8 week old mice were injected IP with 2mg tamoxifen or mock solution (ethanol and sunflower seed oil) per day on 5 consecutive days followed by rest of 14-21 days. All mice were maintained and used in accordance with the University of California Los Angeles Chancellor's Animal Research Committee.

B cell isolation

Splenocytes were harvested and purified as previously published (Chapter 2,3). B cells were isolated using via negative selection according to manufacturer's instructions (Miltenyi 130-090-862).

mRNA isolation, reverse transcription and quantitative PCR analysis

RNA was isolated using TriZol reagent as previously described (9). 2µg RNA was reverse-transcribed using Superscript II reverse transcriptase (Invitrogen) according to the manufacturer's instructions using random hexamer and oligo(dT)₂₀ as primers. The iCycler thermocycler was used for quantitative PCR analysis according to manufacturer's instructions (BioRad). A final volume of 25µl was used for each quantitative PCR reactions as previously described (9). The following gene-specific primers were used for amplification: L32F-5'-AAGCGAAACTGGCGGAAAC-3', L32(R)-5'-TAACCGATGTTGGGCATCAG-3', NFATc1(F)-5'-GCCTCGTAT CAGTGGGCGAAG-3', NFATc1(R)-5'-CGAAGCTCGTATGGACCA-3', IκBα(F)-5'-CTGCAGGCCACCAACTACAA-3', IκBα(R)-5'-CAGCACCCAAAGTCACCAAGT-3', Dlg1 total(F)-5'-AGATCGCATCATATCGGTGAA-3', Dlg1 total(R)-5'-

TCAAACGACTGTACTCTTCGG-3', Dlg1AB(F)-5'- CGCACACAGGCAAA -3', Dlg1AB(R)-5'- TACTTGAGTCATCTCCAATGTGTG-3'. All quantitative PCR products were normalized to L32 ribosomal protein quantitative PCR products.

Immunoprecipitations and blotting

For immunoprecipitation: WeHi cell lysates were incubated with 20 μ l 50% (v/v) protein G sepharose beads (GE Healthcare 17-5132-01) for 2hrs at 4°C. Sepharose beads were removed and lysates were incubated with 2 μ g α Dlg1 antibody (BD Biosciences 610875) or IgG1 κ control antibody (BD Pharmingen 554121) for 1hr at 4°C, then 40 μ l 50% protein G sepharose beads in PBS were added and incubated over night (~12hrs) at 4°C. Beads were washed and boiled with Laemmle buffer. Blotting was performed using antibodies directed against Dlg1 (BD Biosciences 610875), Syk (Cell Signaling 2712), Lyn (Cell Signaling 2796), or p38 (clone C20; Santa Cruz SC535), Blots were imaged using ECL Plus Western Blotting Substrate (Pierce 32132) or LiCor Odyssey Imaging System.

In vitro kinase assays

WeHi B cells (40x10⁶) were lysed using IP Lysis buffer (Pierce) in the presence of protease and phosphatase inhibitors (Pierce). Resulting lysates were cleared by centrifugation and incubated with WT or Y222F GST-Dlg1 fusion proteins bound to glutathione sepharose beads slurry, then washed twice with kinase buffer (Cell Signaling). Resulting bead complexes were incubated at 30°C for 20 minutes in 50 μ l kinase buffer in the presence or absence of ATP (Cell Signaling).

Intracellular p-p38

For measurement of p38 phosphorylation: expanded primary B cells were harvested, counted and placed in fresh media at a concentration of 2x10⁶ cells per ml. Cells were allowed to rest for 4hrs at 37°C in 6-well dishes at volume of 2mls per well and were transferred to 12-well plates coated with IgM 10 μ g/ml goat anti-mouse IgM Fab (Jackson 115-006-020) and 1 μ g/ml CD40

(clone IC10) with a final volume of 1ml per well (2×10^6 cells) and incubated for 5min or 15min at 37°C to stimulate. Cells were fixed in paraformaldehyde (4% final concentration) for 30min followed by permeabilization using the FoxP3 staining buffer set (eBioscience 00-5523-00) according to manufacturer's instructions. Phosphorylated p38 T180/Y182 was detected using Alexa Fluor 647 conjugated α -p38 antibody (T180/Y182; BD Phosflow 612595) at 1:20.

Intracellular Cytokines

Primary mouse B cells were restimulated with 10g/ml IgM and 1 μ g/ml CD40 for 6 hrs in the presence of GolgiPLUG (BD 555029). Cells were surface stained with B220-PE in FACS wash buffer (PBS + 3% FCS + 0.1% sodium azide) prior to overnight fixation and permeabilization with BD Cytotfix/Cytoperm (BD 51-2090KZ) at 4°C. Cells were then washed in BD Permeabilization wash solution, stained for 30 mins with IFN γ -APC or IL-4-APC, washed and data collected using a BD FACS-Calibur.

Statistical methods

Standard deviations (SD) and standard error of the mean (SEM) were calculated using Excel (Microsoft). Significance was assessed by two-tailed t test. P values < 0.05 were considered significant.

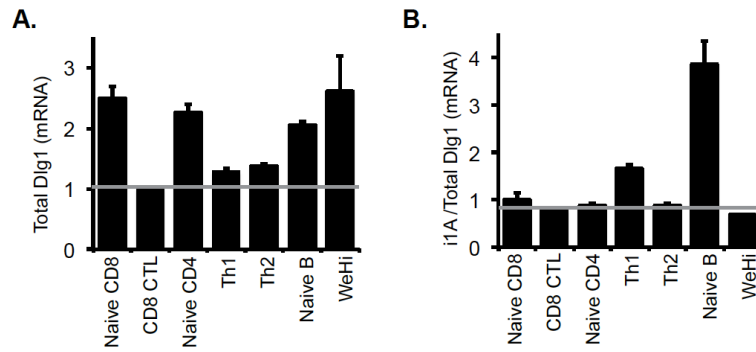


Figure 5-1: Dlg1 expression profiles in T and B lymphocytes. (A-B) mRNA was isolated from a panel of primary T cells and B cells from mice or cell lines followed by reverse transcription and quantitative PCR using primers specific for total Dlg1 (A) or Dlg1AB splice variant (B). Data are representative of two independent experiments.

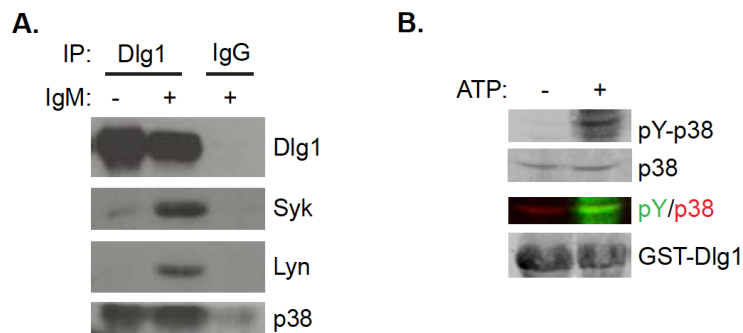


Figure 5-2: Dlg1 forms a BCR-inducible complex with Lyn, Syk and p38 that facilitates p38 phosphorylation *in vitro*. (A) Dlg1 immunoprecipitations from WeHi B cells unstimulated or stimulated for 15 min with IgM, followed by separation using SDS-PAGE and blotting with Dlg1, Syk, Lyn or p38 antibodies. (B) GST pulldown using GST-Dlg1 fusion proteins in WeHi B cell lysates. Resulting complexes were washed and incubated with ATP in the presence or absence of PP2. Immunoblots were performed using pY (pY-p38), p38 or GST (GST-Dlg1). Data are representative of two independent experiments.

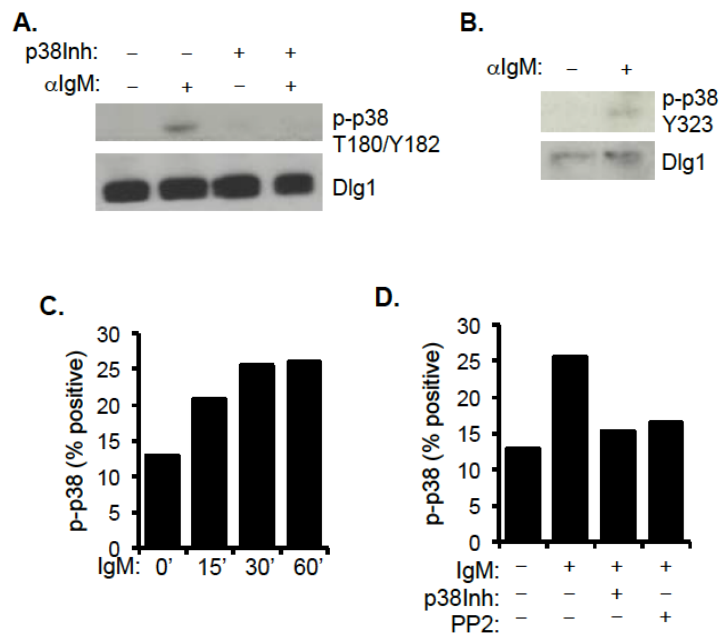


Figure 5-3: BCR-inducible alternative p38 activation occurs in IgM+ B cells. (A-B) WeHi hybridomas were left unstimulated or stimulated using IgM and CD40 for 15 min in the presence or absence of 20uM SB203580 (p38Inh). Whole cell lysates were separated on SDS-PAGE gels and blotted using Dlg1 (A-B), p-p38 T180/Y182 (A) and p-p38 Y323 (B). (C-D) B cells were sorted from total mouse splenocyte cells using negative selection to >95% purity. Cells were stimulated using IgM and CD40 for 0, 15, 30 or 60 min (C) or 30 min in the presence of 20M SB203580 (p38Inh) or 10uM PP2 and then stained for intracellular p-p38 T180/Y182. Results are presented as percent positive. Data are representative of two independent experiments.

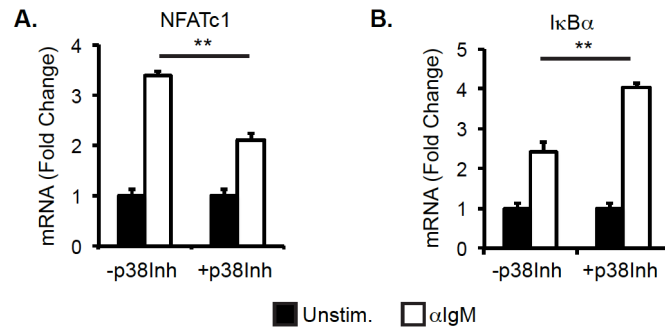


Figure 5-4: BCR-induced NFAT-, but not NFκB-dependent transcription is p38-dependent. (A-B) Total B cells isolated from spleens of C57Bl/6 mice were left unstimulated or stimulated for 2hs in the presence or absence of 20M SB203580 (p38Inh). Quantitative PCR was performed on cDNA from samples using primers specific for NFAT-dependent gene (NFATc1) or NFκB-dependent gene (IκBα).

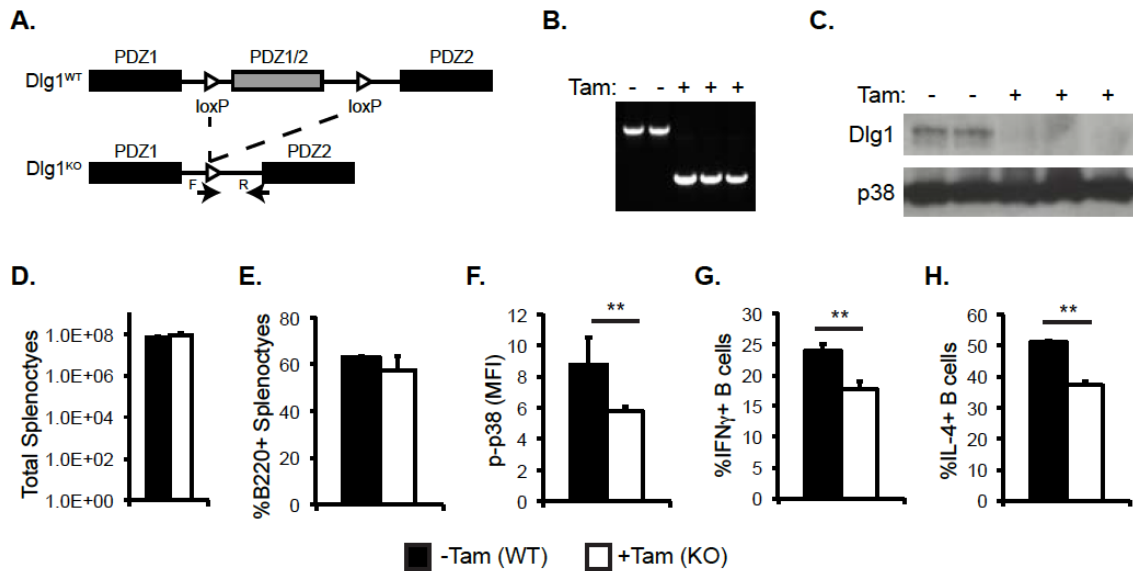


Figure 5-5: Dlg1 knockout impairs BCR-induced p38 phosphorylation and cytokine production in IgM+ B cells. (A) Schematic of the *Dlg1* knockout locus. Two loxP sites are inserted flanking exon 8 that codes for parts of the PDZ1 and PDZ1 domains. Expression of cre recombinase leads to loss of exon 8 and loss of *Dlg1* protein expression. (B-H) Total splenocytes were isolated from *Dlg1*^{flox/flox} ER-CRE mice. (B) Genomic DNA from mice was amplified using primers that flank exon 8. (C) Whole cell lysates were separated using SDS_PAGE and blotted using *Dlg1* and p38. (D) Total number of splenocytes. (E) Percent B220+ B cells in total splenocytes. (F-G) Total splenocytes were stimulated with IgM and CD40 or 30min (F) or 48hrs (G-H). Cells were fixed and stained for intracellular p-p38 (F), IFN γ (G) or IL-4 (H).

REFERENCES

1. Dal Porto JM, Gauld SB, Merrell KT, Mills D, Pugh-Bernard AE, Cambier J. B cell antigen receptor signaling 101. *Molecular immunology* 2004, **41**(6-7): 599-613.
2. Finnegan A, Ashaye S, Hamel KM. B effector cells in rheumatoid arthritis and experimental arthritis. *Autoimmunity* 2012, **45**(5): 353-363.
3. Ashwell JD. The many paths to p38 mitogen-activated protein kinase activation in the immune system. *Nature reviews Immunology* 2006, **6**(7): 532-540.
4. Cook R, Wu C-C, Kang yJ, Han J. The Role of the p38 Pathway in Adaptive Immunity. *Cellular and Molecular Immunology* 2007, **4**(4): 253-259.
5. Salvador JM, Mittelstadt PR, Guszczynski T, Copeland TD, Yamaguchi H, Appella E, *et al.* Alternative p38 activation pathway mediated by T cell receptor-proximal tyrosine kinases. *Nature immunology* 2005, **6**(4): 390-395.
6. Mittelstadt PR, Yamaguchi H, Appella E, Ashwell JD. T cell receptor-mediated activation of p38alpha by mono-phosphorylation of the activation loop results in altered substrate specificity. *The Journal of biological chemistry* 2009, **284**(23): 15469-15474.
7. Jirmanova L, Sarma DN, Jankovic D, Mittelstadt PR, Ashwell JD. Genetic disruption of p38a Tyr323 phosphorylation prevents T-cell receptor-mediated p38a activation and impairs interferon-g production. *Blood* 2009, **113**: 2229-2237.
8. Jirmanova L, Giardino Torchia ML, Sarma ND, Mittelstadt PR, Ashwell JD. Lack of the T cell-specific alternative p38 activation pathway reduces autoimmunity and inflammation. *Blood* 2011, **118**(12): 3280-3289.
9. Round JL, Humphries LA, Tomassian T, Mittelstadt P, Zhang M, Miceli MC. Scaffold protein Dlg1 coordinates alternative p38 kinase activation, directing T cell receptor signals toward NFAT but not NF-kappaB transcription factors. *Nature immunology* 2007, **8**(2): 154-161.
10. Liu W, Chen E, Zhao XW, Wan ZP, Gao YR, Davey A, *et al.* The Scaffolding Protein Synapse Associated Protein 97 is Required for Enhanced Signaling Through Isotype-Switched IgG Memory B Cell Receptors. *Science Signaling* 2012, **5**(235): ra54.
11. Salvador JM, Hollander MC, Nguyen AT, Kopp JB, Barisoni L, Moore JK, *et al.* Mice Lacking the p53-Effector Gene Gadd45a Develop a Lupus-Like Syndrome. *Immunity* 2002, **16**: 499-508.
12. Salvador JM, Mittelstadt PR, Belova GI, Fornace AJ, Jr., Ashwell JD. The autoimmune suppressor Gadd45alpha inhibits the T cell alternative p38 activation pathway. *Nature immunology* 2005, **6**(4): 396-402.
13. Zanin-Zhorov A, Lin J, Scher J, Kumari S, Blair D, Hippen KL, *et al.* Scaffold protein Disc large homolog 1 is required for T-cell receptor-induced activation of regulatory T-cell function. *Proceedings of the National Academy of Sciences of the United States of America* 2012, **109**(5): 1625-1630.

CHAPTER SIX

Conclusions and Future Directions

The T cell receptor is unique in its ability to discriminate subtleties in antigenic peptide presentation and translate these differences into distinct biological outcomes. A better understanding of the molecular events that underlie this specificity will allow us to design targeted therapeutics capable of impacting a particular pathway while leaving the majority of the immune response intact. Previous work has shown that MAGUK family scaffolds are one tool that the TCR utilizes to specify T cell function (1-6). The data presented here extend these findings to B cells, and demonstrate that Dlg1 function is guided by both post-transcriptional and post-translational modifications. While Dlg1 has been appreciated as a regulator of signaling and cytoskeletal events downstream of the TCR, we now present a unified molecular mechanism by which Dlg1 controls these pathways individually and together. We propose that expression, utilization and/or recruitment of Dlg1 splice variants along with Dlg1 phosphorylation events allow TCR signals to be integrated and translated into specific functional consequences. This chapter will describe our findings and speculate on their role in translating TCR signals into cellular function.

Dlg1 Modifications Uncouple TCR-mediated Cytoskeletal and Signaling Events

We have provided data demonstrating that at least two Dlg1 variants are expressed in T cells through alternative splicing: Dlg1AB and Dlg1B. We have also shown that these variants can differentially regulate functionality downstream of the TCR. In attempting to understand the role of Dlg1 splice variants in regulating T cell function we identified Dlg1AB as a unique ligand of Dlg1AB, but not Dlg1B. The association of Lck with the proline rich region of Dlg1 encoded by the i1A region is supported by reports that this interaction occurs between the Lck SH3 domain and the N-terminal region of Dlg1 (4, 6). Consistent with a role for Lck in the alternative p38 pathway, Dlg1AB, but not Dlg1B was able to facilitate p38 phosphorylation, NFAT-dependent transcription and up regulation of pro-inflammatory cytokine genes. Conversely, both Dlg1AB and Dlg1B facilitate TCR-induced cytoskeletal functions including F-actin polymerization and release of cytotoxic granules during contact dependent lysis. We show that these functions are

dependent on WASp activity. Further, we demonstrate that both Dlg1AB and Dlg1B increase the portion of WASp in the open/active conformation. These results are supported by previous work mapping WASp association to the SH3 domain of Dlg1, which is expressed in both the Dlg1AB and Dlg1B isoforms (4). Collectively, our results identify that Dlg1 splice variants as a method to uncouple Dlg1-mediated signaling and cytoskeletal functions. Initial studies examining Dlg1 splice variant expression demonstrate that the total amount of Dlg1 as well as the ratio of Dlg1AB to Dlg1B varying across cell types (Figure 5-1). These results are supported by a recently published RNASeq study that identified Dlg1-i1A as one of the most highly spliced exons in response to TCR stimulation (7). Future studies will be focused on the mechanisms that dictate splicing in different cell types and in response to different levels of TCR stimulation.

We demonstrate that TCR-induced Dlg1 tyrosine phosphorylation is a key point of control required for alternative p38 activation downstream of the TCR. We show that phosphorylation occurs preferentially on the Dlg1AB variant, and is mediated by a Dlg1-associated kinase. Upon investigating candidate kinases, we find that Lck, but not Zap70 can phosphorylate Dlg1. While our data suggest that several tyrosine residues of the Dlg1 protein are phosphorylated we have identified Tyr222 (Y222) as a specific site of Lck-mediated Dlg1 phosphorylation. Phosphorylation of Y222 is required for Dlg1 to facilitate phosphorylation of associated p38. Expression of Dlg1 with a mutation of Y222 to phenylalanine (Y222F) specifically impaired TCR-induced p38 phosphorylation and NFAT-dependent transcription of IFN γ and TNF α . Expression of this mutant had no affect on release of cytotoxic granules required for contact dependent lysis, which is regulated in part by Dlg1B. Our data identify Dlg1 Y222 phosphorylation as vital step that licenses Dlg1AB to coordinate the alternative p38 pathway. Similar phosphorylation events are required for MAGUK scaffold CARMA1 to coordinate JNK and NF κ B in T and B cells (8, 9). Phosphorylation of CARMA1 converts the scaffold from the closed to open conformation, which facilitates association with ligands required for proper function. Since Dlg1 also exists in several closed conformations, we predict that phosphorylation could lead to a similar conformational change (10-15). Alternatively,

phosphotyrosines can form binding sites for SH2 domain containing proteins (16). The most likely candidate for association with pY222 is Zap70 as it contains tandem SH2 domains. While we have not observed consistent loss of the Dlg1:Zap70 association in Y222F mutants, we cannot rule out a role for Y222 in Zap70 juxtaposition as it often binds using both of its SH2 domains. Therefore, the yet unidentified phosphotyrosine site may be sufficient to facilitate a tentative association between Dlg1 and Zap70 while still disrupting proper Zap70 position and therefore p38 phosphorylation. Future experimentation will be required to delineate these details.

Together these data have allowed us to propose a mechanism by which Dlg1-mediated signaling and cytoskeletal functions can be regulated individually or together in order to customize the T cell response to antigen (Figure 6-1). TCR-triggered cytoskeletal functions, including actin polymerization and effector molecule release, are regulated by WASp interaction with the SH3 domain of either Dlg1AB or Dlg1B. Conversely, p38 phosphorylation and NFAT-dependent transcription of pro-inflammatory cytokines can only be coordinated by Dlg1AB. Our data suggest a mechanism where Lck associates with and phosphorylates Dlg1AB at several sites including Y222, which likely causes a conformational shift required for p38 phosphorylation and downstream activation of NFAT-dependent transcription of pro-inflammatory cytokines IFN γ and TNF α . The release of these cytokines, however, is likely mediated by Dlg1-mediated WASp-dependent events. This model predicts that decreased expression or phosphorylation of Dlg1AB would selectively decrease the production of pro-inflammatory cytokines, but not the formation of the immune synapse or release of other effectors such as cytotoxic granules or IL-2. Therefore, the specific targeting of the Dlg1AB pathway could facilitate inhibition of pro-inflammatory signals while rendering the rest of the immune response unharmed. For example, a peptide designed to block the interaction between Lck and Dlg1 would inhibit production of IFN γ and TNF α , while maintaining the individual functions of both Lck and Dlg1. Future studies will allow us to explore the therapeutic potential of targeting Dlg1-mediated pathways.

In CD8+ CTLs, a low level of TCR stimulation is sufficient to mediate contact dependent lysis, but high levels of stimulation are required for pro-inflammatory cytokine production (18-20). Additionally, the activation of Lck and the expression of Dlg1AB are highly dependent on the degree of TCR stimulation (7, 18). We predict that Lck-dependent phosphorylation of Dlg1 only occurs under conditions where antigen quality and quantity are high in order to control the production of potentially harmful pro-inflammatory cytokines. Additionally, we predict that the levels of Dlg1AB expressed in CTLs decreases upon high levels of stimulation as a mechanism to down regulate pro-inflammatory cytokine production while maintaining other vital effector functions such as target cell killing. Studies to investigate these predictions are currently underway.

B cells: New Cell Type, New Possibilities

While the role of Dlg1 in specifying TCR-dependent signals has been described, its role in B cells remains controversial. Here we show that Dlg1 coordinates p38 phosphorylation in B cells. Using an *in vitro* system we demonstrate that Dlg1 forms a complex with Lyn, Syk and p38 that is analogous to the complex that mediates p38 phosphorylation in T cells. Dlg1 complexes isolated from BCR-stimulated B cells are associated with p38 phosphorylated at Y323, suggesting that activation occurs through the alternative pathway. Further, loss of Dlg1 in either IgM or IgG B cells leads to impaired p38 phosphorylation in response to BCR-stimulation. Together these data demonstrate that Dlg1 coordinates the alternative p38 pathway downstream of the BCR in both IgM and IgG B cells. In T cells, NFAT, but not NFκB is activated downstream of the alternative p38 pathway leading to transcription of IFNγ (6). We find that BCR-induced NFAT, but not NFκB is p38 dependent suggesting that a similar mechanism of specificity exists in B cells. Additionally, p38 has been implicated in proliferation, class switching and cytokine production in B cells. Initial studies suggest that Dlg1-mediated p38 activation will play a role in these functions, however further experimentation is needed to clarify these results.

In addition to its role in p38 activation, we show that Dlg1 is present at the immune synapse and co-localizes with the mIgG upon BCR stimulation. However, Dlg1 is not able to associate with the short cytoplasmic tail of mIgM. These results suggest that Dlg1 plays a role in IgG BCR clustering and oligomerization, which could lead to the enhanced signaling observed upon stimulation of IgG BCRs. While Dlg1 association with mIg may enhance BCR-induced signaling, it is not required for Dlg1-mediated p38 activation. Therefore, we predict that Dlg1 plays a dual role in B cells (i) regulating BCR-induced alternative p38 phosphorylation (ii) regulating BCR clustering and other cytoskeletal events. It is likely that the regulatory mechanisms found in T cells including alternative splice variants and phosphorylation will play a role in regulating Dlg1 function in B cells. We have determined that Dlg1AB is expressed in B cells; however future experimentation is required to determine fully examine the role of Dlg1 splice variants and phosphorylation in shaping Dlg1-mediated B cell function.

Future Directions: Inducible Dlg1 Knockout System

We and others have defined a role for Dlg1 as an important regulator of T cell development and effector function (4, 6, 21-23). Due to the perinatal lethality of Dlg1 knockouts, these initial studies have been performed using a variety of Dlg1 knockdown methods, which are limited to *in vitro* studies on mature cell types. A collaborative study from our lab examining three conditional and germline Dlg1 knockout systems, observed no or minor defects in T cell development, morphology, migration, signaling, activation or proliferation (24). Another group has observed variable outcomes in proliferation and CD4⁺ memory formation in their knockout systems (25, 26). Because developmental compensatory mechanisms have been reported to mask functional changes in Dlg1 knockouts in neurons, an inducible Dlg1 knockout system was created. Using this system we have confirmed the importance of Dlg1 in mediating TCR-induced signaling and cytoskeletal event in CD8⁺ CTLs (Chapter 3), identified a role for Dlg1 in B cell signaling (Chapter 5), and defined a role of Dlg1 in coordinating *in vivo* responses to LCMV and influenza (Chapter 2, Figure 6-2 & Figure 6-3). The successes of these initial studies

make our inducible Dlg1 knockout system the method of choice for further dissecting the role of Dlg1 specifying the adaptive immune response.

Production of an appropriate immune response to influenza is a balancing act between effector functions that mediate viral clearance and those that induce tissue pathology (19, 20, 27, 28). Indeed, the ability to cause inflammatory-induced tissue pathology is credited with the high level of morbidity and mortality seen in pandemic influenza viruses (27, 28). The role of CD8+ CTLs in mediating the immune response to influenza is well documented; however, scrutiny of the individual contributions of pro-inflammatory cytokine production and target cell killing have remained elusive. Initial studies point to a role for Dlg1 in mediating immunity to influenza (Figure 6-2). Adoptive transfer of CD8+ CTLs re-expressing Dlg1AB or Dlg1B into mice, followed by influenza infection could allow us to uncouple the role of these two functions during influenza. We predict that cells expressing either variant will be able to clear influenza infection, but that cells expressing Dlg1B only will cause less lung damage due to a lack of pro-inflammatory cytokine production. Studies to test this hypothesis have been planned.

Concluding Remarks

How exactly lymphocytes sense external stimuli in order to elicit distinct biological outcomes is a complex question. Immunoreceptors such as the TCR and BCR are accompanied by a variety of other surface receptors that adapt extracellular signals into intracellular cues. Signaling from these receptors leads to a web of activated early kinases and cytoskeletal mediators that must be translated into discrete biological responses. MAGUK scaffold proteins Dlg1 and CARMA1 form specific signaling complexes that provide the framework to translate these early signals into an organized signaling network capable of directing distinct biological outcomes. While various adaptors are present in lymphocytes, Dlg1 and CARMA1 provide the only examples of molecules that we know to bifurcate signals downstream of the immunoreceptor. A role for CARMA1 in channeling PKC θ signals toward JNK and NF κ B in both T and B cells has been described, while the ability of Dlg1 to harness proximal

signals from Lck and Zap70 to activate p38 and NFAT has only been examined in T cells. Here, we present the first data demonstrating a role for Dlg1-mediated p38 activation in B cells. We predict that further investigation into this pathway will lend insight into selective activation of effector functions downstream of the BCR. In addition we have defined two Dlg1-mediated pathways in T cells: an Lck-dependent pathway responsible for p38 activation and cytokine production and a WASp-dependent pathway responsible for actin polymerization and granule release. While either Dlg1 variant coordinates the WASp-dependent pathway, the Lck-dependent pathway is specific to the Dlg1AB variant, and requires a Dlg1 phosphorylation event at Y222. Therefore, we speculate that differential expression, utilization, recruitment and modification of Dlg1 variants can tune the level of pro-inflammatory cytokine production while maintaining cytoskeletal re-arrangements required for the release of other vital effector molecules. Indeed, the Dlg1 i1A region is one of the most highly regulated exons in response to TCR stimulation, lending credence to our hypothesis. Certainly future studies into the regulation of Dlg1 splice variant expression and post-translational modification will further elucidate the dynamic interplay between immune cells and their environment. Identification of mechanisms that dictate signal specificity downstream of immunoreceptors is the first step to understanding how the immune response is adapted to specific pathogens, how aberrant signals can lead to pathology, and what points of control can be targeted in the creation of improved therapeutics.

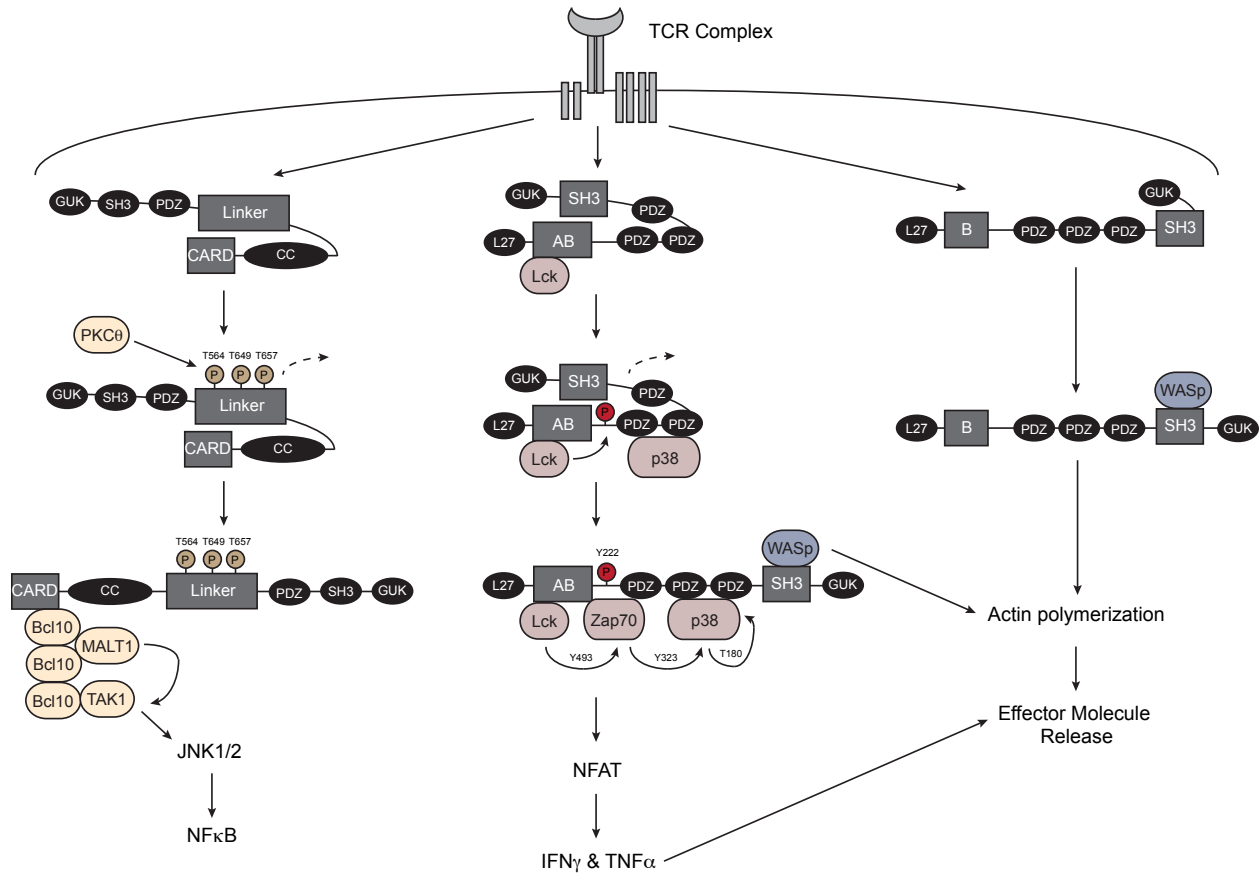


Figure 6-1: Current Model of MAGUK-Mediated Signaling. MAGUK scaffold proteins Dlg1 and CARMA1 bifurcate signal transduction downstream of the TCR in order to elicit specific biological outcomes. CARMA1 (left) is phosphorylated by PKC θ in the linker region, which opens the scaffold allowing association with Bcl10, MALT1 and TAK1 leading to the activation of MAPKs JNK1/2 and transcription factor NF κ B. Two Dlg1 splice variants are expressed in T cells: Dlg1AB (center) and Dlg1B (right). Dlg1AB (center) associates with Lck and is phosphorylated by Lck at Y222, which is thought to open the scaffold allowing proper juxtaposition of Zap70 and p38 followed by p38 phosphorylation and activation of NFAT-dependent transcription including cytokines IFN γ and TNF α . Dlg1AB or Dlg1B (right) can associate with WASp leading to actin polymerization and secretion of effector molecules including the IFN γ and TNF α produced via the Dlg1AB pathway.

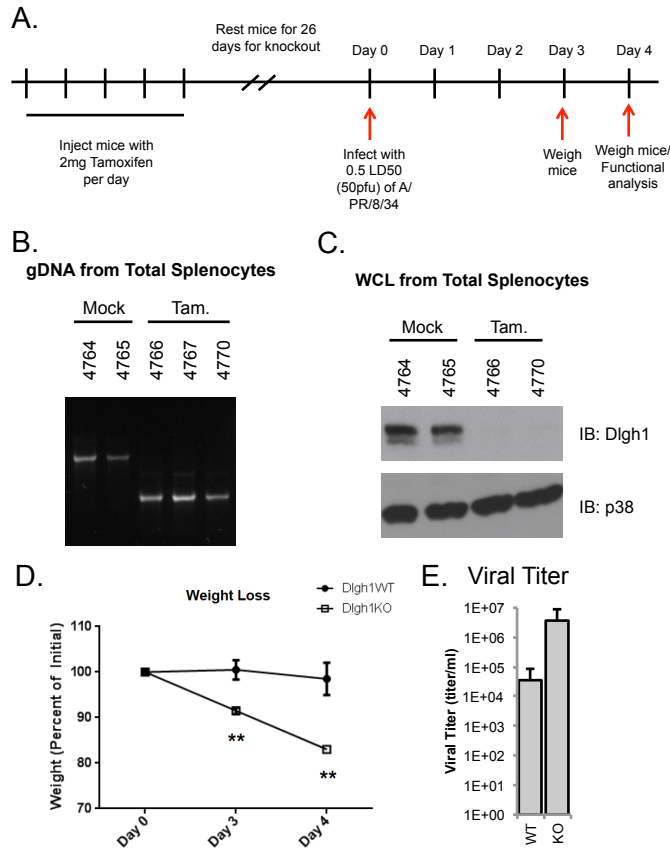


Figure 6-2: Dlg1 knockout impairs response to H1N1 influenza. (A-D) Dlg1^{fl/fl} ER-Cre mice were treated with 2mg tamoxifen per day for five consecutive days followed by 26 days of rest. They were infected with 0.5 LD50 A/PR/8/34 influenza through inhalation. (B) gDNA and (C) protein from splenocytes were analyzed to confirm Dlg1 knockout. (D) Mice were weighed on day 3 and day 4 and (E) lung viral titers were assessed on day 4. Dots or bars represent the mean +/- SD for three mice per group. Two-tailed t tests were used to assess significance **p<0.05.

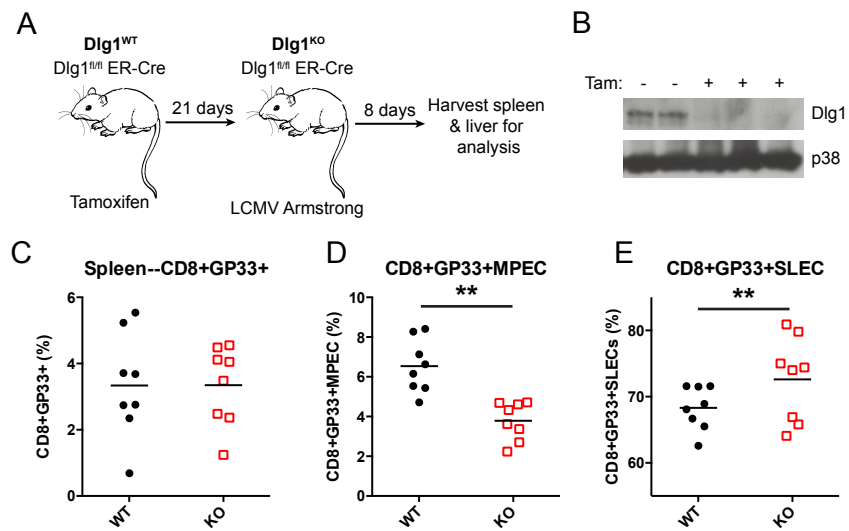


Figure 6-3: (A) Dlg1^{fl/fl} ER-Cre mice were injected with 2mg per day tamoxifen or mock solution followed by LCMV Armstrong infection; spleens were harvested day 8 post-infection. (B) SDS-PAGE of splenic protein lysate assessing Dlg1 knockout. (C-E) Splenocytes were isolated and stained with α CD8 and GP33 tetramer; (D-E) as well as IL7R α and KLRG1 to identify (D) IL7R α ^{hi}KLRG1^{lo} memory precursor (MPEC) and (E) IL7R α ^{lo}KLRG1^{hi} terminal effectors (SLECs). Each dot represents percent positive cells for a single mouse, horizontal line represents the average of the group. Two-tailed t tests were used to assess significance ** $p < 0.05$.

REFERENCES

1. Wang D, You Y, Case SM, McAllister-Lucas LM, Wang L, DiStefano PS, Nunez G, Bertin J, Lin X. 2002. A requirement for CARMA1 in TCR-induced NF-kappa B activation. *Nat Immunol* 3: 830-5
2. Gaide O, Favier B, Legler DF, Bonnet D, Brissoni B, Valitutti S, Bron C, Tschopp J, Thome M. 2002. CARMA1 is a critical lipid raft-associated regulator of TCR-induced NF-kappa B activation. *Nat Immunol* 3: 836-43
3. Thome M. 2004. CARMA1, BCL-10 and MALT1 in lymphocyte development and activation. *Nat Rev Immunol* 4: 348-59
4. Round JL, Tomassian T, Zhang M, Patel V, Schoenberger SP, Miceli MC. 2005. Dlg1 coordinates actin polymerization, synaptic T cell receptor and lipid raft aggregation, and effector function in T cells. *J Exp Med* 201: 419-30
5. Rebeaud F, Hailfinger S, Thome M. 2007. Dlg1 and Carma1 MAGUK proteins contribute to signal specificity downstream of TCR activation. *Trends Immunol* 28: 196-200
6. Round JL, Humphries LA, Tomassian T, Mittelstadt P, Zhang M, Miceli MC. 2007. Scaffold protein Dlg1 coordinates alternative p38 kinase activation, directing T cell receptor signals toward NFAT but not NF-kappaB transcription factors. *Nat Immunol* 8: 154-61
7. Martinez NM, Pan Q, Cole BS, Yarosh CA, Babcock GA, Heyd F, Zhu W, Ajith S, Blencowe BJ, Lynch KW. 2012. Alternative splicing networks regulated by signaling in human T cells. *RNA* 18: 1029-40
8. Matsumoto R, Wang D, Blonska M, Li H, Kobayashi M, Pappu B, Chen Y, Wang D, Lin X. 2005. Phosphorylation of CARMA1 plays a critical role in T Cell receptor-mediated NF-kappaB activation. *Immunity* 23: 575-85
9. Sommer K, Guo B, Pomerantz JL, Bandaranayake AD, Moreno-Garcia ME, Ovechkina YL, Rawlings DJ. 2005. Phosphorylation of the CARMA1 linker controls NF-kappaB activation. *Immunity* 23: 561-74
10. Marcette J, Hood IV, Johnston CA, Doe CQ, Prehoda KE. 2009. Allosteric control of regulated scaffolding in membrane-associated guanylate kinases. *Biochemistry* 48: 10014-9
11. Newman RA, Prehoda KE. 2009. Intramolecular interactions between the SRC homology 3 and guanylate kinase domains of discs large regulate its function in asymmetric cell division. *J Biol Chem* 284: 12924-32
12. Wu H, Reissner C, Kuhlendahl S, Coblenz B, Reuver S, Kindler S, Gundelfinger ED, Garner CC. 2000. Intramolecular interactions regulate SAP97 binding to GKAP. *EMBO J* 19: 574-5751
13. Nakagawa T, Futai K, Lashuel HA, Lo I, Okamoto K, Walz T, Hayashi Y, Sheng M. 2004. Quaternary structure, protein dynamics, and synaptic function of SAP97 controlled by L27 domain interactions. *Neuron* 44: 453-67

14. Tully MD, Grossmann JG, Phelan M, Pandelaneni S, Leyland M, Lian LY. 2012. Conformational characterization of synapse-associated protein 97 by nuclear magnetic resonance and small-angle X-ray scattering shows compact and elongated forms. *Biochemistry* 51: 899-908
15. Lin EI, Jeyifous O, Green WN. 2013. CASK regulates SAP97 conformation and its interactions with AMPA and NMDA receptors. *J Neurosci* 33: 12067-76
16. Filippakopoulos P, Muller S, Knapp S. 2009. SH2 domains: modulators of nonreceptor tyrosine kinase activity. *Curr Opin Struct Biol* 19: 643-9
17. Lopez-Santalla M, Salvador-Bernaldez M, Gonzalez-Alvaro I, Castaneda S, Ortiz AM, Garcia-Garcia MI, Kremer L, Roncal F, Mulero J, Martinez AC, Salvador JM. 2011. Tyr323-dependent p38 activation is associated with rheumatoid arthritis and correlates with disease activity. *Arthritis Rheum* 63: 1833-42
18. Corse E, Gottschalk RA, Allison JP. 2011. Strength of TCR-peptide/MHC interactions and in vivo T cell responses. *J Immunol* 186: 5039-45
19. Hufford MM, Kim TS, Sun J, Braciale TJ. 2011. Antiviral CD8+ T cell effector activities in situ are regulated by target cell type. *J Exp Med* 208: 167-80
20. Hamada H, Bassity E, Flies A, Strutt TM, Garcia-Hernandez Mde L, McKinstry KK, Zou T, Swain SL, Dutton RW. 2013. Multiple redundant effector mechanisms of CD8+ T cells protect against influenza infection. *J Immunol* 190: 296-306
21. Zanin-Zhorov A, Lin J, Scher J, Kumari S, Blair D, Hippen KL, Blazar BR, Abramson SB, Lafaille JJ, Dustin ML. 2012. Scaffold protein Disc large homolog 1 is required for T-cell receptor-induced activation of regulatory T-cell function. *Proc Natl Acad Sci U S A* 109: 1625-30
22. Lasserre R, Charrin S, Cuche C, Danckaert A, Thoulouze MI, de Chaumont F, Duong T, Perrault N, Varin-Blank N, Olivo-Marin JC, Etienne-Manneville S, Arpin M, Di Bartolo V, Alcover A. 2010. Ezrin tunes T-cell activation by controlling Dlg1 and microtubule positioning at the immunological synapse. *EMBO J* 29: 2301-14
23. Adachi K, Davis MM. 2011. T-cell receptor ligation induces distinct signaling pathways in naive vs. antigen-experienced T cells. *Proc Natl Acad Sci U S A* 108: 1549-54
24. Humphries LA, Shaffer MH, Sacirbegovic F, Tomassian T, McMahon KA, Humbert PO, Silva O, Round JL, Takamiya K, Haganir RL, Burkhardt JK, Russell SM, Miceli MC. 2012. Characterization of in vivo Dlg1 deletion on T cell development and function. *PLoS One* 7: e45276
25. Stephenson LM, Sammut B, Graham DB, Chan-Wang J, Brim KL, Huett AS, Miletic AV, Kloeppel T, Landry A, Xavier R, Swat W. 2007. DLGH1 is a negative regulator of T-lymphocyte proliferation. *Mol Cell Biol* 27: 7574-81
26. Gmyrek GB, Graham DB, Sandoval GJ, Blaufuss GS, Akilesh HM, Fujikawa K, Xavier RJ, Swat W. 2013. Polarity gene discs large homolog 1 regulates the generation of memory T cells. *Eur J Immunol* 43: 1185-94
27. Sun J, Madan R, Karp CL, Braciale TJ. 2009. Effector T cells control lung inflammation during acute influenza virus infection by producing IL-10. *Nat Med* 15: 277-84

28. Brandes M, Klauschen F, Kuchen S, Germain RN. 2013. A systems analysis identifies a feedforward inflammatory circuit leading to lethal influenza infection. *Cell* 154: 197-212